ACTIVE NOISE CONTROL IN A DUCT WITH FLOW

by

Osman Yüksel

B.S., Chemical Engineering, Boğaziçi University, 2008

Submitted to the Institute for Graduate Studies in

Science and Engineering in partial fulfillment of

the requirements for the degree of

Master of Science

Graduate Program in Mechanical Engineering

Boğaziçi University

2012

ACKNOWLEDGEMENTS

ABSTRACT

ACTIVE NOISE CONTROL IN A DUCT WITH FLOW

In this thesis, active noise control in a duct with flow is investigated. A one dimensional acoustic duct model, in which fluid medium inside the duct has a mean flow velocity, is presented. The acoustic duct model is solved in Laplace domain and infinite dimensional system transfer functions are obtained. For controller designs, appropriate microphone and noise canceling source locations inside the duct are determined. In numerical studies, ideal boundary condition case (open end) and general boundary condition case (frequency dependent impedance end) are investigated. For these boundary conditions, low order finite dimensional transfer function approximations of actual system transfer functions are obtained. It is found that, in a selected frequency range, approximations represent actual system in a satisfactory way. By using approximated system transfer functions, low order optimal H_2 and H_∞ controllers are synthesized via linear matrix inequalities method found in linear time invariant finite dimensional control theory. Closed loop frequency response and time domain simulations show that the controllers successfully suppress unwanted sound which propagates along the duct.

ÖZET

AKIŞLI BORUDA AKTİF GÜRÜLTÜ KONTROLÜ

Bu tez çalışmasında akışlı bir borudaki aktif gürültü kontrolü incelenmiştir. Boru içindeki akışkanın ortalama bir hızının olduğu, tek boyutlu akustik bir boru modeli sunulmuştur. Akustik boru modeli Laplace alanında çözülmüş ve sonsuz boyutlu sistem transfer fonksiyonları elde edilmiştir. Kontrolcü tasarımları için, borunun içinde, uygun mikrofon ve gürültü kesici kaynak konumları belirlenmiştir. Nümerik çalışmalarda, ideal sınır koşulu durumu (açık uç) ve genel sınır koşulu durumu (frekansa bağlı impedanslı uç) ele alınmıştır. Bu sınır koşulları için gerçek sistem transfer fonksiyonlarının düşük dereceli sonlu boyutlu transfer fonksiyon tahminleri elde edilmiştir. Seçilen bir frekans aralığında, tahminlerin, gerçek sistemi tatmin edici bir şekilde yansıttığı bulunmuştur. Tahmin edilen sistem transfer fonksiyonları kullanılarak, doğrusal, zamanla değişmeyen, sonlu boyutlu kontrol teorisinde yer alan doğrusal matris eşitsizlikleri metodu ile, düşük dereceli optimal H_2 ve H_∞ kontrolcüleri sentezlenmiştir. Kapalı döngü frekans cevabı ve zaman alanı simülasyonları sonucunda, boru boyunca iletilen istenmeyen sesleri, kontrolcülerin başarılı şekilde bastırdığı görülmüştür.

TABLE OF CONTENTS

LIST OF FIGURES

LIST OF TABLES

LIST OF SYMBOLS

$\mathbf{a_{est}}$	Estimated parameters vector of A_i's for open BC case
$\mathbf{A}$	Approximated system's corresponding state space matrix
$\mathbf{A_c}$	Controller's corresponding state space matrix
A_i	ith least squares estimate for transfer function approximations
$\mathbf{b_{est}}$	Estimated parameters vector of B_i's for open BC case
$\mathbf{B}$	Approximated system's corresponding state space matrix
$\mathbf{B_c}$	Controller's corresponding state space matrix
B_i	ith least squares estimate for transfer function approximations
c	Speed of sound
$\mathbf{C}$	Approximated system's corresponding state space matrix
$\mathbf{C_c}$	Controller's corresponding state space matrix
$C(s)$	Controller transfer function in Laplace domain
d	Disturbance
$d(s)$	Disturbance in Laplace domain
$d(t)$	Disturbance signal coming into the duct
$\mathbf{D_c}$	Controller's corresponding state space matrix
f	Frequency in Hz
f_{di}	Damped natural frequency of the ith mode
f_n	nth natural frequency of the duct for no flow case for open BC
f'_n	nth natural frequency of the duct for mean flow case for open BC
f_m	Frequency at which microphone located at x_m measures zero pressure for no flow case for open BC
f'_m	Frequency at which microphone located at x_m measures zero pressure for mean flow case for open BC
f_s	Frequency at which source located at x_s creates zero pressure for no flow case for open BC
f'_s	Frequency at which source located at x_s creates zero pressure for mean flow case for open BC

$G_{appx}(s)$	Finite dimensional transfer function approximation
$G_d(x,s)$	$d(s)$ to $P(x,s)$ transfer function
$G_q(x,s)$	$q(s)$ to $P(x,s)$ transfer function
$\mathbf{H}$	Matrix variable in LMIs
$\mathbf{K}$	Matrix variable in LMIs
L	Length of the duct
Ma	Mach number
$\mathbf{N}$	Matrix variable in LMIs
$p(x,t)$	Acoustic pressure
$P(s)$	Acoustic pressure at duct end $x = L$ in Laplace domain
$P(t)$	Acoustic pressure at duct end $x = L$
$P(x_m,s)$	Acoustic pressure in Laplace domain at microphone point
$P(x,s)$	Acoustic pressure at x inside the duct in Laplace domain
$P_c(t)$	Capacitor voltage in electrical circuit analogy for acoustic impedance approximation
P_0	Equilibrium pressure
q	Input
$q(s)$	Input of source in Laplace domain
$q_s(t)$	Mass injection rate per unit area by point source
r	Radius of the duct
$\mathbf{R}$	Matrix variable in LMIs
s	Laplace variable
T_0	Equilibrium temperature
$u(x,t)$	Velocity change of fluid particle
u_0	Mean flow velocity of fluid inside the duct
$V(s)$	Fluid velocity at duct end $x = L$ in Laplace domain
$V(t)$	Fluid velocity at duct end $x = L$
$V_m(t)$	Inductance current in electrical circuit analogy for acoustic impedance approximation
$\tilde{\mathbf{x}}$	Closed loop transfer function's state vector
$\mathbf{x_c}$	Controller's state vector

x_i	Corresponding ith regressor for transfer function approximations in frequency dependent impedance BC case
x_i^m	ith regressor for imaginary part of transfer function approximations in open BC case
x_i^r	ith regressor for real part of transfer function approximations in open BC case
x_m	Microphone location
x_p	Performance point
$\mathbf{x_{pl}}$	Plant's state vector
x_s	Source location
$\mathbf{X}$	Matrix variable in LMIs
$\mathbf{X_{fdie}}$	Regressor matrix for transfer function approximations in frequency dependent impedance BC case least squares formulation
$\mathbf{X_{imag}}$	Regressor matrix for imaginary part of transfer function approximations in open BC case least squares formulation
$\mathbf{X_{real}}$	Regressor matrix for real part of transfer function approximations in open BC case least squares formulation
y	Measured output
$\mathbf{y_{fdie}}$	Vector of exact transfer function responses in frequency dependent impedance BC case least squares formulation
$\mathbf{y_{imag}}$	Vector of imaginary parts of the exact transfer function in open BC case least squares formulation
$\mathbf{y_{real}}$	Vector of real parts of the exact transfer function in open BC case least squares formulation
$\mathbf{Y}$	Matrix variable in LMIs
z	Controlled output
z_i	Corresponding ith regressor for transfer function approximations in frequency dependent impedance BC case
$Z_L(s)$	Frequency dependent specific acoustic impedance of the duct end at $x = L$

$\hat{\boldsymbol{\beta}}$	Vector of estimated parameters for transfer function approximations for frequency dependent impedance BC least squares formulation
$\delta(x)$	Dirac delta function
ζ_i	Damping ratio for the ith mode
λ	Wavelength
λ_n	Wavelength of the nth mode
$\rho(x,t)$	Density change of fluid particle
ρ_0	Equilibrium density of fluid
τ	Temperature change
ω_{di}	Damped natural frequency for the ith mode
ω_i	Undamped natural frequency for the ith mode

LIST OF ACRONYMS/ABBREVIATIONS

ANC	Active Noise Control
BC	Boundary Condition
FEA	Finite Element Analysis
HVAC	Heating Ventilating Air Conditioning
IC	Initial Condition
LMI	Linear Matrix Inequality
LQG	Linear Quadratic Gaussian
LTI	Linear Time Invariant
ODE	Ordinary Differential Equation
PDE	Partial Differential Equation
PID	Proportional Integral Derivative
SISO	Single Input Single Output
SITO	Single Input Two Outputs

1.   INTRODUCTION

Acoustic noise is an important problem that can influence human health and comfort negatively. It can cause several hazards including stress and pain to the human body. In the modern world, noise is originated and generated by technological developments such as automobiles, jet engines, fans, exhausts and any kind of machines. Although they provide lots of benefits and ease people's lives, they also make noise and disturb people. So it is a crucial task to provide less noisy and peaceful environments while benefiting from the blessings of the modern world.

1.1. Noise Control Strategies

Noise control is basically the attenuation of unwanted sound. Here, we briefly discuss the two strategies namely; passive and active noise control.

1.1.1. Passive Noise Control

Traditionally, passive control techniques are mostly used in noise control practices. Passive control aims to modify the environment to achieve noise reduction in a way that either by changing the flow direction of acoustic energy or by reducing the total sound power that flows away. Changing the flow direction of acoustic energy can be achieved by a wall or barrier as can be seen along busy highways. On the other hand reduction of acoustic power can be achieved by acoustic insulation materials which absorb acoustic energy and turns it into small amount of heat, or by coating vibrating surfaces, or by changing the acoustic impedance as in the car muffler case [1].

1.1.2. Active Noise Control

Active noise control is a technique that uses superposition principle of waves in order to suppress unwanted sound. In this technique noise is canceled via introduction of an additional sound field which has the same magnitude but that is out of phase

with the noise field. When these two fields meet, the result is a less noisy environment according to the principle of destructive interference.

Typical application of an active noise control system consists of a reference microphone, an error microphone, a controller and an actuator which is usually a loudspeaker [1–3]. Reference microphone picks up incoming noise, converts it into electrical signal and sends it to controller. Controller uses that information to create a sound wave, which has the same magnitude but 180° out of phase with the noise signal. Controller sends this information to the actuator as an electrical signal. This signal is converted into mechanical energy in the actuator (in loudspeaker mechanical energy is obtained by moving diaphrams). Thus, a canceling sound field which coincides with original noise field is created. Error microphone is used to check the residual noise and to adapt the system.

Some of the applications of Active Noise Control (ANC) include: active mufflers for automobiles and other kind of transportation vehicles; aircraft cabin silencing; active noise reducing head-phones, earmuffs, headrests; active noise control systems in HVAC (Heating Ventilating Air Conditioning) equipments, ducts, pipes; active control of fan noise, helicopter rotor noise; electrical transformer noise; intake and exhaust noise; car and van interior noise; aircraft jet engine noise [2–8]. Among them the most successful ANC applications are for controlling low-frequency noise (plane wave noise) problems in ducts [2, 3, 6, 7].

The idea of active control of noise fields was first mentioned 75 years ago in Lueg's patent application [9]. He claimed to reduce incident single tone noise in a duct by using a microphone, an amplifier, and a loudspeaker. Microphone detects sound and creates a signal, and this signal is sent to the loudspeaker through the amplifier in a way that the loudspeaker produces a canceling sound wave. The exact 180° out of phase shift is obtained by arranging the distance between microphone and loudspeaker.

Although promising, Lueg's idea was impractical because it only deals with single pure tonal noise and if the frequency of noise changes the residual noise could be

worsened as stated in [10]. The technology of 1930's also made it impractical for realization [9]. However, Lueg understood the physical applicability of active noise control since speed of electrical signals are much higher than the speed of sound waves. Once an incoming noisy sound wave is detected, there is enough time to process and create an anti-sound wave which coincides with the original noisy sound field and results in reduction of sound amplitude [4, 10].

After Lueg's early work Olson *et al.* [11] introduced electronic sound absorber in 1953. That device consists of a microphone, an amplifier and a loudspeaker as Lueg's case, but it reduces the sound field near microphone whereas in Lueg's patent the microphone is used to obtain information about the incident wave. In active noise control terminology, if reference microphone is used to get information about the incoming wave and used to attenuate noise in somewhere else then it is called feedforward configuration, but if it is used to attenuate the noise in the vicinity of the microphone then that configuration is feedback. From that point of view, Lueg's work is feedforward whereas Olson's work is feedback. Olson obtained reduction in noise levels in a small volume for low frequency portion of the audio range [11]. But frequency range and physical noise reduction extent of Olson's device was limited as well as performance diminishes quickly from a short distance away from the control point [10].

In 1957 Conover *et al.* patented a system for transformer noise problem [12]. In [12] loudspeakers were placed near transformer's wall in order to cancel the transformer noise in the near field. The controlled frequencies of the noise are periodic such that fundamental at 120 Hz and its harmonics at 240 Hz and 360 Hz. Conover obtained noise reduction in certain areas but the noise levels were increased in some other areas as well [10].

As a result of early failures active noise control was abandoned till the end of 1960's. In 1968, the interest to the field increased with the publications of Jessel and Kido [10]. They realized that active noise control systems can be utilized for reducing low frequency noise problems. They reached such a conclusion because of the high cost, large bulk and back-pressure problems of existing passive hardware when dealing

with low frequency noise [10].

After briefly reviewing some early attempts of active noise control we leave the review of research done from 1970's to today in the "Literature Review" section of the thesis and also we limit that section only to the studies done on "Active Noise Control in Ducts".

1.2. Noise Control in Ducts

Here, we begin our discussion with passive noise reduction techniques used in ducts and then we give our attention primarily to ANC in ducts.

1.2.1. Passive Noise Reduction Techniques in Ducts

Passive noise control approaches in ducts fall into two categories, which are reactive techniques and dissipative techniques. In reactive techniques, the aim is to alter the duct impedance whereas in dissipative techniques the aim is to absorb acoustic energy in the duct. Reactive techniques are used in low frequency noise control problems and dissipative techniques are used primarily in mid and high frequency noise problems. Examples for reactive techniques used in ducts are side-branch resonator, expansion chamber and Helmholtz filter. A side-branch resonator is useful when dealing with pure tone noise in a duct. An expansion chamber is a large opening in the duct and provides sound attenuation over a wider range of frequencies compared to side-branch resonator. Helmholtz filter is used to suppress noise in flowing gas and it is an extension of the expansion chamber. But in Helmholtz filter low frequency attenuation is limited so it is considered as a low pass filter. Dissipative techniques use a porous lining material which is placed on the walls of the duct in order to absorb the acoustic energy that propagates along the duct. Dissipative techniques work best for higher order duct modes and their performance for plane wave mode is very poor [1].

There are some serious problems encountered when dealing with low frequency noise problems in ducts. A problem with duct silencers is that in order to achieve low

frequency noise reduction the silencer must be long since they can affect the sound which has similar or smaller wavelength compared to silencer's dimensions [8]. That is to say, we need large passive silencers [3]. When volume of the duct-silencer couple increases it also reflects as an increase in weight which can be important in aerospace or automotive industries. Large space needed to implement duct-silencer couple can be problematic in industries where effective usage of total area is important. Another problem with duct silencers is that since they reduce the duct area, they cause pressure drop inside the duct [13]. This would be problematic in systems (such as server rooms) where large amount of gas/air flow is needed to operate the system properly.

On the other hand, the problem with lining materials (absorbing materials) in low frequencies is that acoustic wavelengths become large compared to the thickness of these materials [6]. As the thickness of the lining material increases, the absorption of lower frequency noise is improved [8, 13]. Thus, when the noise frequency decreases, thicker and heavier absorbing materials are needed. Thicker absorbing materials inhibit ventilation [14]. As a result, to obtain noise reduction, we increase the weight of the duct and inhibit ventilation.

1.2.2. Active Noise Control in Ducts

As mentioned earlier the most important ANC application is plane wave noise reduction in ducts. Plane waves propagate between 20 Hz and plane wave cut-off frequency [8]. Plane wave cut-off frequency is inversely proportional to the duct's cross-sectional dimensions [8]. ANC application in ducts frequently has feedforward configuration in which a reference microphone sends primary knowledge about incoming noise along the duct to a controller arrangement. Controller proceeds this information and sends an input to actuator in order to attenuate the incident noise at target location. After interference, an error microphone detects the residual noise downwards the duct and sends this information to the controller, in order to make controller adapt the weights used in the algorithm to adjust the control system to meet certain specifications. This is the most widely encountered configuration [1-3, 13]. The other configuration is feedback in which an error microphone sends information to controller

and controller's task is to attenuate the noise level at the vicinity of error microphone [2, 3].

Feedforward controllers are usually preferred against feedback controllers because reference signal combined with error signal increase the stability of the system [2]. One disadvantage of feedforward controllers over feedback controllers is that the control source output is also captured by reference microphone [2]. Application of the ANC in a duct for low frequency noise is simple because of the plane wave propagation along the duct since a few microphones and a single canceling loudspeaker is satisfactory for control applications [5, 8, 10].

Typically, passive noise reduction techniques work best above 250 Hz in mid and high frequency range whereas ANC works best at low frequency range between 31 Hz and 250 Hz [8]. The low frequency range mentioned in [13] is between 40 and 400 Hz. Thus, instead of implementing passive techniques into ducts for plane wave frequencies it is a better choice to handle low frequency noise problem with ANC. By this, unnecessary increase in weight, bulk, pressure-drop and cost will be eliminated. As an illustrative quantitative example, power loss due to passive silencers in a large size HVAC duct ranges between 2 to 40 kiloWatts whereas the electrical energy needed for ANC system in a HVAC duct is less than 40 Watts [8].

Advantages of ANC systems over passive methods in ducts can be summarized as; improved low frequency noise reduction performance, reduction in size and weight compared to conventional passive control techniques, zero or very low pressure drop values.

After introducing basic principles regarding ANC in ducts, Literature Review on this subject is given next.

1.3. Literature Review

ANC studies in ducts can be grouped into two. The first one utilizes signal processing and system identification tools for ANC in ducts [15], and then implement an adaptive control algorithm to achieve noise reduction [16]. Adaptive ANC in ducts need secondary path identification in some of the studies [17–20]. In adaptive ANC systems, disturbance to error microphone transfer function is called primary path, control source to error microphone transfer function is called secondary path and control source to reference microphone transfer function is called feedback path. Reference microphone provides primary information about the incoming noise whereas error microphone is used to adapt the system [21].

Physical model based ANC systems in ducts constitute the second group. Adaptive systems could be used for noise reduction purposes, but it is beneficial to see the limitations and possible theoretical noise reduction levels as well. These can be observed by using the physical model based ANC systems. In our thesis, we would like to determine the physical limitations and possible noise reduction performances of ANC applications in ducts with flow. Thus, we give our emphasis to model based studies which are derived by principles of physical acoustics. In this section, we partition physical model based studies into two group such that, studies with flow and studies without flow.

Before starting our review we would like to mention that, all the studies in this section were done for rigid walled (hard walled) ducts. The studies, which does not consider flow of fluid inside the duct (no flow case), are reviewed first. Then, studies which include mean flow of fluid medium inside the duct (mean flow case), are investigated.

1.3.1. Studies Without Flow Inside The Duct

Eghtesadi and Leventhall proposed an active noise cancelation scheme [22] using a microphone placed centrally between the two canceling loudspeakers. By this con-

figuration, in the upstream of the duct standing waves were produced whereas in the downstream section noise cancelation was achieved. In the microphone section, the two loudspeaker inputs canceled each other so that only primary noise was detected by the microphone. This study was supported by experiments conducted in both circular and rectangular ducts. Noise reduction was achieved both for pure tones and random noise signals. Flow of the acoustic wave propagation medium (air) was not considered. After [22], they also discussed the active noise cancelation problem in ducts by using just one secondary (canceling) source in [23]. In the absence of air flow the primary noise signal was picked up by a microphone and downstream of the duct the noise was canceled using a secondary source. They suggested a way to get rid of acoustic feedback towards reference microphone caused by using only one canceling loudspeaker. Experiments conducted in rectangular duct and noise reduction for pure tone and random noise signals was achieved. In a later theoretical study [24], they derived a general expression for various number of sources and spacings between them. They concluded; as the number of sources increases, the effective bandwidth of noise reduction as well as isolation of reference microphone from canceling source signals are improved.

In [25], Trinder and Nelson discussed a feedback control scheme for the purpose of active sound attenuation in a finite length duct. The primary plane wave noise, caused by a loudspeaker mounted on one side of the square duct, was canceled via a second canceling loudspeaker at the downstream of the duct. The feedback microphone and the canceling source was collocated, i.e., their longitudinal coordinate along the duct was the same. In experiments, they obtained low frequency broadband noise reduction especially at the longitudinal duct resonance frequencies in an open ended duct with no flow.

Hull *et al.* [26], developed a state space representation of a one dimensional acoustic duct system by applying separation of variables technique to governing partial differential equations. Their model was an adiabatic system with no mean flow and had totally reflective boundary condition at one end, whereas partially reflective boundary condition at the other. They obtained an infinite order, diagonal state space model. Hull and Radcliffe [27], conducted experiments in order to verify the model developed

in [26]. In [28], Hull *et al.* developed a truncated state estimator for the purpose of active noise control since all the states of the duct system was not available for the pole placement control action. The truncated state space model and state estimator were adequate to design a finite dimensional feedback controller for low frequency active noise reduction purposes. Finally, by using [26] and [28], Hull *et al.* developed a feedback control law for active noise control of this one-dimensional acoustic duct by using pole placement feedback algorithm [29]. Frequency and time domain simulations together with experiments were performed. In time domain simulations, a pure tone sine wave was used whereas in experiments a band limited random noise signal was used.

In [30], Hu discussed active noise control in finite length ducts by transfer function approach. He obtained transfer functions that relate control inputs to acoustic pressure in any location of the duct. He studied effects of collocated and noncollocated sensor and actuator configurations on feedback stability of the system. In his mathematical work, the flow of the acoustic medium was not considered. In his discussion, he used both totally and partially reflected boundary conditions. He also developed a feedback controller in order to suppress unwanted periodic noise. He performed some simulations resulted in noise reduction at feedback microphone region.

Bai and Shieh [31], obtained modal equations of a finite length duct with the help of orthogonality of eigenfunctions. Later, they applied modal truncation in order to obtain finite number of modal equations for control purposes. Their acoustic wave propagation medium (air) was stationary. They also put truncated modal equations into modal state form and they derived an optimal controller by using Linear Quadratic Gaussian (LQG) algorithm. Their modal state observer was designed based on the Kalman-Bucy filter. Their controller was designed for suppressing zero mean white Gaussian noise field and they only considered the steady state case. They performed numerical simulations taking into account various parameters such as type of primary noise, number of controlled modes, number of sensors, number of actuators, location of sensors, location of actuators, and the ratio of relative importance of the control error to control energy.

In [32], Hong *et al.* developed the state space model of a rectangular duct open at both ends and with no flow conditions. The governing partial differential equations of the system was derived via three fundamental equations: equation of state, equation of continuity and linearized inviscid force equation. The model consisted of one control actuator and one control sensor in which control speaker was considered as a point mass source. By using separation of variables and incorporating a speaker model with acoustic duct model a state space representation of the system was obtained. Some model parameters were determined via experimental identification. In those experiments, it was found that finite speaker size did not have a significant effect on duct's acoustic response which confirmed the point source assumption. Then, a precompensated LQG type controller were synthesized in order to minimize the H_2 norm of the transfer function of the state space realization of the closed-loop system at a selected performance point. The synthesized controller's order was truncated by standard techniques and reduced order controller was implemented digitally in experiments. For collocated sensor and actuator configuration, this feedback controller showed noise reductions at performance point (performance point was also selected as sensor location) and at the end of the duct away from the disturbance source.

Wu *et al.* [33], developed a one dimensional time domain model describing acoustical pressure response in a duct with no flow. Their system consisted of two semi infinite regions and one finite region which was between semi infinite regions. Primary source (disturbance source) and secondary source(s) (canceling source(s)) were located in the finite region. In their model, they also included a passive viscous damping term acting on the finite duct section. State space formulation which relates the duct dynamics, disturbance, input and output to each other, was obtained by solving governing partial differential equations analytically for semi infinite regions, whereas for finite region solution a standard numerical method (finite difference method) was used. The discrete and analytical results were then related by the application of boundary conditions at the intersection points of finite and semi infinite regions; thus completing the derivation of the state space model. Then, feedback control algorithms utilizing LQG optimal control theory were designed by using derived state space model. Various noise control systems with several sensor and actuator arrangements were studied for

both full state-feedback and state observer based feedback controllers.

Lee [34], modeled acoustic response in a one dimensional finite length duct by using finite element method. The medium in his model was stationary. He derived state space representation of the duct system by using finite element formulation. In order to design a suitable controller, he truncated the state space system, thus only the few important modes were included to represent low frequency behavior of the system. He compared the frequency responses of analytical and finite element solutions, and also discussed the effects of truncation. After convinced that the truncated state space model was adequate, he designed a feedback controller by using linear quadratic optimal control technique and a truncated state observer. He performed frequency and time domain simulations in order to see the performance of the proposed controller. Frequency response simulations showed noise reduction in low frequency range. In time domain simulations, a pure tone sinusoidal wave was used as disturbance and noise reduction was also observed in this case as well.

Grad [35], theoretically discussed the achievable global noise reduction in a one dimensional duct in which there exists a disturbance point source, a controller point source and a sensor. She considered totally reflective and partially reflective boundary conditions and assumed no mean flow in the duct. She obtained the transfer function relating the pressure measured at some point in the duct to disturbance pressure applied at disturbance source location by taking laplace transform of the governing partial differential equations. Then, she formulated the global noise reduction problem as an H_∞ model matching problem. By saying global, it was indicated that the purpose of noise reduction is not only for a single performance point but also for several performance points altogether. In order to apply finite dimensional H_∞ control theory, she approximated the infinite dimensional system to a finite dimensional system by using Legendre polynomial based Galerkin approximation method, linear spline based Galerkin approximation method, and finite difference method. She concluded Legendre polynomials and linear splines were suitable for approximation of this duct model with their advantages and disadvantages. In order to solve the model matching problem she employed Nevanlinna-Pick interpolation method. Finally, she discussed the global

noise reduction for feedback and feedforward configurations while considering several configurations of the actuator, sensor and performance points.

Morris [36] theoretically discussed the achievable noise reduction in a one dimensional acoustic duct by deriving an infinite dimensional H_∞ optimal control law for suppressing noise at a specified performance point in a duct. She used a similar model as in [35] except that the totally reflective boundary condition was replaced with disturbance end boundary condition. In her model, the medium was stationary as well. She obtained a transfer function which relates the control pressure input to output pressure obtained in any location of the duct by taking laplace transform of the governing partial differential equations an solving them by using standard linear ordinary differential equation solution methods. After that she formulated the control problem as an H_∞ optimization problem in order to minimize the acoustic response at a desired performance point. Youla parameter function was utilized while obtaining optimal controller for perfect cancelation, but it was found that when using this controller the controlled system became unstable. Instead, a suboptimal controller which stabilizes the closed loop system was considered for determining performance of the proposed system. Feedforward and feedback configurations were analyzed. In feedforward case, it was emphasized that; when using a performance point, which is located downstream of the actuator, noise levels at downstream of the actuator was reduced at the expense of increased noise levels at upstream of the actuator; whereas when using a performance point located upstream of the actuator, the noise reduction was achieved only at that point and noise levels at other locations were increased. In feedback case, performance was limited by feedback delay and imaginary axis zeros of the system transfer function. It was mentioned that sensor, actuator locations and relative impedance of partially reflective duct end had effect on performance.

Pota and Kelkar [37], modeled a one dimensional acoustic duct with no flow by obtaining transfer function that relates actuator input to pressure value at any spatial position along the duct, for open-open end, closed-closed end, open-closed end boundary conditions. They also considered the general boundary conditions which take into account the impedances at both ends of the duct. For comparison of their

theoretical and experimental frequency response values, they modeled the loudspeaker as a second order dynamic system and microphone as a constant gain system. They theoretically discussed an infinite dimensional feedforward controller to suppress the acoustic noise in their infinite dimensional analytical model. But to implement on real systems, they obtained finite dimensional models describing the infinite dimensional system for low frequency range by three approximation methods. Among Maclaurin series expansion, modal representation and zero phase functions methods, they choosed the last one as proper approximation scheme. After that, they designed a noncollocated feedback controller which was a combination of a feedforward passifier, a resonant compensator and a feedback compensator. They conducted experiments and achieved noise reduction at microphone sensing point.

In [38], Toochinda studied the two sensor one actuator ANC design in a one dimensional acoustic duct with no flow. He used a state space approximation of duct and a transfer function model of the speaker to describe the acoustic dynamics of the duct. He compared this analytical model with an experimental model and a finite element model which was constructed by using a commercial software. He found that there was some discrepancy between analytical model and the other two models but he also observed that Finite Element Analysis (FEA) model tends to converge to the analytical model as the duct length increases. He used this mathematical model in order to discuss the fundamental limitations of Single Input Two Outputs (SITO) systems on active noise reduction in ducts. He discussed the effects of different sensor/actuator configurations on closed loop noise control performance and stability. He also studied the superiority of two sensor designs over one sensor designs. In order to analyse the control system he designed an H_∞ controller, by using a software, which aims to reduce the noise levels at error microphone. Designed controller used two inputs to calculate the proper control output which was fed to the system as input. One of the inputs to the controller came from measurement microphone (feedforward arrangement), whereas the other one came from error microphone (feedback arrangement).

In [39], Zimmer et $al.$ developed a one dimensional acoustic duct model for Active Noise Control in a duct. In their system, one end of the duct was closed by a disturbance

loudspeaker whereas the other end was open. Open end was modeled as partially reflective and partially absorptive boundary condition. They approximated the specific acoustic impedance of the open end by a rational function and coupled it to the duct system in the frequency domain. For the disturbance end, they coupled the loudspeaker dynamics to the duct system and formed disturbance end boundary condition, again in the frequency domain. The classical one dimensional wave propagation equations in a duct without fluid flow were treated in the frequency domain together with boundary conditions and formed boundary value problem was solved by using a standard Green's function method. Then, system transfer functions were obtained. They conducted experiments for a circular duct. They obtained similar frequency response behavior both for theoretical and physical systems. Then, an infinite dimensional H_∞ optimal controller was designed in [40] by Morris, in order to suppress unwanted noise at some desired performance point in the duct by using derived transfer function models. A single sensor feedforward configuration was preferred and Youla parameter function was employed to solve the model matching problem. Simulations were performed to analyse the proposed system's performance. If performance point was selected at downstream of the control actuator, then noise reduction occurred at points downstream of canceling actuator whereas noise amplification occurred at upstream of this actuator. Some other configurations of performance points yielded unstability and limited noise reduction.

In [41], Yang studied ANC in a one dimensional duct in the absence of flow. He slightly modified Hull's state space duct model [26, 27] and obtained transfer functions from disturbance and canceling inputs to output acoustic pressures. He obtained a state space model of loudspeaker and converted it to the transfer function description as well. The whole duct system was then defined using these descriptions. Disturbance boundary condition was totally reflective, whereas the other boundary condition was partially reflective. Terminal impedance of partially reflective end was identified, by System Identification Toolbox in Matlab, as some complex constant value. In laboratory tests, model and real system were compared. After that, ANC problem was formulated as a disturbance attenuation problem using a negative feedback controller. Standard control design problems were formulated and several simple Proportional Integral Derivative (PID) controllers were developed for the truncated infinite dimen-

sional system which considers certain modes. Fixed feedback controllers were designed for collocated sensor and control actuator configuration. In real time simulations, a previously recorded low frequency machine noise was used. In physical tests, a low frequency narrowband noise and a sweep signal were used. Additionally, he designed a simple lag compensator in [42] and a feedforward controller filter in [43] with Hicks, in order to study active noise reduction in the same duct system.

The studies reviewed so far [22–43] did not consider the flow in the duct. However, the flow of medium inside the duct should be taken into account since real physical systems such as HVAC or exhaust ducts include gas flow inside. In the literature, there exists relatively few studies which also consider mean flow of fluid medium inside the duct.

1.3.2. Studies With Flow Inside The Duct

Swinbanks [44] discussed the active attenuation of sound waves in a long duct (infinitely long duct). His aim was to suppress a plane wave sound field which is propagating downwards through a uniform flow along the duct. He proposed a mechanism which produces a unidirectional plane wave downstream of the duct in order to attenuate the noise field down the duct. On the other hand, this unidirectional plane wave had no influence on upstream of the duct so the incoming noise was not influenced by canceling noise signal. Swinbanks made his analysis for both circular and square long ducts. The actuator mechanism consist of two or three separated rings of sources in which there were three (for circular) or four (for square) equally spaced point sources.

In [45], Poole and Leventhall conducted some experiments on active cancelation of sound in ducts by using Swinbanks' theoretical method. They constructed a unidirectional array of secondary (canceling) sources in a finite length rectangular duct. They obtained good noise reduction in some pure low frequency tones but as bandwidth of the noise signal was widened the noise reduction levels were diminished. They also did not consider the effect of air flow, i.e., there was no air flow in the duct in none of the experiments conducted. Later in [46], they modified their experimental setup

and improved the results obtained in previous work [45]. In [46], they also included the effect of low Mach number flow in their experiments.

In their theoretical study [47], Berengier and Roure proposed a system similar to Swinbanks' system [44] but they used vibrating pistons as sound sources instead of point sources. Their theoretical waveguide was an infinitely long rectangular duct carrying uniformly flowing fluid. Again the purpose was to create a unidirectional acoustic field in order to suppress downstream noise while incident noise was not affected by canceling system as in [44]. They discussed the effects of using various number of canceling sources on noise reduction performance.

In [48], Hong *et al.* studied two different feedback configurations. They developed a theory to cancel the unwanted plane wave noise caused by a noise source in a long duct. Their first feedback scheme consisted of a tight coupled monopole source, i.e. the feedback microphone and loudspeaker were in close proximity. The attenuator region was lined with absorptive material also and that lining effect was also considered in theory. Then, they extended their theory to a tandem attenuator, i.e. two tight-coupled monopole attenuators cascaded in series. The loudspeakers were considered as vibrating rigid pistons. Experiments were conducted to compare theoretical and measured results. Experiments showed tight-coupled tandem attenuator was superior than tight-coupled monopole attenuator for both suppressing band limited random noise and low frequency pure tonal noise. Tests that were done by airflow showed a decline in performance because of the flow turbulence.

In [49], Bai and Lin studied the active noise control problem in a one dimensional duct by using H_∞ robust control theory. They modeled sound fields in a rectangular duct by considering the effects of physical conditions which were lining, viscosity, temperature and flow. After obtaining the transfer function between monopole source point and any field point they synthesized an H_∞ robust feedback controller which satisfies the mixed sensitivity condition. For the proposed feedback active noise control configuration numerical simulations were performed to discuss the effects of flow, temperature, radiation impedance at open end of the duct (the other end of the duct

was closed) and time delay. Their work was limited to fixed controller and feedback configuration only. For some plant uncertainties, no fixed controller met the design requirements.

Sawada and Ohsumi [50], studied active noise attenuation in a one-dimensional duct with flow. They modeled various number of baffle board speakers and microphones in their duct model. They combined the governing ordinary differential equations (ODEs) of each baffle board displacements and wave propagation equation along the duct. The boundary conditions were chosen as external disturbances caused by a theoretical fan. These disturbances as well as the measurement noises were modeled by a standard white Gaussian noise. In order to obtain a state space model of the system they employed the modal expansion method. After that they designed a finite dimensional controller based on this model by applying (LQG) theory. By using the stationary Kalman filter as the state estimator they obtained an optimal control law which aims to reduce the noise outflowing from the exit of the duct. Only numerical simulations were performed. In the simulations, one baffle board was used as actuator and three microphones as sensors. A pure tone sine function was used as a disturbance noise. However, in those simulations, the velocity of the mean flow of air was taken as zero.

1.4. Motivation of The Study

As it can be seen from Section 1.3.2, relatively low number of studies have been done for ANC in a duct in which mean flow of fluid exists. Therefore, there are still some works that have not been done. Here, we discuss our motivation for this thesis.

There are various theoretical studies on ANC designs that show the capacities and limitations of these systems. However, the ANC designs in some of these studies are hard to realize due to certain physical limitations. From engineering point of view, low cost and efficient ANC systems are needed in real life. By using low order, optimal controllers and less amount of microphones and sources (e.g., a single microphone and a single canceling source loudspeaker), these requirements can be met. Although [44,

47] include flow, these studies can be improved in certain aspects. They considered infinitely long ducts, many sources and microphones, and unidirectional plane wave which is a hard thing to obtain in real life without using several electronic devices and their special arrangements. In [46, 48], in addition to theory, experiments were also conducted but, optimal controllers were not utilized.

In [49, 50], flow is also considered and modern control theory is utilized. However, in those studies, transfer function approximations of system were obtained, for ideal open boundary condition (BC) case, with modal analysis. Modal analysis can possess weaknesses for representing the actual system, if a low order truncated model is used. A possible negative outcome is mismatch in resonance frequencies. Instead, if the system model is solved in Laplace domain, exact system resonance frequencies are obtained. Thus, the only remaining thing to synthesize a low order, finite dimensional controller is, to find a suitable low order approximating scheme that fits the original data. By employing Laplace domain solution, both open BC and frequency dependent impedance BC transfer functions can be obtained easily.

Moreover, in [50], flow is neglected in numerical simulations and more than one microphone were used. Only pure tone sine function was used, which is not a realistic scenario, since, pure tone noises are rarely encountered in real physical world. In [49], the effects of mean flow and frequency dependent radiation impedance at duct end are studied separately. In order to have a more realistic flow duct system, mean flow and frequency dependent impedance end should be considered together.

In addition to those mentioned above, linear matrix inequalities (LMIs) were not utilized in the literature often [51]. If a control problem can be written in terms of LMIs, a solvable convex optimization problem is obtained. For H_2 and H_∞ optimal control problems, LMIs are valuable tools. Moreover, none of the studies mentioned in the literature did not compare the closed loop performances of H_2 and H_∞ optimal controllers. It is beneficial to make comparison of these and choose the appropriate one that fits our needs.

In the light of preceding discussions, we summarize our motivations for this study as:

- Designing a physically applicable single input single output (SISO) ANC system in ducts with flow, which aims to reduce low frequency acoustic noise.
- Analyzing ideal (open BC) and realistic (frequency dependent impedance BC) duct systems with flow, in Laplace domain.
- Studying the effects of mean flow of fluid medium inside the duct and frequency dependent specific acoustic impedance of the duct end, at the same time.
- Obtaining low order, real, rational, finite dimensional approximations for system transfer functions in frequency domain.
- Synthesizing physically applicable, low order, finite dimensional optimal H_2 and H_∞ controllers with LMI method.
- Comparing the H_2 and H_∞ controllers' noise reduction performances.

2. MODEL OF THE ACOUSTIC DUCT SYSTEM

Here we give the governing equations for an acoustic duct system which includes mean flow of acoustic medium inside. We then use this model for our active noise control study.

2.1. Model Assumptions

Following assumptions are made for the duct model:

- Fluid inside the duct is inviscid.
- There are no dissipative effects and no heat interaction inside the duct.
- The process is adiabatic.
- Duct is rigid walled.
- There is uniform flow of fluid medium with velocity u_0 along the duct axis.
- Acoustic pressure p, density ρ, temperature τ and velocity u changes are small compared to equilibrium pressure P_0, density ρ_0, temperature T_0 and mean flow velocity u_0; so that high order nonlinear effects can be neglected.
- Transverse dimensions of the duct are small compared to acoustic wavelengths considered, i.e., only plane waves inside the duct can progress.
- Gravitational effects inside the duct are neglected.

Rigid walled duct together with inviscid fluid assumption declare that there is no shear force acting on fluid by the walls of the duct. So the plane pressure field does not change along the duct cross section. In other words, acoustic pressure at some axial coordinate x is same throughout the cross sectional plane $y - z$ located at that x coordinate. So, the pressure inside the duct is just a function of axial coordinate x and time, i.e., $p(x,t)$. Rigid walled assumption is encountered in all of our Literature Survey [22–50]. This assumption, also, does not change the mean flow profile, i.e., the flow velocity everywhere in the duct is same as u_0. Since one of our primary goals is to study the effects of flow field on active noise control performance, this simplification

seems quite reasonable.

In this study, we disregard the turbulence and viscosity effects. Turbulence can cause additional sound field in the duct. On the other hand, viscosity makes the acoustic medium dispersive and we should take into account transfer of heat in the duct, which alters our adiabatic process assumption. To cope with this problem, we consider low Mach number flow, i.e., the fluid acts like an ideal gas and there is no turbulence in the duct.

One dimensional duct assumption can be explained as follows: When transverse dimensions of the duct (whether it is rectangular or circular that doesn't matter) is much less than the wavelength of sound, the higher modes other than the plane wave mode quickly vanish below a certain cut-off frequency, which is related to the duct cross-sectional dimensions [52]. So as mentioned previously, the only propagating wave mode along the duct at low frequencies is plane wave mode. We also only concentrate on plane wave mode in this study and choose the transverse dimensions and length of the duct accordingly, for later simulation purposes. All acoustic variables such as particle displacement, density, pressure etc. have constant amplitudes on plane waves [53].

2.2. The Wave Equation

Our acoustic wave propagation equation along the duct is given as;

$$\frac{\partial^2 p}{\partial t^2} + 2u_0 \frac{\partial}{\partial x}\frac{\partial p}{\partial t} + (u_0^2 - c^2)\frac{\partial^2 p}{\partial x^2} = c^2 \left[\frac{\partial[q_s(t)\delta(x - x_s)]}{\partial t} + u_0 \frac{\partial[q_s(t)\delta(x - x_s)]}{\partial x} \right] \quad (2.1)$$

Equation 2.5 can also be written as;

$$\frac{\partial^2 p}{\partial t^2} + 2u_0 \frac{\partial}{\partial x}\frac{\partial p}{\partial t} + (u_0^2 - c^2)\frac{\partial^2 p}{\partial x^2} = c^2 \frac{d}{dt}[q_s(t)\delta(x - x_s)] \quad (2.2)$$

by using the total derivative definition.

The source term has units $\frac{\text{kg}}{\text{m}^3\text{s}}$, indicating mass flow rate per unit volume. Dirac

delta function $\delta(x - x_s)$ has unit m^{-1}, and $q_s(t)$ has unit $\frac{\text{kg}}{\text{m}^2\text{s}}$. Final governing Equation 2.5 and 2.2 are dimensionally consistent.

Our nonhomogeneous one dimensional wave propagation model can be found in [44], [54] and [55].

Homogeneous version of this model can be found in some major references such as [52] and [56].

Please note that, when the medium is stationary, i.e., $u_0 = 0$, then our homogeneous wave model reduces to the well known wave equation in one dimension:

$$\frac{\partial^2 p}{\partial t^2} = c^2 \frac{\partial^2 p}{\partial x^2} \tag{2.3}$$

In this case ($u_0 = 0$) the nonhomogeneous version reduces to:

$$\frac{1}{c^2}\frac{\partial^2 p}{\partial t^2} - \frac{\partial^2 p}{\partial x^2} = \frac{\partial}{\partial t}[q_s(t)\delta(x - x_s)] \tag{2.4}$$

and this can be found in references such as [32], [37] and [57–59].

2.3. The Complete Duct System

Here, we define our duct system completely by indicating initial and boundary conditions.
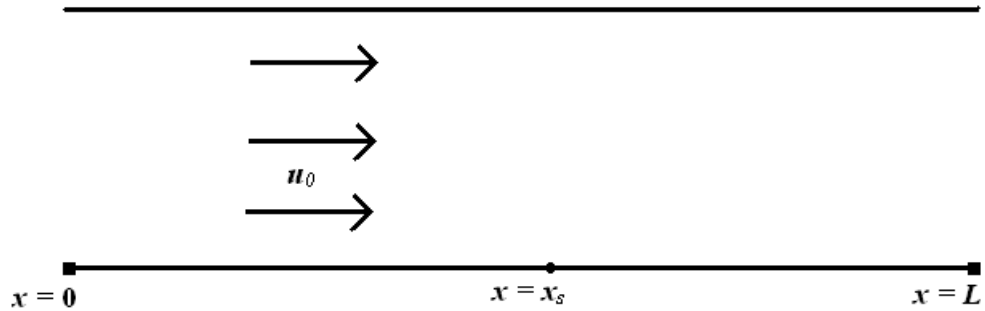
Figure 2.1. Duct system with flow.

Governing partial differential equation (PDE) of the duct system is:

$$\frac{\partial^2 p}{\partial t^2} + 2u_0 \frac{\partial}{\partial x}\frac{\partial p}{\partial t} + (u_0^2 - c^2)\frac{\partial^2 p}{\partial x^2} = c^2 \left[\frac{\partial[q_s(t)\delta(x - x_s)]}{\partial t} + u_0 \frac{\partial[q_s(t)\delta(x - x_s)]}{\partial x} \right] \quad (2.5)$$

Initial conditions of the system are:

$$p(x, 0) \ = \ 0 \quad\quad (2.6)$$

$$\dot{p}(x, 0) = \frac{\partial p(x, 0)}{\partial t} \ = \ 0 \quad\quad (2.7)$$

Boundary conditions of the system are:

$$p(0, t) \ = \ d(t) \quad\quad (2.8)$$

$$-\frac{\partial p(L, t)}{\partial x} \ = \ \rho_0 \left(\frac{\partial u(L, t)}{\partial t} + u_0 \frac{\partial u(L, t)}{\partial x} \right) \quad\quad (2.9)$$

where p is the acoustic pressure, c is the speed of sound, u_0 is the mean flow velocity of the fluid, L is the length of the duct, $d(t)$ is the disturbance coming into the duct, x_s is the point source location in the duct, $q_s(t)$ is the time dependent forcing term of the point mass source, $\delta(x - x_s)$ is the spatial Dirac delta function indicating the application location of forcing input into the system, $u(L, t)$ is the velocity change of fluid particle at $x = L$, ρ_0 is the equilibrium density of fluid particle.

For the purpose of obtaining transfer functions of the system, we have chosen "zero" initial conditions as encountered widely in control theory.

Disturbance to the system is taken as exterior by using the boundary condition at $x = 0$, i.e., $p(0, t) = d(t)$.

Equation 2.9 indicates frequency dependent impedance boundary condition at $x = L$. It represents the fact that momentum equation (Equation 2.10) should be satisfied at $x = L$. Later, in the next chapter, it will be related with the acoustic impedance of the duct end, which states some of the acoustic noise is radiated away

from the duct while the remaining is reflected back into the duct. Momentum equation is given below:

$$-\frac{\partial p}{\partial x} = \rho_0 \left(\frac{\partial u}{\partial t} + u_0 \frac{\partial u}{\partial x} \right) \qquad (2.10)$$

The above system constitutes the most difficult problem of our study. But, we will also give the solutions for simpler problems which are for no flow case and open boundary condition at $x = L$.

3.   SYSTEM TRANSFER FUNCTIONS

3.1. Obtaining Infinite Dimensional Transfer Functions

To obtain the transfer functions of the system, we will apply the classical Laplace transform method encountered in the literature [30, 35-37]. A comprehensive review about the Laplace transform method to solve boundary value PDE problems can be obtained in [60]. Now, we will apply this technique to solve our most complicated problem which has both mean flow of fluid medium and frequency dependent impedance boundary condition. Simpler cases (no flow and/or open BC ($p(L,t) = 0$) cases) can also be solved by the same methodology. Recall that our governing partial differential equation of the system is;

$$\frac{\partial^2 p}{\partial t^2} + 2u_0 \frac{\partial}{\partial x}\frac{\partial p}{\partial t} + (u_0^2 - c^2)\frac{\partial^2 p}{\partial x^2} = c^2 \left[\frac{\partial[q_s(t)\delta(x-x_s)]}{\partial t} + u_0\frac{\partial[q_s(t)\delta(x-x_s)]}{\partial x}\right] \quad (3.1)$$

together with the initial conditions (ICs):

$$p(x,0) \quad = \quad 0 \quad\quad\quad (3.2)$$

$$\dot{p}(x,0) = \frac{\partial p(x,0)}{\partial t} \quad = \quad 0 \quad\quad\quad (3.3)$$

$$q_s(0) \quad = \quad 0 \quad\quad\quad (3.4)$$

and with the boundary conditions (BCs):

$$p(0,t) \quad = \quad d(t) \quad\quad\quad (3.5)$$

$$-\frac{\partial p(L,t)}{\partial x} \quad = \quad \rho_0 \left(\frac{\partial u(L,t)}{\partial t} + u_0\frac{\partial u(L,t)}{\partial x}\right) \quad\quad (3.6)$$

When we take Laplace transform with respect to time to Equation 3.1 we obtain

such an equation in the frequency domain:

$$s^2 P(x,s) - sp(x,0) - \dot{p}(x,0) + 2u_0 \frac{\partial[sP(x,s) - p(x,0)]}{\partial x} + (u_0^2 - c^2)\frac{\partial^2 P(x,s)}{\partial x^2}$$
$$= c^2 \left[[sq(s) - q_s(0)]\delta(x - x_s) + u_0 \frac{\partial[q(s)\delta(x - x_s)]}{\partial x} \right] \quad (3.7)$$

where $P(x,s)$ is the Laplace transform of $p(x,t)$ and $q(s)$ is the Laplace transform of $q_s(t)$. Since; $p(x,0) = 0, \dot{p}(x,0) = 0, q_s(0) = 0$, then Equation 3.7 simplifies to;

$$s^2 P(x,s) + 2u_0 s \frac{\partial P(x,s)}{\partial x} + (u_0^2 - c^2)\frac{\partial^2 P(x,s)}{\partial x^2}$$
$$= c^2 \left[sq(s)\delta(x - x_s) + u_0 q(s)\frac{\partial[\delta(x - x_s)]}{\partial x} \right] \quad (3.8)$$

Please note that Equation 3.8 is an ordinary differential equation (ODE) for variable x and now Laplace variable s and functions of s behave like constants. So we just need to solve ODE in Equation 3.8 in order to get the transfer functions.

When considering $\frac{\partial P(x,s)}{\partial x} = P'(x,s)$ and $\frac{\partial[\delta(x - x_s)]}{\partial x} = \delta'(x - x_s)$; Equation 3.8 can further be simplified as;

$$s^2 P(x,s) + 2u_0 s P'(x,s) + (u_0^2 - c^2)P''(x,s)$$
$$= c^2 \left[sq(s)\delta(x - x_s) + u_0 q(s)\delta'(x - x_s) \right] \quad (3.9)$$

In the same manner, when we take Laplace transform of BCs in Equation 3.5 and 3.6 we obtain;

$$P(0,s) = d(s) \quad (3.10)$$
$$-\frac{\partial P(L,s)}{\partial x} = \rho_0 \left(su(L,s) + u_0 \frac{\partial u(L,s)}{\partial x} \right) \quad (3.11)$$

Now, we will put Equation 3.11 in a more useful form. Define the acoustic

impedance at $x = L$ as;

$$Z_L(s) = \frac{P(L, s)}{u(L, s)} \tag{3.12}$$

Then, putting Equation 3.12 into Equation 3.11 we get;

$$-\frac{\partial P(L, s)}{\partial x} = \rho_0 \left(s \frac{P(L, s)}{Z_L(s)} + \frac{u_0}{Z_L(s)} \frac{\partial P(L, s)}{\partial x} \right) \tag{3.13}$$

Rearranging Equation 3.13 we finally get;

$$P(L, s) = -\left(\frac{Z_L(s)}{\rho_0 s} + \frac{u_0}{s} \right) \frac{\partial P(L, s)}{\partial x} \tag{3.14}$$

$Z_L(s)$ is the frequency dependent specific acoustic impedance of the duct end at $x = L$. $Z_L(s)$ is approximated with a rational transfer function in [39] and below we also derive and use this approximation in detail.

In [61] radiation impedance of the plane circular piston vibrating sinusoidally in the end of a long tube is approximated by the electrical circuit analogy [61] shown below:
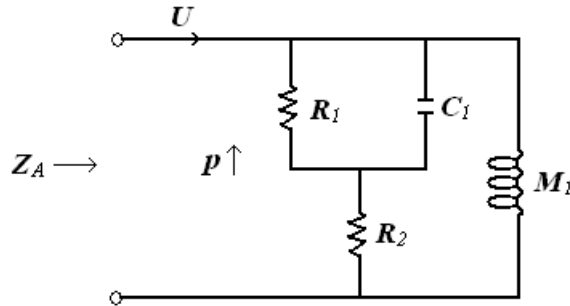
Figure 3.1. Electrical circuit analogy for the duct end impedance.

where $V(t)$ is the fluid velocity, $P(t)$ is the acoustic pressure and R_1, R_2, C_1, M_1 are analogous circuit's resistance, capacitance and inductance type elements. Values of these parameters are given in [61] as;

- $R_2 = \rho_0 c / \pi r^2$
- $R_1 = 0.504 R_2$
- $C_1 = 5.44 r^3 / \rho_0 c^2$
- $M_1 = 0.1952 \rho_0 / r$

where r is the radius of the duct.

These circuit's differential equations are obtained by using the guide in [61] as follows:

$$\frac{dV_m(t)}{dt} = \frac{1}{M_1} P(t) \tag{3.15}$$

$$P(t) = \frac{P_c(t)}{R_1} R_2 + C_1 \frac{dP_c(t)}{dt} R_2 + P_c(t) \tag{3.16}$$

$$V(t) = \frac{P_c(t)}{R_1} + C_1 \frac{dP_c(t)}{dt} + V_m(t) \tag{3.17}$$

where $V_m(t)$ is the inductance current and $P_c(t)$ is the capacitor voltage.

Taking Laplace transform of Equation 3.15, 3.16, 3.17 and rearranging gives the following:

$$\frac{P(s)}{V(s)} = \frac{C_1 R_1 R_2 M_1 s^2 + M_1 s (R_1 + R_2)}{s^2 M_1 C_1 R_1 + (M_1 + C_1 R_1 R_2) s + (R_1 + R_2)} \tag{3.18}$$

In order to obtain specific acoustic impedance, we should multiply Equation 3.18 with cross-sectional area of the duct since $V(t) = \pi r^2 v(t)$ [61] and we get;

$$Z_L(s) = \pi r^2 \frac{C_1 R_1 R_2 M_1 s^2 + M_1 (R_1 + R_2) s}{M_1 C_1 R_1 s^2 + (M_1 + C_1 R_1 R_2) s + (R_1 + R_2)} \tag{3.19}$$

To sum up, we collect our ODE boundary value problem variables below (which are stated in Equation 3.9, 3.10 and 3.14):

$$
\begin{aligned}
s^2 P(x,s) + 2u_0 s P'(x,s) + (u_0^2 - c^2) P''(x,s) &= c^2 \left[sq(s)\delta(x - x_s) + u_0 q(s)\delta'(x - x_s) \right] \\
P(0,s) &= d(s) \\
P(L,s) &= -\left(\frac{Z_L(s)}{\rho_0 s} + \frac{u_0}{s} \right) \frac{\partial P(L,s)}{\partial x}
\end{aligned}
$$

where $Z_L(s)$ is found from Equation 3.19.

Now, Equation 3.9 together with Equation 3.10 and 3.14 form our ODE boundary value problem.

We solve this boundary value problem by using a commercial software and obtain the results shown in oncoming subsections. We once again would like to indicate that Laplace variable s and functions of s alone $(q(s), d(s))$ in Equation 3.9, 3.10, 3.14 and 3.19 behaves like constants and when we solve the ODE with respect to x, they remain same as s and can be directly used in transfer function formulation.

Now, we will obtain the disturbance to $P(x,s)$ and input to $P(x,s)$ transfer functions of the system for open BC, frequency dependent impedance BC and for no flow, mean flow cases. $P(x,s)$ denotes the pressure value observed at any location x in the duct at frequency domain.

3.2. Transfer Functions for Open Boundary Condition

3.2.1. No Flow Case

For obtaining open end duct's transfer functions for no flow case, we will use Equation 3.9 while taking $u_0 = 0$, Equation 3.10 and below open end boundary condi-

tion which is:

$$P(L, s) = 0 \tag{3.20}$$

3.2.1.1. Disturbance to Output Pressure Transfer Function. Solving equation system just mentioned above gives disturbance to output pressure transfer function as:

$$\frac{P(x, s)}{d(s)} = \frac{e^{-\frac{xs}{c}} - e^{-\frac{(2L-x)s}{c}}}{1 - e^{-\frac{2Ls}{c}}} \tag{3.21}$$

3.2.1.2. Input to Output Pressure Transfer Function. Solving equation system at the beginning of this subsection mentioned above gives the input to output pressure transfer function as;

for $x < x_s$

$$\frac{P(x, s)}{q(s)} = \frac{c(1 - e^{-\frac{2xs}{c}})(e^{-\frac{x_s s}{c}} - e^{-\frac{(2L-x_s)s}{c}})}{2e^{-\frac{xs}{c}}(1 - e^{-\frac{2Ls}{c}})} \tag{3.22}$$

for $x \geq x_s$

$$\frac{P(x, s)}{q(s)} = \frac{c\left[(1 - e^{-\frac{2xs}{c}})(e^{-\frac{x_s s}{c}} - e^{-\frac{(2L-x_s)s}{c}}) + (1 - e^{-\frac{2Ls}{c}})(e^{-\frac{(2x-x_s)s}{c}} - e^{-\frac{x_s s}{c}})\right]}{2e^{-\frac{xs}{c}}(1 - e^{-\frac{2Ls}{c}})} \tag{3.23}$$

3.2.2. Mean Flow Case

By solving ODE boundary value problem formed by Equation 3.9, 3.10 and 3.20, we will obtain disturbance to output pressure and input to output pressure transfer functions of the open end duct for mean flow case.

3.2.2.1. Disturbance to Output Pressure Transfer Function.

Disturbance to output pressure transfer function is obtained as:

$$\frac{P(x,s)}{d(s)} = e^{xs\frac{u_0}{c^2-u_0^2}} \frac{e^{-\frac{xs}{c}\frac{c^2}{c^2-u_0^2}} - e^{-\frac{(2L-x)s}{c}\frac{c^2}{c^2-u_0^2}}}{1 - e^{-\frac{2Ls}{c}\frac{c^2}{c^2-u_0^2}}} \tag{3.24}$$

3.2.2.2. Input to Output Pressure Transfer Function.

Input to output pressure transfer function is obtained as:

for $x < x_s$

$$\frac{P(x,s)}{q(s)} = \frac{c^2}{2(c^2-u_0^2)}(a_{12})\left[c(a_4) + u_0(a_5)\right] \tag{3.25}$$

for $x \geq x_s$

$$\frac{P(x,s)}{q(s)} = \frac{c^2}{2(c^2-u_0^2)}(a_{12})\left[c(a_8 + a_9) + u_0(a_{10} - a_{11})\right] \tag{3.26}$$

where,

$$a_1 = \frac{e^{-x_s s\frac{u_0}{c^2-u_0^2}} e^{xs\frac{u_0}{c^2-u_0^2}}}{e^{-\frac{xs}{c}\frac{c^2}{c^2-u_0^2}}}$$

$$a_2 = e^{-\frac{2xs}{c}\frac{c^2}{c^2-u_0^2}}$$

$$a_3 = e^{-\frac{2Ls}{c}\frac{c^2}{c^2-u_0^2}}$$

$$a_4 = e^{-\frac{x_s s}{c}\frac{c^2}{c^2-u_0^2}} - e^{-\frac{(2L-x_s)s}{c}\frac{c^2}{c^2-u_0^2}}$$

$$a_5 = e^{-\frac{x_s s}{c}\frac{c^2}{c^2-u_0^2}} + e^{-\frac{(2L-x_s)s}{c}\frac{c^2}{c^2-u_0^2}}$$

$$a_6 = e^{-\frac{(2x-x_s)s}{c}\frac{c^2}{c^2-u_0^2}} - e^{-\frac{x_s s}{c}\frac{c^2}{c^2-u_0^2}}$$

$$a_7 = e^{-\frac{(2x-x_s)s}{c}\frac{c^2}{c^2-u_0^2}} + e^{-\frac{x_s s}{c}\frac{c^2}{c^2-u_0^2}}$$

$$a_8 = (1 - a_2)(a_4)$$

$$a_9 = (1 - a_3)(a_6)$$

$$a_{10} = (1 - a_2)(a_5)$$
$$a_{11} = (1 - a_3)(a_7)$$
$$a_{12} = \frac{(a_1)(1 - a_2)}{(1 - a_3)}$$

3.3. Transfer Functions for Frequency Dependent Impedance Boundary Condition

3.3.1. No Flow Case

By solving Equation 3.9 while taking $u_0 = 0$, for boundary conditions Equation 3.10 and Equation 3.11, we obtain disturbance to output pressure and input to output pressure transfer functions as below.

3.3.1.1. <u>Disturbance to Output Pressure Transfer Function.</u> Disturbance to output pressure transfer function for frequency dependent impedance boundary condition for no flow case is obtained as:

$$\frac{P(x,s)}{d(s)} = e^{\frac{sx}{c}} \frac{\left[e^{\frac{-2sx}{c}} e^{\frac{2Ls}{c}} c(c\rho_0 + Z_L(s)) + (-c)(c\rho_0 - Z_L(s)) \right]}{\left[e^{\frac{2Ls}{c}} c(c\rho_0 + Z_L(s)) + (-c)(c\rho_0 - Z_L(s)) \right]} \tag{3.27}$$

where $Z_L(s)$ is given by Equation 3.19, ρ_0 is the density of the acoustic medium.

3.3.1.2. <u>Input to Output Pressure Transfer Function.</u> Input to output pressure transfer function for frequency dependent impedance boundary condition for no flow case is obtained as:

for $x < x_s$

$$G_{qPxltxs} = \frac{P(x,s)}{q(s)} = \frac{[(b_1)(b_7) + (b_2)(b_8)]}{2\left[e^{\frac{2Ls}{c}}(b_3) + (b_4)\right]} \tag{3.28}$$

for $x \geq x_s$

$$\frac{P(x,s)}{q(s)} = G_{qPxltxs} + \frac{[(b_9)(b_5) + (b_{10})(b_6)]}{2\left[e^{\frac{2Ls}{c}}b_3 + b_4\right]} \tag{3.29}$$

where,

$$
\begin{aligned}
b_1 &= (c\rho_0 + Z_L(s))c^2 \\
b_2 &= (c\rho_0 - Z_L(s))c^2 \\
b_3 &= (c\rho_0 + Z_L(s))c \\
b_4 &= (c\rho_0 - Z_L(s))(-c) \\
b_5 &= (d_5)c^2 - (d_3)c^2 \\
b_6 &= (d_6)c^2 - (d_2)c^2 \\
b_7 &= d_2 - d_1 \\
b_8 &= d_3 - d_4 \\
b_9 &= (c\rho_0 - Z_L(s)) \\
b_{10} &= (c\rho_0 + Z_L(s)) \\
d_1 &= (a_{13})(a_{15})(a_{17}) \\
d_2 &= (a_{14})(a_{15})(a_{17}) \\
d_3 &= (a_{13})(a_{16}) \\
d_4 &= (a_{14})(a_{16}) \\
d_5 &= (a_{14})(a_{15}) \\
d_6 &= (a_{13})(a_{16})(a_{17})
\end{aligned}
$$

$$a_{13} = e^{\frac{-sx}{c}}$$

$$a_{14} = e^{\frac{sx}{c}}$$

$$a_{15} = e^{\frac{-sx_S}{c}}$$

$$a_{16} = e^{\frac{sx_S}{c}}$$

$$a_{17} = e^{\frac{2Ls}{c}}$$

3.3.2. Mean Flow Case

By solving Equation 3.9 for boundary conditions Equation 3.10 and Equation 3.11, we obtain disturbance to output pressure and input to output pressure transfer functions for mean flow case for frequency dependent impedance boundary condition as below.

3.3.2.1. Disturbance to Output Pressure Transfer Function. Disturbance to output pressure transfer function for frequency dependent impedance boundary condition for mean flow case is obtained as:

$$\frac{P(x,s)}{d(s)} = g_1 \frac{[g_2(c+u_0)(c\rho_0 + Z_L(s)) + (-c+u_0)(c\rho_0 - Z_L(s))]}{[g_3(c+u_0)(c\rho_0 + Z_L(s)) + (-c+u_0)(c\rho_0 - Z_L(s))]} \tag{3.30}$$

where $Z_L(s)$ is given by Equation 3.19, ρ_0 is the density of the acoustic medium, u_0 is the mean flow velocity of medium, c is the speed of sound.

where,

$$g_1 = e^{\frac{sx}{c}\frac{c^2}{c^2-u_0^2}} e^{\frac{sxu_0}{c^2}\frac{c^2}{c^2-u_0^2}}$$

$$g_2 = e^{\frac{-2sx}{c}\frac{c^2}{c^2-u_0^2}} e^{\frac{2Ls}{c}\frac{c^2}{c^2-u_0^2}}$$

$$g_3 = e^{\frac{2Ls}{c}\frac{c^2}{c^2-u_0^2}}$$

3.3.2.2. Input to Output Pressure Transfer Function. Input to output pressure transfer function for frequency dependent impedance boundary condition for mean flow case is obtained as:

for $x < x_s$

$$G_{qPxltxs} = \frac{P(x,s)}{q(s)} = \frac{c^2}{2(c^2 - u_0^2)} \frac{[(h_1)(h_7) + (h_2)(h_8)]}{[(l_7)(h_3) + (h_4)]} \tag{3.31}$$

for $x \geq x_s$

$$\frac{P(x,s)}{q(s)} = G_{qPxltxs} + \frac{c^2}{2(c^2 - u_0^2)} \frac{[(h_9)(h_5) + (h_{10})(h_6)]}{[(l_7)h_3 + h_4]} \tag{3.32}$$

where,

$$
\begin{aligned}
h_1 &= (c\rho_0 + Z_L(s))(c + u_0)^2 \\
h_2 &= (c\rho_0 - Z_L(s))(c - u_0)^2 \\
h_3 &= (c\rho_0 + Z_L(s))(c + u_0) \\
h_4 &= (c\rho_0 - Z_L(s))(-c + u_0)) \\
h_5 &= (k_5)(c^2 - u_0^2) - (k_3)(c - u_0)^2 \\
h_6 &= (k_6)(c^2 - u_0^2) - (k_2)(c + u_0)^2 \\
h_7 &= k_2 - k_1 \\
h_8 &= k_3 - k_4 \\
h_9 &= (c\rho_0 - Z_L(s)) \\
h_{10} &= (c\rho_0 + Z_L(s)) \\
k_1 &= (l_1)(l_3)(l_4)(l_6)(l_7) \\
k_2 &= (l_2)(l_3)(l_4)(l_6)(l_7) \\
k_3 &= (l_1)(l_3)(l_5)(l_6) \\
k_4 &= (l_2)(l_3)(l_5)(l_6)
\end{aligned}
$$

$$k_5 = (l_2)(l_3)(l_4)(l_6)$$

$$k_6 = (l_1)(l_3)(l_5)(l_6)(l_7)$$

$$l_1 = e^{\frac{-sx}{c} \frac{c^2}{(c^2-u_0^2)}}$$

$$l_2 = e^{\frac{sx}{c} \frac{c^2}{(c^2-u_0^2)}}$$

$$l_3 = e^{\frac{sxu_0}{c^2} \frac{c^2}{(c^2-u_0^2)}}$$

$$l_4 = e^{\frac{-sx_s}{c} \frac{c^2}{(c^2-u_0^2)}}$$

$$l_5 = e^{\frac{sx_s}{c} \frac{c^2}{(c^2-u_0^2)}}$$

$$l_6 = e^{\frac{-sx_s u_0}{c^2} \frac{c^2}{(c^2-u_0^2)}}$$

$$l_7 = e^{\frac{2Ls}{c} \frac{c^2}{(c^2-u_0^2)}}$$

3.4. Effects of Mean Flow on System Resonance Frequencies

We can obtain some basic information from open BC solution mentioned above. When considering $P(x,s)/d(s)$ transfer functions for no flow case, Equation 3.21 and mean flow case Equation 3.24 we can see that they have the same form except that the extra $c^2/(c^2 - u_0^2)$ term in each individual exponential term.

This term shifts the resonance frequencies by a factor of $(c^2/(c^2 - u_0^2))^{-1}$. For example, if $c = 340$ m/s and $u_0 = 34$ m/s resonance frequency of the first mode is shifted from 50 Hz to 49.5 Hz. Similarly, if $c = 340$ m/s and $u_0 = 68$ m/s are selected, then the first resonance frequency is predicted at 48 Hz.

Second, third and higher resonance frequencies can also be predicted in the same way since; nth resonance frequency for no flow case occurs at $n \times f$, where f is the first (fundamental) resonance frequency; and nth resonance frequency for mean flow case occurs at $(c^2/(c^2 - u_0^2))^{-1} \times n \times f$.

The same results are observed when considering $P(x,s)/q(s)$ transfer functions for no flow case and mean flow case as well. Again the resonance frequencies are shifted by the factor $(c^2/(c^2 - u_0^2))^{-1}$.

From the results obtained for the ideal situations, we can conclude that we expect a shift in resonance frequency due to flow. The shift, given by the factor $(c^2/(c^2 - u_0^2))^{-1}$ for open BC case, provides a good approximation for resonance frequency shifts encountered in frequency dependent impedance BC case.

Figure 3.2 and 3.3 show this shifting concept for $d(s)$ to $P(x, s)$ transfer function, both for open BC and frequency dependent impedance BC cases, respectively. The parameters in Figure 3.2 and 3.3 are specified as; $c = 340$ m/s, $L = 3.4$ m, $x = 2.8$ m. For comparison, mean flow velocities of fluid (u_0's) are taken as; 0 m/s, 34 m/s and 102 m/s, i.e., effect of mean flow on system resonance frequencies are observed for Mach numbers; 0, 0.1 and 0.3, respectively.

Both in Figure 3.2 and 3.3, shift in resonance frequencies occur according to the discussion mentioned above. In Figure 3.3, it is also observed that, mean flow has a damping effect for frequency dependent impedance BC case.
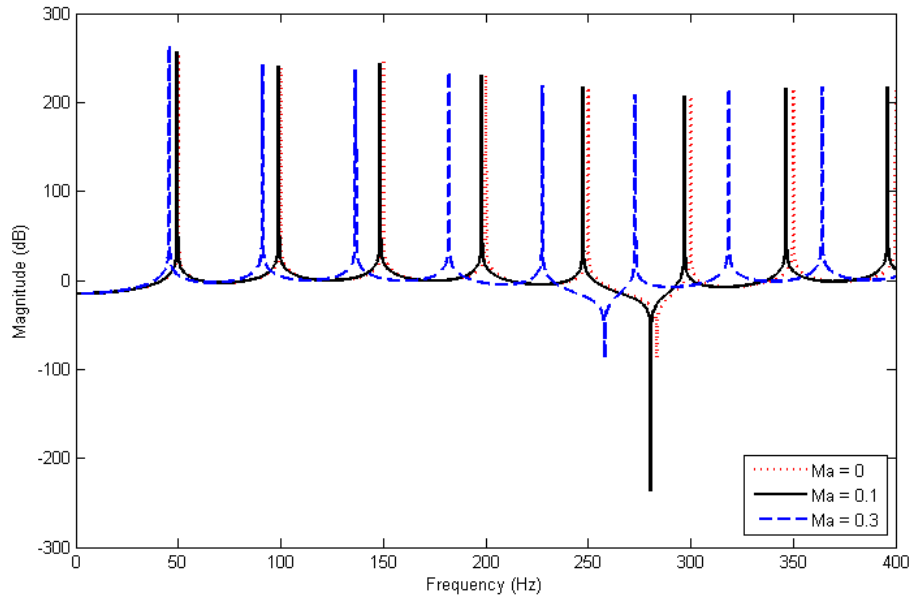
Figure 3.2. Frequency response of $d(s)$ to $P(x, s)$ transfer function for three different Mach numbers for open BC. (red dotted line - $Ma = 0$, black solid line - $Ma = 0.1$, blue dashed line - $Ma = 0.3$).
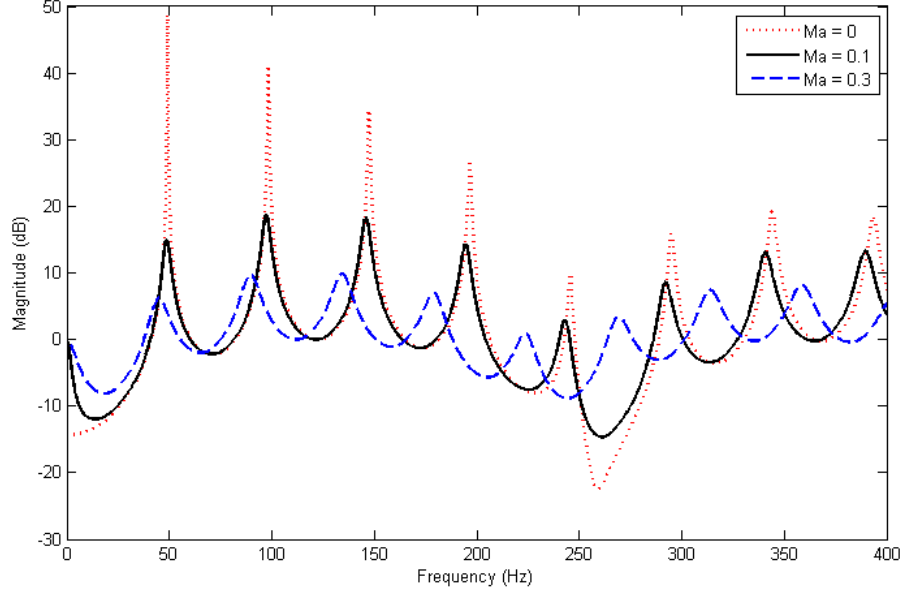
Figure 3.3. Frequency response of $d(s)$ to $P(x, s)$ transfer function for three different Mach numbers for frequency dependent impedance BC. (red dotted line - $Ma = 0$, black solid line - $Ma = 0.1$, blue dashed line - $Ma = 0.3$).

3.5. Final Remarks

In this section, we have given $d(s)$ to $P(x, s)$ and $q(s)$ to $P(x, s)$ transfer functions for; no flow, mean flow cases and for open end, impedance end boundary condition cases.

We observed that, the resonance frequencies of the mean flow case differs from no flow case by a factor $(c^2/(c^2 - u_0^2))^{-1}$ for ideal open BC case. For the frequency dependent impedance BC case, shift in resonance frequencies also occur, but this factor gives an approximate information about the level of shift.

It should once again be emphasized that the transfer functions obtained in this chapter are infinite dimensional. In order to apply finite dimensional linear time invariant control theory to this acoustic problem, these transfer functions should be approximated by proper finite dimensional ones. Then, tools for finite dimensional

linear time invariant (LTI) control theory can be employed to approximated rational transfer functions, in order to solve active noise control problem in our duct system.

4. MICROPHONE AND SOURCE POSITIONING

In this thesis, our primary objective is to synthesize an optimal controller for noise reduction in a duct with mean flow. Our problem is a single input single output (SISO) control problem so that we need an actuator and a sensor. In order to obtain a reliable and satisfactory noise reduction performance, we need to place the sensor (microphone) and the actuator (source) at the right place.

In this chapter, we will determine our source and microphone locations. Results of this chapter will form our basis to approach our ultimate goal "*H_2-H_∞ Optimal Active Noise Controller Synthesis*".

4.1. Physics for Acoustic Duct System

Here, we will formulate how to obtain natural frequencies and node points of an open-open end duct system in which mean flow exists. Thus, when we specify the parameters; speed of sound, length of the duct and mean flow velocity of fluid medium inside the duct; then we can find the resonances and antiresonances of the duct system immediately, thus poles and zeros.

4.1.1. Natural Frequencies of the Duct

Consider an open-open end duct system. In the absence of flow of fluid in the duct, this duct system satisfies the following relationship:

$$\lambda_n = \frac{2L}{n} \tag{4.1}$$

where λ_n is the nth mode wavelength, L is the length of the duct, n is the mode number.

Following equation gives the relationship between wavelength and frequency:

$$c = \lambda f \tag{4.2}$$

From Equation 4.2, we can find the nth natural frequency of the duct (f_n) as;

$$f_n = \frac{cn}{2L} \tag{4.3}$$

where c is the speed of sound.

As mentioned in the previous chapter, existence of mean flow of fluid medium in the duct shifts the poles and zeros of the system by the factor $(c^2 - u_0^2)/c^2$. Thus for mean flow case, we obtain the following relationship for natural frequencies of our duct system:

$$f_n' = \frac{cn}{2L} \left(\frac{c^2 - u_0^2}{c^2} \right) \tag{4.4}$$

So, as an example, for $c = 340$ m/s, $L = 3.4$ m and $u_0 = 34$ m/s; the nth natural frequency of the system is found as;

$$\begin{aligned}
f_n' &= \frac{340 \times n}{2 \times 3.4} \times \frac{340^2 - 34^2}{340^2} \\
&= n \times 50 \times 0.99 \\
&= n \times 49.5
\end{aligned}$$

which is the same result obtained in the previous chapter.

4.1.2. Nodes of the Duct

In the absence of flow, the nodes of an open-open end duct occur at points which satisfy the Equation 4.5. In Figure 4.1, first three modes of an open-open end duct are given.

$$p(x) = sin\left(\frac{n\pi x}{L}\right) = 0 \tag{4.5}$$

where $p(x)$ is the acoustic pressure, n is the mode number, L is the length of the duct and x is the node.
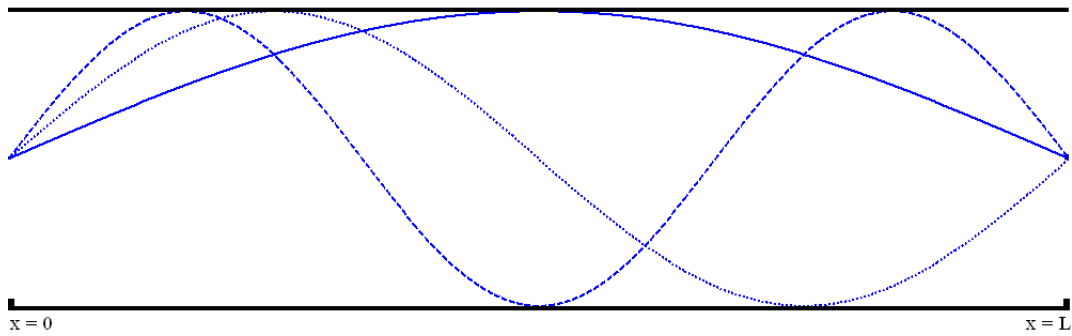
Figure 4.1. First three modes of an open-open end duct. First mode (solid line) - no node inside the duct, second mode (dotted line) - node at $x = L/2$, third mode (dashed line) - nodes at $x = L/3$ and $x = 2L/3$.

Nodes are the locations where the pressure is "zero" inside the duct. So, if we put our microphone or source on a node we can not measure or create a sound pressure from that point at a specific frequency and its harmonics.

We can formulate that at which frequency we can not measure and create a sound pressure in a duct for a given measuring and actuating point as follows:

Suppose we have an open-open end duct with length L in the absence of fluid flow. Assume our microphone is located at x_m and our source is located at x_s inside

the duct.

The frequency f_m at which microphone located at x_m measures zero pressure is found from Equation 4.2 as;

$$c = 2|x - x_m|f_m \tag{4.6}$$

where x is the duct end closest to the x_m. So f_m becomes;

$$f_m = \frac{c}{2(L - x_m)} \qquad \text{if } x_m \text{ is closer to the duct end } (x = L) \tag{4.7}$$

$$f_m = \frac{c}{2x_m} \qquad \text{if } x_m \text{ is closer to the duct end } (x = 0) \tag{4.8}$$

Same formulations are valid for the frequency f_s at which source at x_s creates zero pressure:

$$f_s = \frac{c}{2(L - x_s)} \qquad \text{if } x_s \text{ is closer to the duct end } (x = L) \tag{4.9}$$

$$f_s = \frac{c}{2x_s} \qquad \text{if } x_s \text{ is closer to the duct end } (x = 0) \tag{4.10}$$

If both source and microphone exist inside the open-open end duct, following procedure for determining zeros is applied:

- Firstly, the zeros of the device (microphone/loudspeaker) which is closest to one of the ends are determined.
- Then, the zeros of the other device (loudspeaker/microphone) are determined with respect to the other end.

For the mean flow case, we need to multiply these two frequency values with shifting factor $(c^2 - u_0^2)/c^2$ as is done for the natural frequencies. Thus, zero pressure

frequencies for mean flow case f'_m and f'_s become:

$$f'_m = \frac{c}{2(L - x_m)} \frac{c^2 - u_0^2}{c^2} \qquad \text{if } x_m \text{ is closer to the duct end } (x = L) \quad (4.11)$$

$$f'_m = \frac{c}{2x_m} \frac{c^2 - u_0^2}{c^2} \qquad \text{if } x_m \text{ is closer to the duct end } (x = 0) \quad (4.12)$$

and,

$$f'_s = \frac{c}{2(L - x_s)} \frac{c^2 - u_0^2}{c^2} \qquad \text{if } x_s \text{ is closer to the duct end } (x = L) \quad (4.13)$$

$$f'_s = \frac{c}{2x_s} \frac{c^2 - u_0^2}{c^2} \qquad \text{if } x_s \text{ is closer to the duct end } (x = 0) \quad (4.14)$$

Consider the following numerical example. Assume that there is no mean flow inside the duct, $c = 340$ m/s and $L = 3.4$ m. Suppose we put our microphone at $x_m = 2.8$ m. Then;

$$c = \lambda f$$
$$340 = 2(3.4 - 2.8)f_m$$
$$f_m = 283.3 \text{ Hz}$$

Thus, for $x_m = 2.8$ m we measure the pressure value as "zero" at $f_m = 283.3$ Hz and at its harmonics.

Similarly, if we put our source at $x_s = 1.6$ m, then;

$$340 = 2 \times 1.6 \times f_s$$
$$f_s = 106.2 \text{ Hz}$$

So, at $f_s = 106.2$ Hz and its harmonics we can not create a sound pressure value.

Please note that calculations for nodal frequencies are done for the distance nearest to the one of the duct ends.

These two calculated values of f_m and f_s are for no flow case. For mean flow case results, all we have to do is to multiply these frequency values with the shifting factor $(c^2 - u_0^2)/c^2$. Thus for $u_0 = 34$ m/s corresponding mean flow frequencies become;

$$
\begin{aligned}
f'_m &= 0.99 \times f_m \\
&= 0.99 \times 283.3 \\
&= 280.5 \text{ Hz} \\
f'_s &= 0.99 \times f_s \\
&= 0.99 \times 106.2 \\
&= 105.2 \text{ Hz}
\end{aligned}
$$

Therefore, for mean flow case at $f'_m = 280.5$ Hz and at its harmonics, we measure the acoustic response as "zero" and at $f'_s = 105.2$ Hz and at its harmonics, we create "zero" acoustic pressure.

The results for this ideal open-open BCs will provide us basic knowledge for determining microphone and source locations inside the duct.

4.2. Microphone and Source Locations

4.2.1. Proposed Duct System

As mentioned before, our ultimate goal is to synthesize an optimal controller in order to suppress unwanted noise in the low frequency range. For our duct system, we specify the parameters as below. However, one can choose a different set of parameters.

- $c = 340$ m/s

- $u_0 = 34$ m/s
- $L = 3.4$ m

So, duct resonance frequencies occur nearly at:

$$f_n = nf \frac{c^2 - u_0^2}{c^2} \qquad \text{for } n = 1, 2, ...$$

where $f = c/(2L)$. So f_n becomes;

$$
\begin{aligned}
f_n &= n \times 50 \times \frac{340^2 - 34^2}{340^2} \\
f_n &= 49.5n \qquad \text{for } n = 1, 2, ...
\end{aligned}
$$

Please note that we have already calculated this value for resonance frequency in the previous section.

We choose our target low frequency noise reduction range as $0 - 250$ Hz, i.e., we want to suppress noise levels up to the first five modes of the duct by using Active Noise Controller.

Finally, we use a feedback configuration as shown in Figure 4.2 below. We select $x_m > x_s$, since; source input can travel on both direction to the duct ends and if we place microphone in the duct as $x_m < x_s$, this would cause instability. For the $x_m < x_s$ configuration, a wrong signal is fed to the controller, since we want to attenuate noise at duct end at $x = L$, not the other end. Whereas if we place our microphone at $x_m > x_s$, we can measure noise levels near the target duct end and give appropriate input to suppress unwanted noise.

In the configuration shown in Figure 4.2, microphone placed at x_m measures the acoustic pressure value at x_m and sends it to controller. The controller uses this value $P(x_m, s)$ as input and calculates proper $q(s)$ value to suppress noise resulting from $d(s)$.
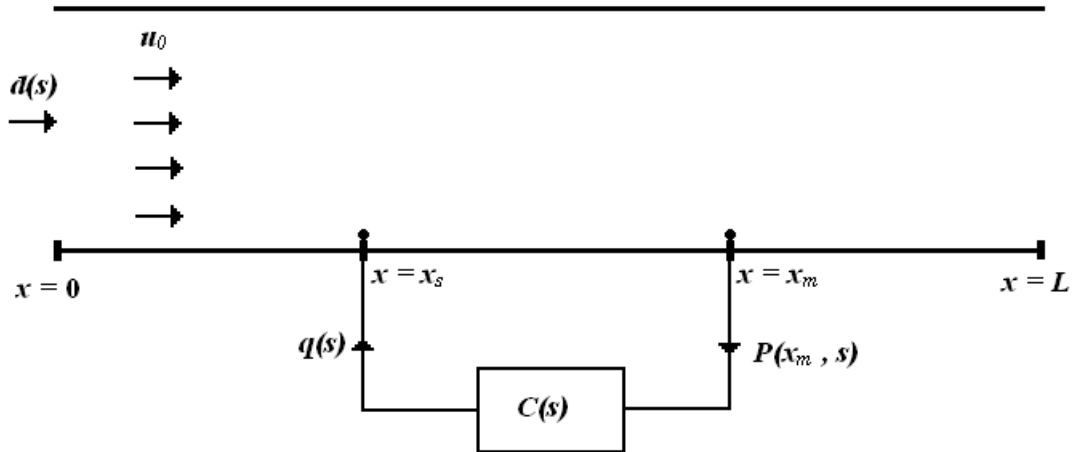
Figure 4.2. Feedback design for ANC in duct

Now, with the parameters specified above, we are ready to discuss the microphone and source locations inside this duct system.

4.2.2. Microphone Location

Since we want to suppress the noise levels up to the first five modes of the duct, we should better to choose a microphone point that has no zeros for $P(x_m, s)/d(s)$ and $P(x_m, s)/q(s)$ transfer functions at the target frequency range $0 - 250$ Hz. Since at zeros; we measure the pressure value as "zero" so we can not create a canceling signal because measured pressure is used as input for our controller.

In mean flow case, for 250 Hz, "zero pressure" point inside the duct can be found for open-open end case by using Equation 4.11 and 4.12 as:

$$250 = \frac{340}{2 \times x_{m1}} \times \frac{340^2 - 34^2}{340^2}$$
$$x_{m1} = 0.67 \text{ m}$$

and,

$$250 = \frac{340}{2 \times (3.4 - x_{m2})} \times \frac{340^2 - 34^2}{340^2}$$

$$x_{m2} = 2.73 \text{ m}$$

Therefore, if we place our measuring point well away at:

$$x_m < 0.67 \text{ m} \qquad (4.15)$$

or,

$$x_m > 2.73 \text{ m} \qquad (4.16)$$

then, we can guarantee that no zeros will occur within our frequency range.

4.2.3. Source Location

As was done in previous section "zero pressure" point for source is calculated for open-open end case from Equation 4.13 and 4.14, for 250 Hz, as:

$$250 = \frac{340}{2 \times x_{s1}} \times \frac{340^2 - 34^2}{340^2}$$

$$x_{s1} = 0.67 \text{ m}$$

and,

$$250 = \frac{340}{2 \times (3.4 - x_{s2})} \times \frac{340^2 - 34^2}{340^2}$$

$$x_{s2} = 2.73 \text{ m}$$

Therefore, if we place our actuating (source) point well away at:

$$x_s < 0.67 \text{ m} \tag{4.17}$$

or,

$$x_s > 2.73 \text{ m} \tag{4.18}$$

then, depending on x_m location, we can avoid the zeros in input to output transfer function which caused by source location.

4.3. Final Duct Configuration for ANC

Here, we describe our complete duct configuration for Active Noise Control (ANC). In the remaining chapters, we will approximate the system transfer functions and synthesize our controllers by using this duct configuration.

We have already determined the parameters, microphone-source configuration and target frequency range, before. Below is the list of parameters:

- speed of sound: $c = 340$ m/s
- mean flow velocity of fluid: $u_0 = 34$ m/s
- length of the duct: $L = 3.4$ m
- target frequency range: $0 - 250$ Hz
- sensor-actuator configuration: $x_m > x_s$

Therefore, we are just left with the exact locations of microphone and source in the duct.

As discussed in "Microphone and Source Locations" section we have found that,

location of microphone should be at:

$$x_m < 0.67 \, \text{m} \quad \text{or} \quad x_m > 2.73 \, \text{m}$$

and, location of source should be at:

$$x_s < 0.67 \, \text{m} \quad \text{or} \quad x_s > 2.73 \, \text{m}$$

For our duct system we have decided that its better to configure microphone-source positioning as $x_m > x_s$. So, above inequalities simplifies to:

$$x_m > 2.73 \, \text{m} \quad \text{and} \quad x_s < 0.67 \, \text{m} \tag{4.19}$$

since, when x_m is closer to the duct end $x = L$, x_s is determined according to Equation 4.14.

Choosing $x_m = 2.8$ m and $x_s = 0.6$ m satisfies Equation 4.19 and finalize our duct system parameters. Here, we choose a symmetric configuration in order to obtain zero information for both source and microphone at the same point. Even we have no zeros at the target frequency range, by choosing a symmetric configuration we get rid of possible uncertain side effects of antisymmetric configuration. By this design, we have captured all the poles in our frequency range and got rid of all the zeros.

5.   OPTIMAL CONTROLLER DESIGNS

System transfer functions obtained in Chapter 3 are infinite dimensional. In order to apply LTI finite dimensional control theory, we need finite dimensional transfer functions which represent the system. In Chapter 6, we will present some approximating schemes utilizing linear least squares in our case studies. We postpone the approximation subject to Chapter 6, and throughout this chapter we assume that we have low order, finite dimensional, real, rational, strictly proper transfer function approximations representing the real system transfer functions. To sum up, throughout this chapter, the transfer functions used in finite dimensional control theory derivations are approximated finite dimensional system transfer functions.

In this chapter, following the discussions made in previous chapters, we will synthesize H_2 and H_∞ optimal controllers to achieve noise reduction at the end of the duct. We will apply linear time invariant (LTI) finite dimensional control theory to approximated low order, finite dimensional, real, rational, strictly proper transfer functions of our acoustic duct system in order to get H_2 and H_∞ controller designs. We will begin this chapter with describing control problem formulation, continue with state space representations of plant and closed loop system, finally conclude with controller designs.

5.1. Control Problem Formulation

In Figure 4.2 we show our proposed duct system. Here, we formulate our control problem:

The transfer function that relates disturbance $(d(s))$ to pressure at a point x inside the duct $(P(x, s))$ is given by:

$$G_d(x, s) = \frac{P(x, s)}{d(s)} \tag{5.1}$$

and, the transfer function that relates control input $(q(s))$ to pressure at a point x inside the duct $(P(x, s))$ is given by:

$$G_q(x, s) = \frac{P(x, s)}{q(s)} \tag{5.2}$$

Then, the total pressure at a point x inside the duct resulting from both disturbance and control input is found by:

$$P(x, s) = G_d(x, s)d(s) + G_q(x, s)q(s) \tag{5.3}$$

As can be seen from Figure 4.2 , our control input is:

$$q(s) = C(s)P(x_m, s) \tag{5.4}$$

where $C(s)$ is the controller transfer function, $P(x_m, s)$ is the measured pressure value by microphone at sensing point.

When we put Equation 5.4 in Equation 5.3 we get;

$$P(x, s) = G_d(x, s)d(s) + G_q(x, s)C(s)P(x_m, s) \tag{5.5}$$

$P(x_m, s)$ is calculated by using x_m instead of x in Equation 5.3:

$$P(x_m, s) = G_d(x_m, s)d(s) + G_q(x_m, s)q(s) \tag{5.6}$$

In the configuration shown in Figure 4.2, microphone located at x_m measures the acoustic pressure $P(x_m)$ at that point, and sends this information to controller. Our controller uses this signal and calculates a proper input, which is fed to the system in order to suppress the unwanted sound downstream of the duct.

Equation 5.3, 5.4 and 5.6 can be formulated as a disturbance attenuation problem shown in Figure 5.1.
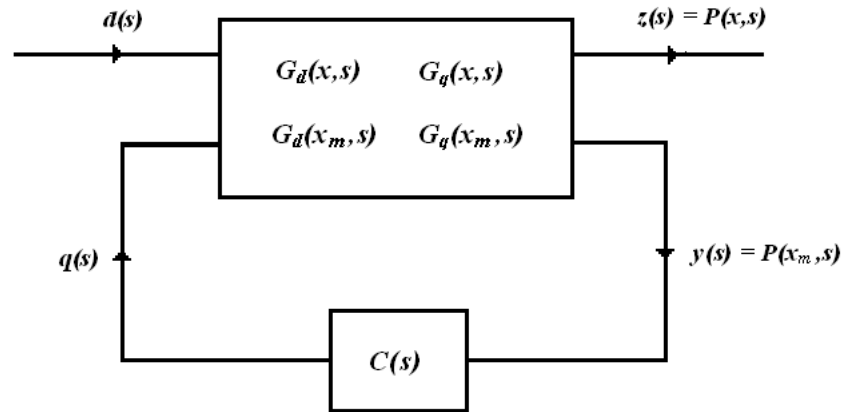
Figure 5.1. Disturbance attenuation problem.

Using Equation 5.4 in Equation 5.6 results in;

$$P(x_m, s) = G_d(x_m, s)d(s) + G_q(x_m, s)C(s)P(x_m, s)$$

$$(1 - G_q(x_m, s)C(s))\,P(x_m, s) = G_d(x_m, s)d(s)$$

$$P(x_m, s) = \frac{G_d(x_m, s)}{1 - G_q(x_m, s)C(s)}d(s) \tag{5.7}$$

Equation 5.7 gives the closed loop system between $P(x_m, s)$ and $d(s)$. Note that, as we have a SISO system, in Equation 5.7, we can use $[1 - G_q(x_m, s)C(s)]$ instead of $[I - G_q(x_m, s)C(s)]$ and conduct a simple division operation to get $P(x_m, s)$. Figure 5.2 shows it in block diagram form.
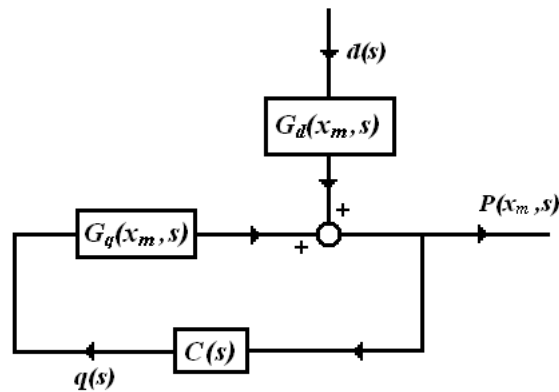
Figure 5.2. Closed loop system between $P(x_m, s)$ and $d(s)$.

When we put Equation 5.7 in Equation 5.5 we get;

$$\frac{P(x,s)}{d(s)} = G_d(x,s) + G_q(x,s)C(s)\frac{G_d(x_m,s)}{1 - G_q(x_m,s)C(s)} \tag{5.8}$$

Equation 5.8 shows the closed loop system between $P(x,s)$ and $d(s)$. Figure 5.3 shows it in block diagram form.
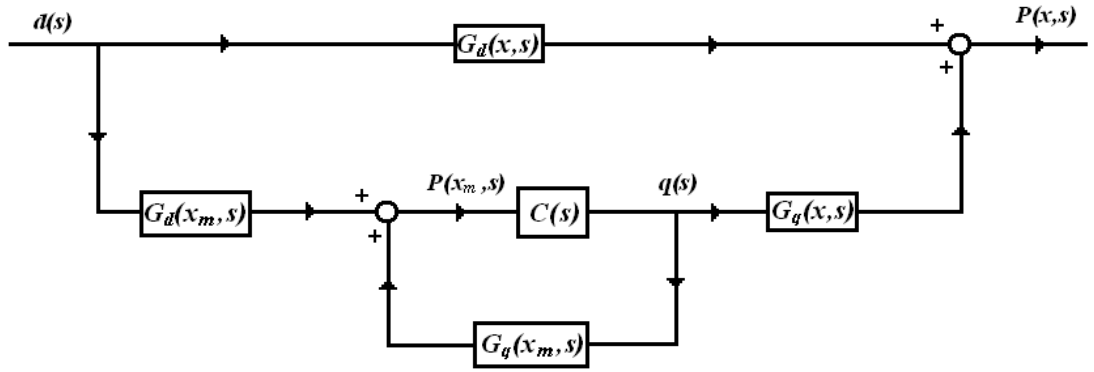
Figure 5.3. Closed loop system between $P(x,s)$ and $d(s)$.

In H_2-design; our task is to synthesize an optimal controller $C(s)$ in order to minimize H_2 norm of closed loop system ($\|P(x,s)/d(s)\|_2$) while maintaining closed loop stability.

In H_∞-design; our task is to synthesize an optimal controller $C(s)$ in order to minimize H_∞ norm of closed loop system ($\|P(x,s)/d(s)\|_\infty$) while maintaining closed loop stability.

Now, we will obtain the required state space descriptions for controller synthesis, in the next section.

5.2. State Space Representations

5.2.1. State Space Description of Plant

Here, we derive the state space description of our plant. In Figure 5.4, general form of our plant can be seen.

Figure 5.4. General plant form.

It has two inputs (d and q) and two outputs (z and y) described before. The relationship between d, q, z and y are;

$$z = G_{dz}d + G_{qz}q \tag{5.9}$$

$$y = G_{dy}d + G_{qy}q \tag{5.10}$$

where $G_{dz}(s)$ is finite dimensional approximation of d to z transfer function, $G_{qz}(s)$ is finite dimensional approximation of q to z transfer function, $G_{dy}(s)$ is finite dimensional approximation of d to y transfer function, $G_{qy}(s)$ is finite dimensional approximation of q to y transfer function.

Since we have finite dimensional transfer functions G_{dz}, G_{qz}, G_{dy} and G_{qy}; we can obtain their state space matrices as;

$$G_{dz}(s) = \mathbf{C_{dz}}(s\mathbf{I} - \mathbf{A_{dz}})^{-1}\mathbf{B_{dz}} \tag{5.11}$$

$$G_{qz}(s) = \mathbf{C_{qz}}(s\mathbf{I} - \mathbf{A_{qz}})^{-1}\mathbf{B_{qz}} \tag{5.12}$$

$$G_{dy}(s) = \mathbf{C_{dy}}(s\mathbf{I} - \mathbf{A_{dy}})^{-1}\mathbf{B_{dy}} \tag{5.13}$$

$$G_{qy}(s) = \mathbf{C_{qy}}(s\mathbf{I} - \mathbf{A_{qy}})^{-1}\mathbf{B_{qy}} \tag{5.14}$$

where $\mathbf{A}$, $\mathbf{B}$ and $\mathbf{C}$ are the corresponding state space matrices.

Writing state space descriptions explicitly, we have;

$$\dot{\mathbf{x}}_{\mathbf{dz}} = \mathbf{A}_{\mathbf{dz}}\mathbf{x}_{\mathbf{dz}} + \mathbf{B}_{\mathbf{dz}}d \tag{5.15}$$

$$y_{dz} = \mathbf{C}_{\mathbf{dz}}\mathbf{x}_{\mathbf{dz}} \tag{5.16}$$

$$\dot{\mathbf{x}}_{\mathbf{qz}} = \mathbf{A}_{\mathbf{qz}}\mathbf{x}_{\mathbf{qz}} + \mathbf{B}_{\mathbf{qz}}q \tag{5.17}$$

$$y_{qz} = \mathbf{C}_{\mathbf{qz}}\mathbf{x}_{\mathbf{qz}} \tag{5.18}$$

$$\dot{\mathbf{x}}_{\mathbf{dy}} = \mathbf{A}_{\mathbf{dy}}\mathbf{x}_{\mathbf{dy}} + \mathbf{B}_{\mathbf{dy}}q \tag{5.19}$$

$$y_{dy} = \mathbf{C}_{\mathbf{dy}}\mathbf{x}_{\mathbf{dy}} \tag{5.20}$$

$$\dot{\mathbf{x}}_{\mathbf{qy}} = \mathbf{A}_{\mathbf{qy}}\mathbf{x}_{\mathbf{qy}} + \mathbf{B}_{\mathbf{qy}}q \tag{5.21}$$

$$y_{qy} = \mathbf{C}_{\mathbf{qy}}\mathbf{x}_{\mathbf{qy}} \tag{5.22}$$

where $\mathbf{x}_{\mathbf{dz}}$, $\mathbf{x}_{\mathbf{qz}}$, $\mathbf{x}_{\mathbf{dy}}$, $\mathbf{x}_{\mathbf{qy}}$ are the corresponding state vectors, y_{dz}, y_{qz}, y_{dy}, y_{qy} are the corresponding outputs.

From Equation 5.9 and 5.10 we have;

$$z = y_{dz} + y_{qz} = \mathbf{C}_{\mathbf{dz}}\mathbf{x}_{\mathbf{dz}} + \mathbf{C}_{\mathbf{qz}}\mathbf{x}_{\mathbf{qz}} \tag{5.23}$$

$$y = y_{dy} + y_{qy} = \mathbf{C}_{\mathbf{dy}}\mathbf{x}_{\mathbf{dy}} + \mathbf{C}_{\mathbf{qy}}\mathbf{x}_{\mathbf{qy}} \tag{5.24}$$

Constructing our plant with Equation 5.15, 5.17, 5.19, 5.21, 5.23 and 5.24 we get;

$$\dot{\mathbf{x}}_{\mathbf{pl}} = \mathbf{A}\mathbf{x}_{\mathbf{pl}} + \mathbf{B}\mathbf{u} \tag{5.25}$$

$$\tilde{\mathbf{y}} = \mathbf{C}\mathbf{x}_{\mathbf{pl}} \tag{5.26}$$

where,

$$
\mathbf{x_{pl}} = \begin{bmatrix} \mathbf{x_{dz}} \\ \mathbf{x_{qz}} \\ \mathbf{x_{dy}} \\ \mathbf{x_{qy}} \end{bmatrix}, \quad \dot{\mathbf{x}}_{pl} = \begin{bmatrix} \dot{\mathbf{x}}_{dz} \\ \dot{\mathbf{x}}_{qz} \\ \dot{\mathbf{x}}_{dy} \\ \dot{\mathbf{x}}_{qy} \end{bmatrix}, \quad \tilde{\mathbf{y}} = \begin{bmatrix} z \\ y \end{bmatrix}, \quad \mathbf{u} = \begin{bmatrix} d \\ q \end{bmatrix}
$$

and,

$$
\mathbf{A} = \begin{bmatrix} \mathbf{A_{dz}} & 0 & 0 & 0 \\ 0 & \mathbf{A_{qz}} & 0 & 0 \\ 0 & 0 & \mathbf{A_{dy}} & 0 \\ 0 & 0 & 0 & \mathbf{A_{qy}} \end{bmatrix}, \quad \mathbf{B} = \begin{bmatrix} \mathbf{B_{dz}} & 0 \\ 0 & \mathbf{B_{qz}} \\ \mathbf{B_{dy}} & 0 \\ 0 & \mathbf{B_{qy}} \end{bmatrix}, \quad \mathbf{C} = \begin{bmatrix} \mathbf{C_{dz}} & \mathbf{C_{qz}} & 0 & 0 \\ 0 & 0 & \mathbf{C_{dy}} & \mathbf{C_{qy}} \end{bmatrix}
$$

Equation 5.25 and 5.26 form our plant's state space description. In Figure 5.5, we can see these in a block diagram form. Our approximated transfer functions are strictly proper. Thus, we do not have any $\mathbf{D}$ matrix. $\mathbf{0}$'s that are found in matrices mentioned above have the proper dimensions consistent with dimensions of $\mathbf{A}$, $\mathbf{B}$, $\mathbf{C}$ matrices as well.
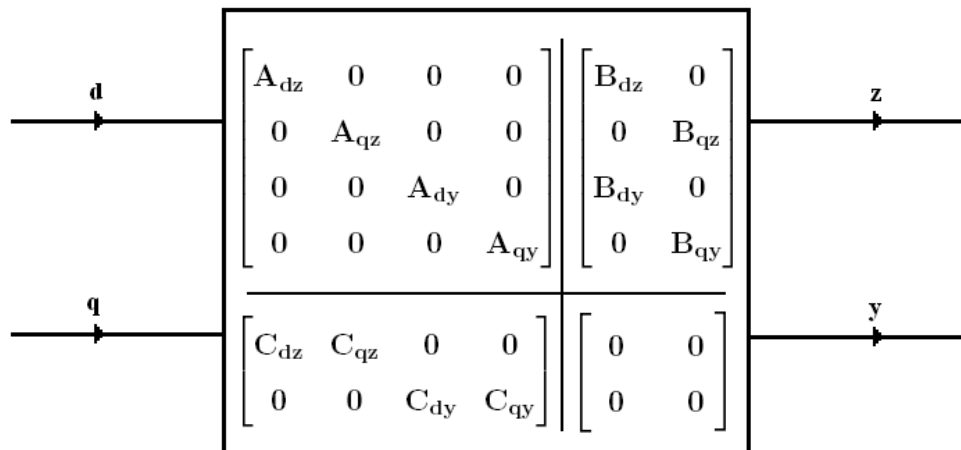
Figure 5.5. State space description of the plant.

In Figure 5.6 we have a more compact form for plant state space description:
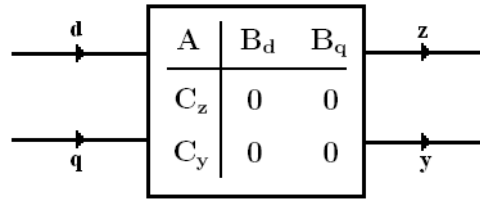
Figure 5.6. Compact form of plant state space description.

where,

$$
\mathbf{A} = \begin{bmatrix} \mathbf{A_{dz}} & \mathbf{0} & \mathbf{0} & \mathbf{0} \\ \mathbf{0} & \mathbf{A_{qz}} & \mathbf{0} & \mathbf{0} \\ \mathbf{0} & \mathbf{0} & \mathbf{A_{dy}} & \mathbf{0} \\ \mathbf{0} & \mathbf{0} & \mathbf{0} & \mathbf{A_{qy}} \end{bmatrix}, \quad \mathbf{B_d} = \begin{bmatrix} \mathbf{B_{dz}} \\ \mathbf{0} \\ \mathbf{B_{dy}} \\ \mathbf{0} \end{bmatrix}, \quad \mathbf{B_q} = \begin{bmatrix} \mathbf{0} \\ \mathbf{B_{qz}} \\ \mathbf{0} \\ \mathbf{B_{qy}} \end{bmatrix},
$$

$$
\mathbf{C_z} = \begin{bmatrix} \mathbf{C_{dz}} & \mathbf{C_{qz}} & \mathbf{0} & \mathbf{0} \end{bmatrix}, \quad \mathbf{C_y} = \begin{bmatrix} \mathbf{0} & \mathbf{0} & \mathbf{C_{dy}} & \mathbf{C_{qy}} \end{bmatrix}
$$

5.2.2. State Space Description of Closed Loop System

When we close the loop between y and q with a controller, we get the following configuration shown in Figure 5.7.
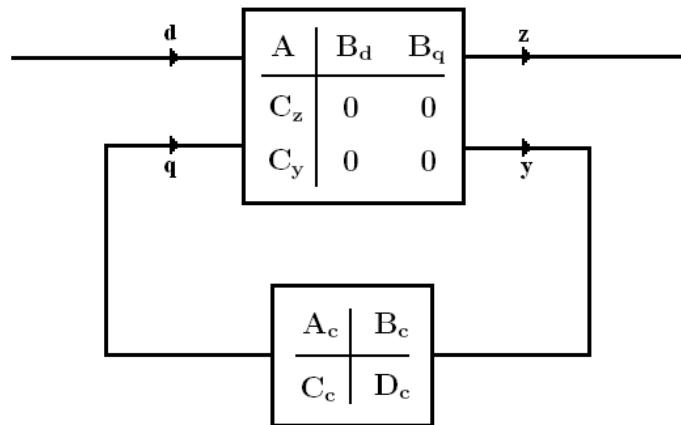
Figure 5.7. Closed loop system.

For plant;

$$\dot{\mathbf{x}}_{\mathbf{pl}} = \mathbf{A}\mathbf{x}_{\mathbf{pl}} + \mathbf{B}_{\mathbf{d}}d + \mathbf{B}_{\mathbf{q}}q \tag{5.27}$$

$$z = \mathbf{C}_{\mathbf{z}}\mathbf{x}_{\mathbf{pl}} \tag{5.28}$$

$$y = \mathbf{C}_{\mathbf{y}}\mathbf{x}_{\mathbf{pl}} \tag{5.29}$$

For controller;

$$\dot{\mathbf{x}}_{\mathbf{c}} = \mathbf{A}_{\mathbf{c}}\mathbf{x}_{\mathbf{c}} + \mathbf{B}_{\mathbf{c}}y \tag{5.30}$$

$$q = \mathbf{C}_{\mathbf{c}}\mathbf{x}_{\mathbf{c}} + \mathbf{D}_{\mathbf{c}}y \tag{5.31}$$

Combining Equation 5.27-5.31 together in which state space descriptions of plant and controller are given, we get;

$$\dot{\mathbf{x}}_{\mathbf{pl}} = (\mathbf{A} + \mathbf{B}_{\mathbf{q}}\mathbf{D}_{\mathbf{c}}\mathbf{C}_{\mathbf{y}})\mathbf{x}_{\mathbf{pl}} + (\mathbf{B}_{\mathbf{q}}\mathbf{C}_{\mathbf{c}})\mathbf{x}_{\mathbf{c}} + \mathbf{B}_{\mathbf{d}}d \tag{5.32}$$

$$\dot{\mathbf{x}}_{\mathbf{c}} = (\mathbf{B}_{\mathbf{c}}\mathbf{C}_{\mathbf{y}})\mathbf{x}_{\mathbf{pl}} + \mathbf{A}_{\mathbf{c}}\mathbf{x}_{\mathbf{c}} \tag{5.33}$$

$$z = \mathbf{C}_{\mathbf{z}}\mathbf{x}_{\mathbf{pl}} \tag{5.34}$$

where $\mathbf{x}_{\mathbf{pl}}$ is the state vector for plant, $\mathbf{x}_{\mathbf{c}}$ is the state vector for controller.

Equation 5.32-5.34 can be written in matrix form as follows:

$$\dot{\tilde{\mathbf{x}}} = \begin{bmatrix} \dot{\mathbf{x}}_{\mathbf{pl}} \\ \dot{\mathbf{x}}_{\mathbf{c}} \end{bmatrix} = \begin{bmatrix} \mathbf{A} + \mathbf{B}_{\mathbf{q}}\mathbf{D}_{\mathbf{c}}\mathbf{C}_{\mathbf{y}} & \mathbf{B}_{\mathbf{q}}\mathbf{C}_{\mathbf{c}} \\ \mathbf{B}_{\mathbf{c}}\mathbf{C}_{\mathbf{y}} & \mathbf{A}_{\mathbf{c}} \end{bmatrix} \tilde{\mathbf{x}} + \begin{bmatrix} \mathbf{B}_{\mathbf{d}} \\ \mathbf{0} \end{bmatrix} d \tag{5.35}$$

$$z = \begin{bmatrix} \mathbf{C}_{\mathbf{z}} & \mathbf{0} \end{bmatrix} \tilde{\mathbf{x}} \tag{5.36}$$

where $\tilde{\mathbf{x}}$ is the closed loop transfer function's state vector.

Equation 5.35 and 5.36 form the state space description of the closed loop transfer

function between d to z. In Figure 5.8 it can be seen in a block diagram form.
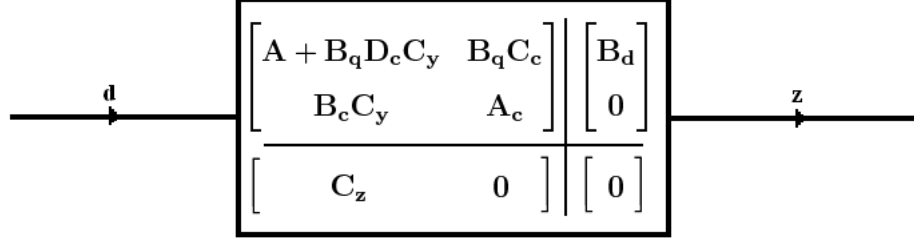
Figure 5.8. State space representation of closed loop transfer function.

5.3. Controller Designs

Since we have obtained our closed loop transfer function form in Equation 5.35 and 5.36, now our task is to find $\mathbf{A_c}$, $\mathbf{B_c}$, $\mathbf{C_c}$, $\mathbf{D_c}$ matrices which provide disturbance attenuation while maintaining closed loop stability. In this section, we give linear matrix inequalities (LMI) formulations for H_2 and H_∞ optimal controller designs.

5.3.1. LMI Formulation for H_2 Optimal Controller

Below, we give our LMI formulation for H_2 optimal controller synthesis.

$$trace(\mathbf{\Lambda}) < \gamma^2 \tag{5.37}$$

$$\begin{pmatrix} \mathbf{E_1} & \mathbf{E_2} & \mathbf{B_d} \\ \mathbf{E_2^T} & \mathbf{E_3} & \mathbf{XB_d} \\ \mathbf{B_d^T} & \mathbf{B_d^TX} & -\mathbf{I} \end{pmatrix} < 0 \tag{5.38}$$

$$\begin{pmatrix} \mathbf{\Lambda} & \mathbf{C_zY} & \mathbf{C_z} \\ \mathbf{YC_z^T} & \mathbf{Y} & \mathbf{I} \\ \mathbf{C_z^T} & \mathbf{I} & \mathbf{X} \end{pmatrix} > 0 \tag{5.39}$$

where,

$$\mathbf{E_1} \quad = \quad \mathbf{AY} + \mathbf{B_q}\mathbf{K} + \mathbf{YA^T} + \mathbf{K^T}\mathbf{B_q^T} \tag{5.40}$$

$$\mathbf{E_2} \quad = \quad \mathbf{A} + \mathbf{B_q}\mathbf{NC_y} + \mathbf{H^T} \tag{5.41}$$

$$\mathbf{E_3} \quad = \quad \mathbf{XA} + \mathbf{RC_y} + \mathbf{A^T}\mathbf{X} + \mathbf{C_y^T}\mathbf{R^T} \tag{5.42}$$

5.3.2. LMI Formulation for H_∞ Optimal Controller

Below, we give our LMI formulation for H_∞ optimal controller synthesis.

$$minimize \; trace(\gamma\mathbf{I}) \tag{5.43}$$

$$\begin{pmatrix} \mathbf{E_1} & \mathbf{E_2} & \mathbf{B_d} & \mathbf{YC_z^T} \\ \mathbf{E_2^T} & \mathbf{E_3} & \mathbf{XB_d} & \mathbf{C_z^T} \\ \mathbf{B_d^T} & \mathbf{B_d^T}\mathbf{X} & -\gamma\mathbf{I} & \mathbf{0} \\ \mathbf{C_z}\mathbf{Y} & \mathbf{C_z} & \mathbf{0} & -\gamma\mathbf{I} \end{pmatrix} < 0 \tag{5.44}$$

$$\begin{pmatrix} \mathbf{Y} & \mathbf{I} \\ \mathbf{I} & \mathbf{X} \end{pmatrix} > 0 \tag{5.45}$$

where $\mathbf{E_1}$, $\mathbf{E_2}$ and $\mathbf{E_3}$ are defined through Equation 5.40-5.42.

5.3.3. Controller Reconstruction for H_2 and H_∞ Designs

Formulations mentioned in the previous subsections are linear with respect to matrix variables $\mathbf{X}$, $\mathbf{Y}$, $\mathbf{H}$, $\mathbf{K}$, $\mathbf{R}$, $\mathbf{N}$. These LMIs will be solved by using a commercial software and these matrix variables will be obtained. Then, they will be placed into the matrix equation below, in order to get the controller matrices $\mathbf{A_c}$, $\mathbf{B_c}$, $\mathbf{C_c}$ and $\mathbf{D_c}$. For further information please refer to [62].

$$\begin{pmatrix} \mathbf{A_c} & \mathbf{B_c} \\ \mathbf{C_c} & \mathbf{D_c} \end{pmatrix} = \begin{pmatrix} \mathbf{U} & \mathbf{XB_q} \\ \mathbf{0} & \mathbf{I} \end{pmatrix}^{-1} \begin{pmatrix} \mathbf{H} - \mathbf{XAY} & \mathbf{R} \\ \mathbf{K} & \mathbf{N} \end{pmatrix} \begin{pmatrix} \mathbf{V^T} & \mathbf{0} \\ \mathbf{C_y Y} & \mathbf{I} \end{pmatrix}^{-1} \tag{5.46}$$

where,

- $\mathbf{U} = \mathbf{I}$
- $\mathbf{V^T} = \mathbf{I} - \mathbf{XY}$
- $\mathbf{I}$ is the identity matrix

With Equation 5.46, we finally can get our controller state space matrices $\mathbf{A_c}$, $\mathbf{B_c}$, $\mathbf{C_c}$ and $\mathbf{D_c}$.

6. RESULTS AND DISCUSSIONS

In this chapter, we give numerical case studies done in the light of the discussions made in the previous sections. Firstly, we specify our system parameters. Then, we obtain finite dimensional, low order, real, rational, strictly proper transfer function approximations of the system transfer functions. Finally, we synthesize H_2 and H_∞ optimal controllers in order to achieve noise reduction at our target low frequency range. We give results for mean flow case, for both open boundary condition case and frequency dependent impedance boundary condition case. Below is the numerical value of parameters. These parameters are the same for all case studies:

- speed of sound: $c = 340$ m/s
- mean flow velocity of fluid: $u_0 = 34$ m/s
- length of the duct: $L = 3.4$ m
- microphone location: $x_m = 2.8$ m
- source location: $x_s = 0.6$ m
- equilibrium density of fluid: $\rho_0 = 1.2$ kg/m^3
- radius of the duct: $r = 0.1$ m
- target frequency range: $0 - 250$ Hz

6.1. Open Boundary Condition Case

In this section, we give results for open boundary condition case. Though not being very realistic, it gives insight for the applicability of ANC in ducts which has mean flow of fluid inside. We first give an approximating scheme to obtain finite dimensional transfer function approximation of system transfer functions at selected target frequency range, then share the optimal controller results which are synthesized via LTI finite dimensional control theory mentioned in Chapter 5.

6.1.1. Transfer Function Approximations

Our system transfer functions are infinite dimensional, i.e., when we want to write them in a traditional rational transfer function form it has infinitely many poles and zeros. However, we want to synthesize optimal controllers via the LTI finite dimensional control theory, since it gives us physically more readily implementable controller configuration. Thus, we need to approximate the system transfer functions with finite dimensional rational ones, particularly in the frequency range of interest. Moreover, our approximate finite dimensional transfer functions should be not only rational but also strictly proper. Since we synthesize an H_2-controller and for the H_2-controller to be synthesized the closed loop disturbance to controlled output transfer function's state space matrix D should be "zero" ($D_{closedloop} = 0$). Thus, in order to guarantee that, we will obtain strictly proper transfer function approximations of the plant.

We want strictly proper, low order, finite dimensional rational transfer function approximations of the system. Here, we propose a method, which satisfies all of these properties.

6.1.1.1. Linear Least Squares Formulation. We write down our transfer function form used in approximations in Equation 6.1.

$$\sum_{i=1}^{5} \frac{A_i + B_i s}{s^2 + \omega_i^2} = G_{appx}(s) \tag{6.1}$$

In Equation 6.1; A_i and B_i are the real coefficients to be determined, ω_i is the ith natural frequency of the duct, and s is the Laplace variable. Since we want to suppress the noise at the first five modes, our summation index goes from 1 to 5. We already knew from the discussions in the previous chapters that at which frequencies resonance occur in our duct system. Therefore, we use this information to determine exact locations of the poles in our approximate transfer function. We do not need to take into account the zeros since we have already avoided all zeros that can occur in our frequency range of interest by properly choosing our duct configuration. However,

we use a term with s in the numerator in order to get the phase information.

Now, we use linear least squares technique in order to get estimates for A_i's and B_i's. When expanding Equation 6.1, we get;

$$G_{appx}(s) = \frac{A_1 + B_1 s}{s^2 + \omega_1^2} + \dots\dots + \frac{A_5 + B_5 s}{s^2 + \omega_5^2} \tag{6.2}$$

Partition Equation 6.2 further to get;

$$G_{appx}(s) = \left(\frac{A_1}{s^2 + \omega_1^2} + \dots\dots + \frac{A_5}{s^2 + \omega_5^2} \right) + \left(\frac{B_1}{s^2 + \omega_1^2} + \dots\dots + \frac{B_5}{s^2 + \omega_5^2} \right) s \tag{6.3}$$

When we put $s = j\omega$ in Equation 6.3:

$$G_{appx}(j\omega) = \left(\frac{A_1}{(j\omega)^2 + \omega_1^2} + \dots\dots + \frac{A_5}{(j\omega)^2 + \omega_5^2} \right)$$
$$+ \left(\frac{B_1}{(j\omega)^2 + \omega_1^2} + \dots\dots + \frac{B_5}{(j\omega)^2 + \omega_5^2} \right) j\omega \tag{6.4}$$

Since $(j\omega)^2 = -\omega^2$ in Equation 6.4, then for any $(j\omega)$ value, our approximate transfer function gives:

$$G_{appx}(j\omega) = \left(\frac{A_1}{-\omega^2 + \omega_1^2} + \dots\dots + \frac{A_5}{-\omega^2 + \omega_5^2} \right)$$
$$+ \left(\frac{B_1}{-\omega^2 + \omega_1^2} + \dots\dots + \frac{B_5}{-\omega^2 + \omega_5^2} \right) \omega j \tag{6.5}$$

The real part of $G_{appx}(j\omega)$ is;

$$real(G_{appx}(j\omega)) = \left(\frac{A_1}{-\omega^2 + \omega_1^2} + \dots\dots + \frac{A_5}{-\omega^2 + \omega_5^2} \right) \tag{6.6}$$

and the imaginary part of $G_{appx}(j\omega)$ is;

$$imag(G_{appx}(j\omega)) = \left(\frac{B_1}{-\omega^2 + \omega_1^2} + \dots\dots + \frac{B_5}{-\omega^2 + \omega_5^2} \right) \omega \tag{6.7}$$

As it can be seen, with this formulation we capture not only the exact resonance frequencies but also the phase information which is $\arctan(imag(G(j\omega))/real(G(j\omega)))$.

Recall that, our transfer functions also have imaginary values at some frequency ω. So in our proposed work, we will treat our exact transfer function values at frequency ω as our observed values and then use them in obtaining least squares estimates of A_i's and B_i's. We apply linear regression to real parts of the approximate and the exact transfer function values in order to obtain estimates for A_i's; whereas for finding B_i's linear regression is applied to imaginary parts of the approximate and the exact transfer function values. Here is the methodology for estimating A_i's,

For data point at $j\omega$ we have:

$$Y_{real\omega} \cong A_1\frac{1}{-\omega^2 + \omega_1^2} + A_2\frac{1}{-\omega^2 + \omega_2^2} + A_3\frac{1}{-\omega^2 + \omega_3^2}$$
$$+ A_4\frac{1}{-\omega^2 + \omega_4^2} + A_5\frac{1}{-\omega^2 + \omega_5^2} \quad (6.8)$$

Say;

$$x_i^r = \frac{1}{-\omega^2 + \omega_i^2}$$

where, $i = 1, ..., 5$ and r denotes the real part.

Then, Equation 6.8 becomes;

$$Y_{real\omega} \cong A_1 x_1^r + A_2 x_2^r + A_3 x_3^r + A_4 x_4^r + A_5 x_5^r \quad (6.9)$$

where x_i^r's are regressors for real part of approximate transfer function, A_i's are parameters to be estimated, $Y_{real\omega}$ is the real part of the exact response at ω.

Equation 6.9 is in the standard form for linear least squares and A_i parameters

are estimated by using N data points as;

$$\mathbf{a_{est}} = (\mathbf{X_{real}^T X_{real}})^{-1} \mathbf{X_{real}^T y_{real}} \tag{6.10}$$

where,

$$\mathbf{X_{real}} = \begin{bmatrix} . & . & . & . & . \\ . & . & . & . & . \\ \dfrac{1}{-\omega^2 + \omega_1^2} & \dfrac{1}{-\omega^2 + \omega_2^2} & \dfrac{1}{-\omega^2 + \omega_3^2} & \dfrac{1}{-\omega^2 + \omega_4^2} & \dfrac{1}{-\omega^2 + \omega_5^2} \\ . & . & . & . & . \\ . & . & . & . & . \end{bmatrix}_{N \times 5}$$

$$\mathbf{y_{real}} = \begin{bmatrix} . \\ . \\ real(G(j\omega)) \\ . \\ . \end{bmatrix}_{N \times 1} , \quad \mathbf{a_{est}} = \begin{bmatrix} A_1 \\ A_2 \\ A_3 \\ A_4 \\ A_5 \end{bmatrix}$$

Similarly B_i's are estimated through the same methodology as;

For data point at $j\omega$;

$$Y_{imag\omega} \cong B_1 \frac{\omega}{-\omega^2 + \omega_1^2} + B_2 \frac{\omega}{-\omega^2 + \omega_2^2} + B_3 \frac{\omega}{-\omega^2 + \omega_3^2}$$
$$+ B_4 \frac{\omega}{-\omega^2 + \omega_4^2} + B_5 \frac{\omega}{-\omega^2 + \omega_5^2} \tag{6.11}$$

Again, say:

$$x_i^m = \frac{\omega}{-\omega^2 + \omega_i^2}$$

where, $i = 1, ..., 5$ and m denotes the imaginary part.

Then, Equation 6.11 becomes;

$$Y_{imagw} \cong B_1 x_1^m + B_2 x_2^m + B_3 x_3^m + B_4 x_4^m + B_5 x_5^m \tag{6.12}$$

where x_i^m's are regressors for the imaginary part of the approximate transfer function, B_i's are parameters to be estimated, $Y_{imag\omega}$ is the imaginary part of the exact response at ω.

Here, Equation 6.12 is in the standard form for linear least squares as well, and B_i parameters are estimated by using N data points as;

$$\mathbf{b_{est}} = (\mathbf{X_{imag}^T X_{imag}})^{-1} \mathbf{X_{imag}^T y_{imag}} \tag{6.13}$$

where,

$$\mathbf{X_{imag}} = \begin{bmatrix} \cdot & \cdot & \cdot & \cdot & \cdot \\ \cdot & \cdot & \cdot & \cdot & \cdot \\ \dfrac{\omega}{-\omega^2 + \omega_1^2} & \dfrac{\omega}{-\omega^2 + \omega_2^2} & \dfrac{\omega}{-\omega^2 + \omega_3^2} & \dfrac{\omega}{-\omega^2 + \omega_4^2} & \dfrac{\omega}{-\omega^2 + \omega_5^2} \\ \cdot & \cdot & \cdot & \cdot & \cdot \\ \cdot & \cdot & \cdot & \cdot & \cdot \end{bmatrix}_{N \times 5}$$

$$\mathbf{y_{imag}} = \begin{bmatrix} \cdot \\ \cdot \\ imag(G(j\omega)) \\ \cdot \\ \cdot \end{bmatrix}_{N \times 1} , \quad \mathbf{b_{est}} = \begin{bmatrix} B_1 \\ B_2 \\ B_3 \\ B_4 \\ B_5 \end{bmatrix}$$

6.1.1.2. Results. We take $N = 25000$ data points, which are equally spaced from 0.01 Hz to 250 Hz. Below, we compare the bode magnitude and phase graphs of the approximated system transfer functions and the exact system transfer functions for various cases.

Figure 6.1 shows the disturbance $(d(s))$ to output pressure at measurement point $(P(x_m, s))$ transfer function's exact and approximate bode magnitude and phase graphs. Figure 6.2 shows the input $(q(s))$ to output pressure at measurement point $(P(x_m, s))$ transfer function's exact and approximate bode magnitude and phase graphs. We show $d(s)$ to $P(x, s)$ and $q(s)$ to $P(x, s)$ Bode graphs for $x = 3.0$ m, in Figure 6.3 and 6.4, respectively.
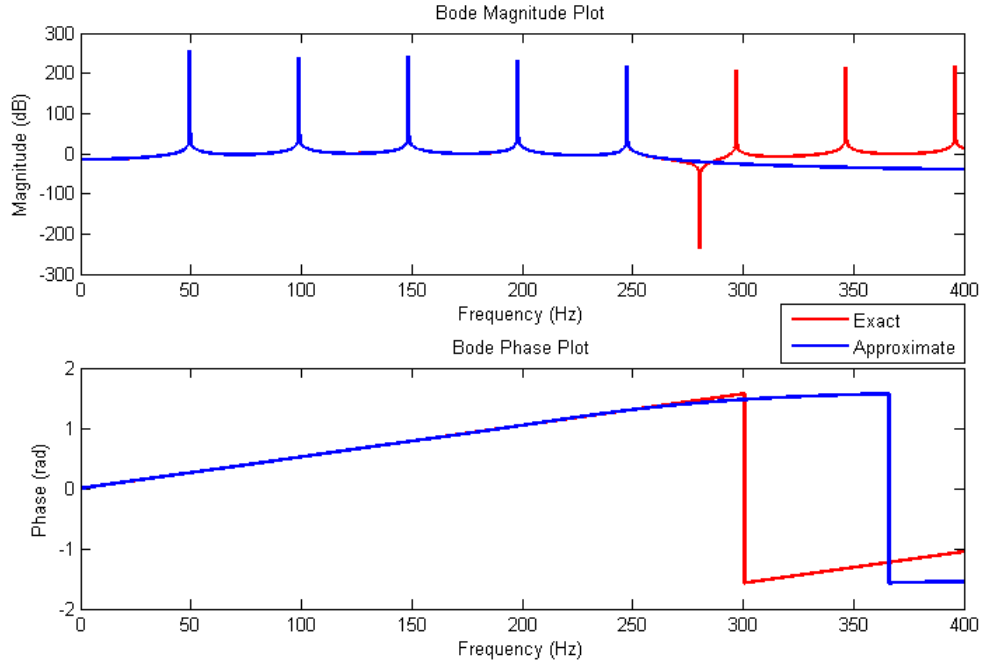
Figure 6.1. Exact and approximate Bode magnitude and phase plot of disturbance $(d(s))$ to output pressure at measurement point $(P(x_m, s))$ transfer function (red - exact, blue - approximate).
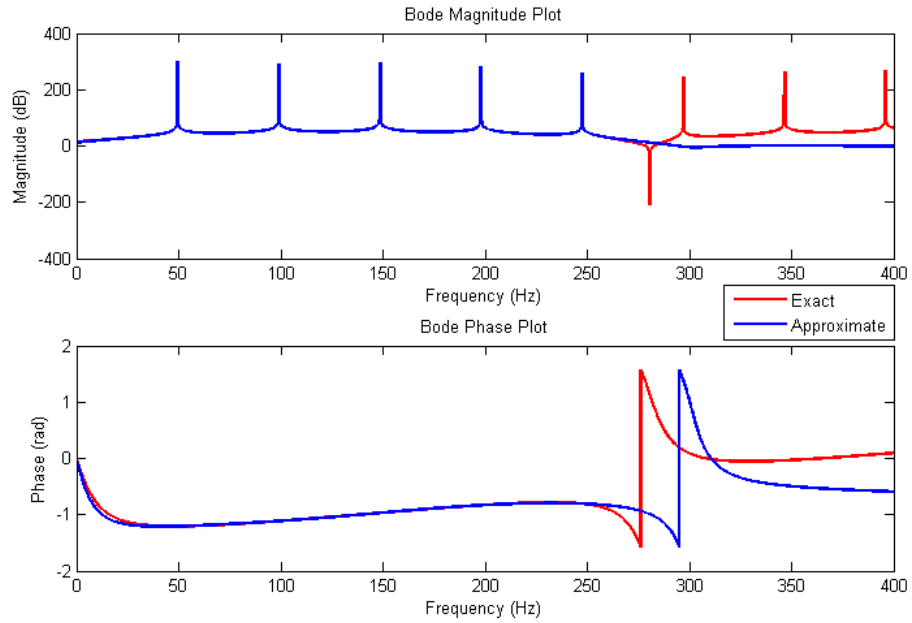
Figure 6.2. Exact and approximate Bode magnitude and phase plot of input ($q(s)$) to output pressure at measurement point ($P(x_m, s)$) transfer function (red - exact, blue - approximate).
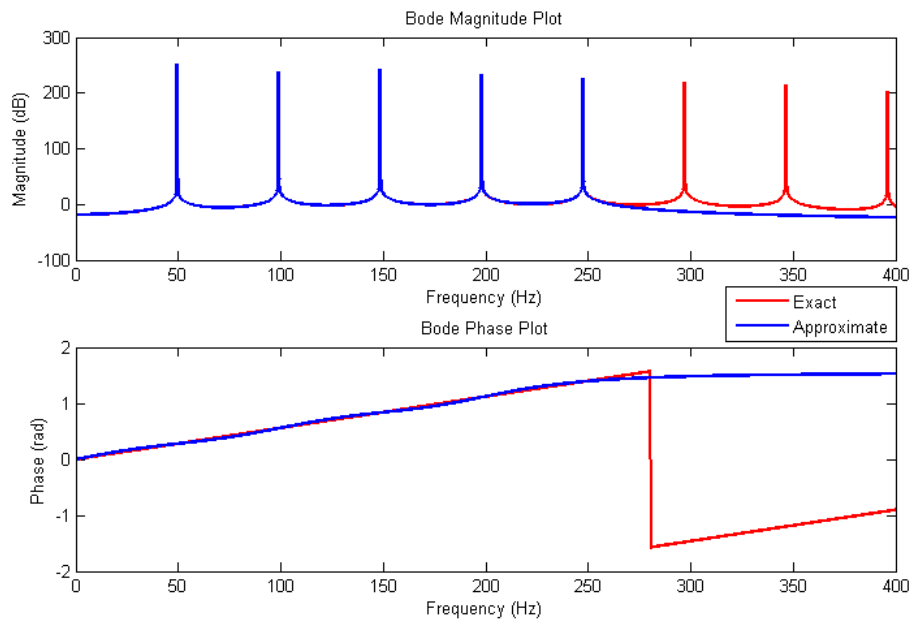
Figure 6.3. Exact and approximate Bode magnitude and phase plot of disturbance ($d(s)$) to output pressure at $x = 3.0$ m ($P(x, s)$) transfer function (red - exact, blue - approximate).
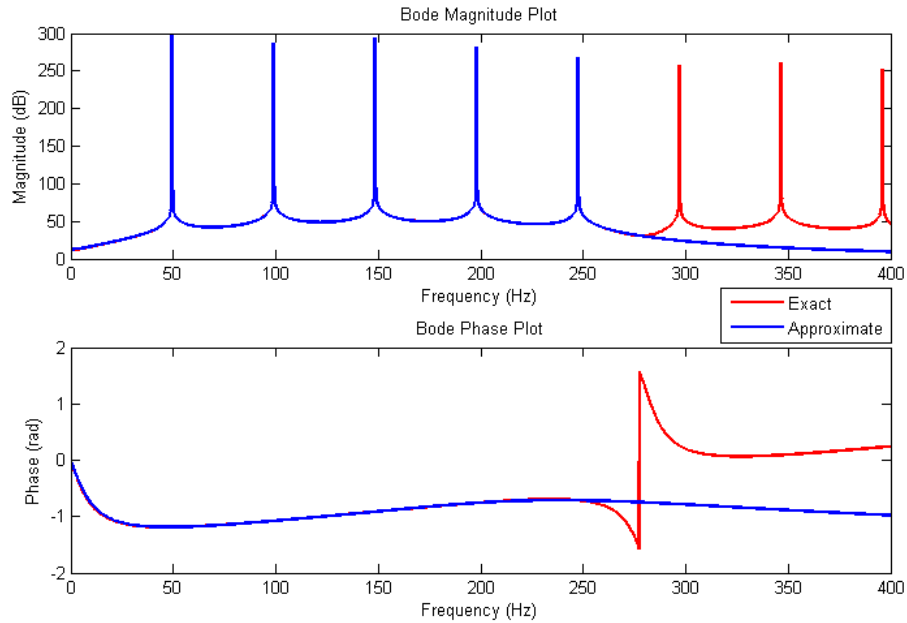
Figure 6.4. Exact and approximate Bode magnitude and phase plot of input $(q(s))$ to output pressure at $x = 3.0$ m $(P(x, s))$ transfer function (red - exact, blue - approximate).

6.1.1.3. Discussions.   As it can be seen from Figure 6.1-6.4 our rational transfer function approximation represents the original system quite well within the selected frequency range $(0 - 250$ Hz$)$. Beyond that range, both Bode magnitude and phase plots of approximated transfer functions begin to deviate from the original plots.

These obtained approximations are real, rational, low order, finite dimensional and strictly proper as we seek for. The degree of the denominator of our approximated transfer functions is 10 and the numerator's degree is 9. Low order approximations make the controller's degree low as well, which is crucial in real life implementations.

So, it can be concluded that our approximating scheme is satisfactory for the selected frequency range, thus it can be used for controller synthesis using LTI control theory.

6.1.2. Performance of Controllers

Here we represent the performance of synthesized controllers, which are designed according to Chapter 5. Our aim is to reduce the noise levels towards the end section of the duct. We take measurements from $x_m = 2.8$ m and reduce the noise levels at some performance point x_p which can be located between $x = 2.8$ m and $x = 3.4$ m. We select our performance point as $x = 2.8$ m as well and suggest that if we succeed to achieve noise reduction at that performance point, we also achieve noise reduction at any point in the end section of the duct.

In the design scheme shown in Equation 5.25, we have $\mathbf{A_{dz}}$, $\mathbf{A_{qz}}$, $\mathbf{A_{dy}}$ and $\mathbf{A_{qy}}$. But, recall that in our approximation scheme all of these are equal since we have same poles everywhere (resonance frequencies are the same). In other words, our individual plant transfer functions all have same dynamics but we have different $\mathbf{B}$ and $\mathbf{C}$ matrices. Thus, in our controller synthesis, we can avoid unnecessary modes, that is, instead of having 40×40 state matrix we can obtain 10×10 state matrix for representing plant dynamics.

After having obtained minimal and balanced plant realizations, we used LMI formulations mentioned in Sections 5.3.1 and 5.3.2 to synthesize H_2 and H_∞ optimal controllers. We give our controllers' performance results below.

6.1.2.1. Frequency Domain Results. In this section, we give the frequency domain results for uncontrolled and controlled system transfer functions. System transfer functions used in frequency responses are approximated finite dimensional ones.

Figure 6.5 shows the uncontrolled and controlled system frequency response results for performance point $x_p = 2.8$ m. Figure 6.6 shows the uncontrolled and controlled system frequency response results for $x = 3.0$ m in the duct.
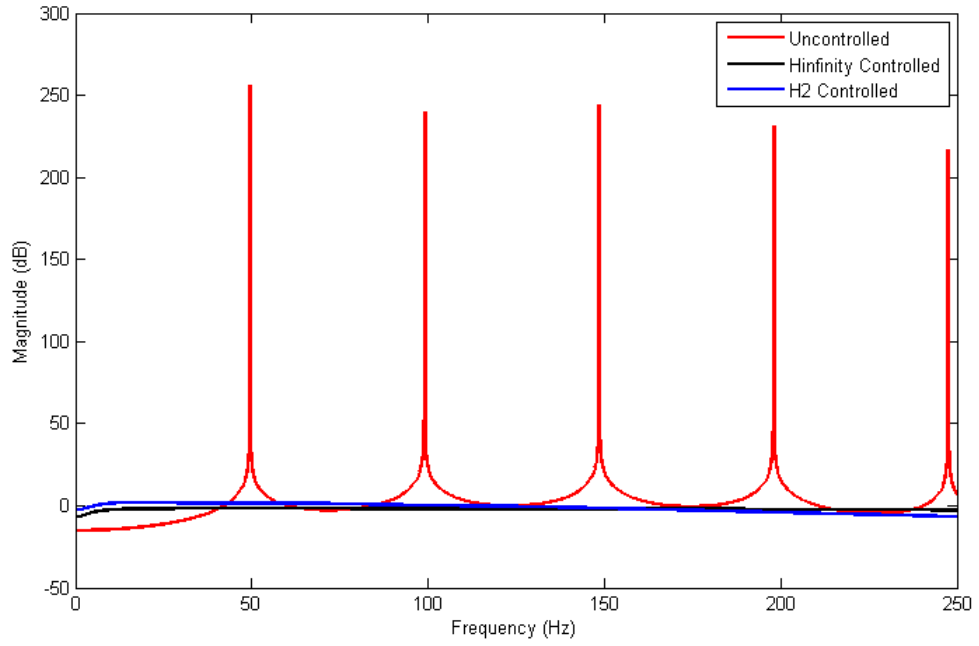
Figure 6.5. Uncontrolled and controlled system frequency response plot at $x = 2.8$ m (red - uncontrolled, blue - H_2 controlled, black - H_∞ controlled).
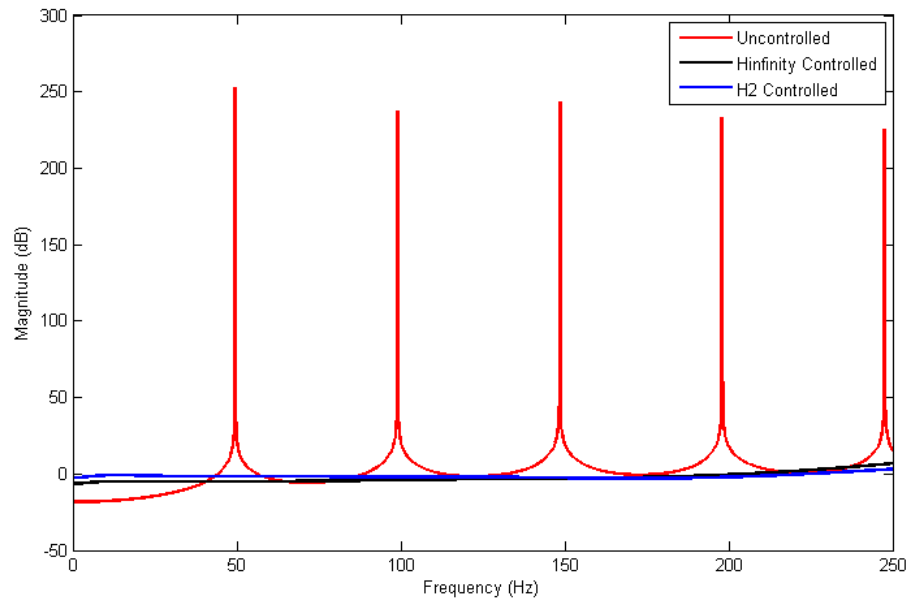
Figure 6.6. Uncontrolled and controlled system frequency response plot at $x = 3.0$ m (red - uncontrolled, blue - H_2 controlled, black - H_∞ controlled).

6.1.2.2. Time Domain Results. In this section, we give time domain simulation results obtained from Simulink by using approximated system transfer functions.

The disturbance signal used in time domain simulations is a summation of ten sine waves. All of these sine waves have amplitude 1 Pa. Ten different frequencies for these sine waves are: 25, 49.5, 75, 99, 125, 148.5, 175, 198, 225 and 247.5 Hz. Note that 49.5, 99, 148.5, 198, 247.5 Hz frequencies are duct's first five resonance frequencies. This broadband disturbance signal is shown in Figure 6.7.

Time domain uncontrolled and controlled system response to disturbance signal shown in Figure 6.7 at $x_m = 2.8$ m, is shown in Figure 6.8. Similarly, time domain uncontrolled and controlled system response to disturbance signal shown in Figure 6.7 at $x = 3.0$ m, is shown in Figure 6.9.
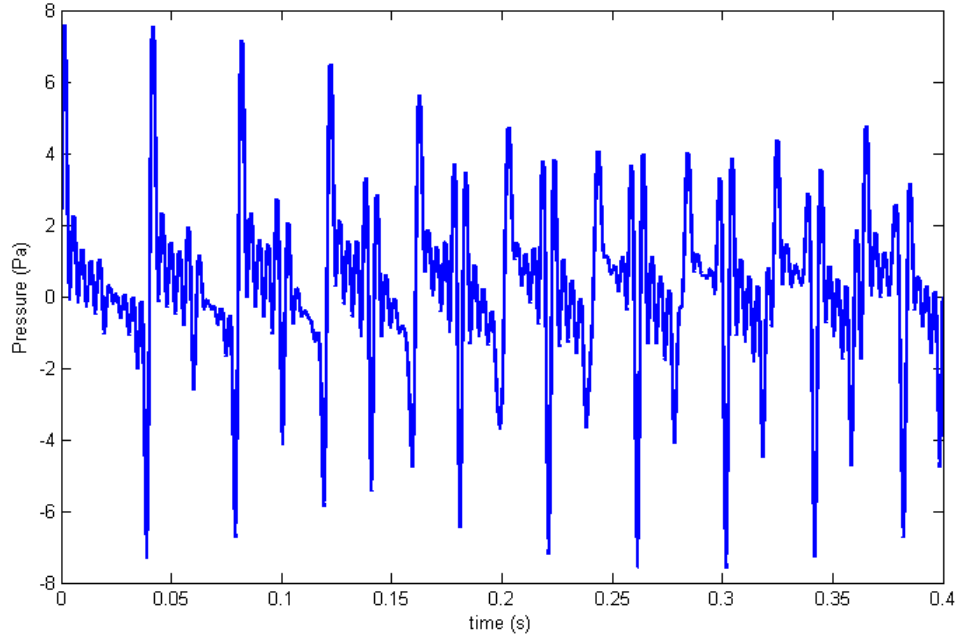
Figure 6.7. Disturbance signal used in time domain simulations for open boundary condition.
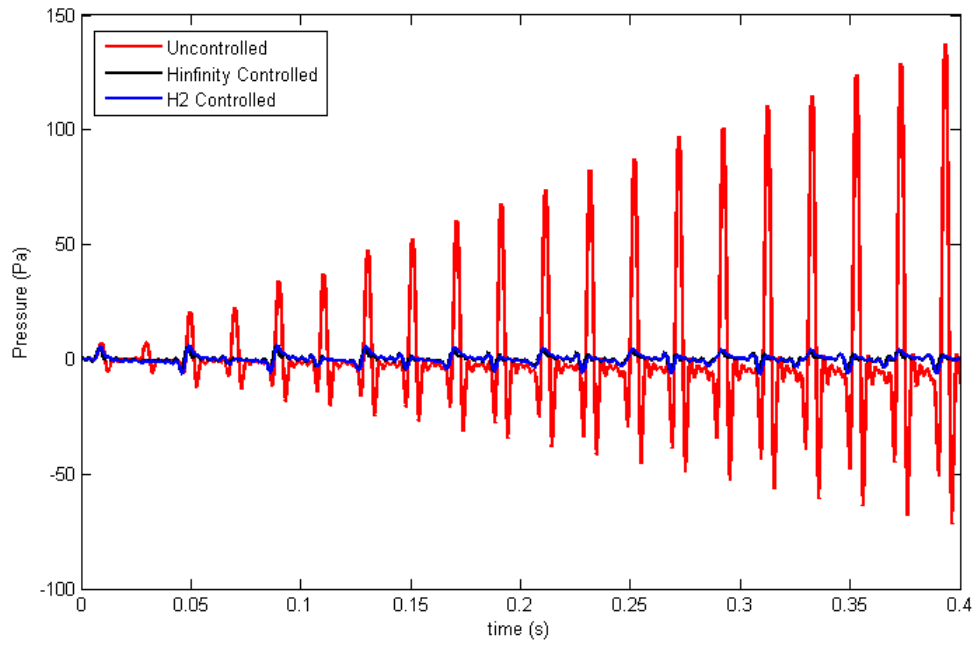
Figure 6.8. Uncontrolled and controlled system time domain simulation at $x_m = 2.8$ m (red - uncontrolled, blue - H_2 controlled, black - H_∞ controlled).
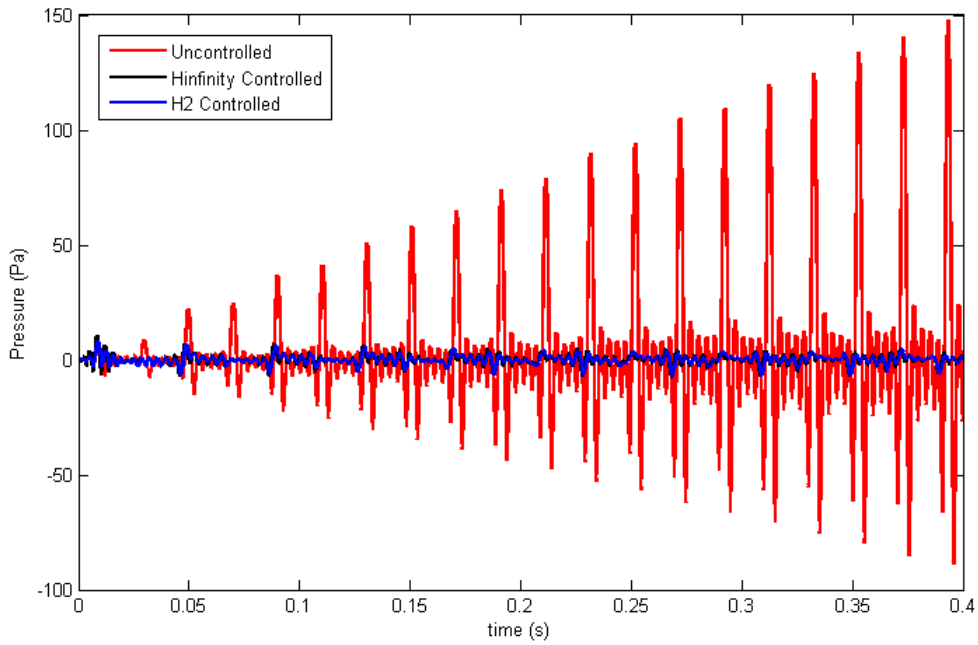
Figure 6.9. Uncontrolled and controlled system time domain simulation at $x = 3.0$ m (red - uncontrolled, blue - H_2 controlled, black - H_∞ controlled).

6.1.2.3. Discussions.   As can be seen from Figure 6.5 and 6.6, our synthesized optimal controllers suppress all the noise in $0 - 250$ Hz frequency range. H_2 optimal controller gives better results at higher frequencies whereas, H_∞ optimal controller gives better results at lower frequencies. But the overall performance of H_∞ optimal controller is superior than H_2 optimal controller.

Even though our design is with respect to the performance point at $x_p = 2.8$ m, at $x = 3.0$ m good noise reduction is also achieved. Since resonance frequencies do not change along the duct, as presumed earlier, our controller design gives good results.

These frequency domain results are supported by the time domain simulations as well, in which a broadband disturbance signal is used. As can be seen from Figure 6.8 and 6.9 this disturbance signal causes large pressure fluctuations at the corresponding points in the duct (red lines in those Figures), but due to the control signal produced, these unwanted pressure fluctuations are omitted (blue lines for H_2 performance, black lines for H_∞ performance).

Even though these results are quite satisfactory, open boundary condition does not represent a very realistic duct system. To obtain more realistic results, we investigate frequency dependent impedance boundary condition in the next section.

6.2. Frequency Dependent Impedance Boundary Condition Case

In this section, we present results for a more realistic case, which has been described with a general boundary condition mentioned in Equation 2.9 for the time domain and in Equation 3.13 for the frequency domain. Frequency dependent specific acoustic impedance of the duct end is given by Equation 3.19.

Again, we first obtain finite dimensional transfer function approximations of system transfer functions by least squares, then present closed loop performance results of synthesized optimal controllers, as we did for the open end case.

6.2.1. Transfer Function Approximations

In this part, we propose an approximating scheme for the frequency dependent impedance end case. Our finite dimensional transfer function approximations are real, rational, low order and strictly proper. These transfer function approximations are obtained via linear least squares, which is described in detail, below.

6.2.1.1. Linear Least Squares Formulation. We begin with, writing down the transfer function form used in approximations in Equation 6.14.

$$\sum_{i=0}^{5} \frac{A_i + B_i s}{s^2 + 2\zeta_i \omega_i s + \omega_i^2} = G_{appx}(s) \tag{6.14}$$

In Equation 6.14, A_i and B_i are the real coefficients to be determined, ω_i is the ith natural frequency of the duct, ζ_i is the damping ratio corresponding to the ith mode, and s is the Laplace variable. Since we want to suppress the noise at first five modes, our summation index goes from 0 to 5. Note that we have included a mode with index 0, representing the mode near zero frequency. We already knew from the discussions in previous chapters that approximately at which frequencies resonance occur in our duct system. Therefore, we use this information to determine the exact locations of the poles in our approximate transfer function. We do not need to take into account the zeros since we have already avoided all zeros that can occur in our frequency range of interest by properly choosing our duct configuration. Please note that we also have the phase information because of the s terms which exist in both the numerator and the denominator.

Here, we discuss how to obtain ω_i's and ζ_i's where i ranges from 1 to 5.: ζ_i's are obtained approximately by the following procedure found in [63]. A sketch describing this approximation is given in Figure 6.10. From the frequency response data of the transfer function for which finite dimensional approximation will be done:

(i) Determine the ith mode's maximum bode magnitude value in dB ($|H(\omega_{di})|_{\text{dB}}$).

(ii) Determine the frequency value corresponding to that maximum (ω_{di}).

(iii) Search for the Bode magnitude values which satisfies the following relationship at both sides of ω_{di}, as shown in Figure 6.10.

$$|H(\omega_{di})| - 3 \text{ dB } = |H(\omega_a)| = |H(\omega_b)| \tag{6.15}$$

(iv) Find the corresponding frequencies of ω_a and ω_b for $|H(\omega_a)|$ and $|H(\omega_b)|$, respectively.

(v) Find the ζ_i by the following relationship.

$$\zeta_i = \frac{\omega_b - \omega_a}{2\omega_{di}} \tag{6.16}$$

After finding ζ_i, the ω_i is obtained by damped natural frequency formulation;

$$\omega_i = \frac{\omega_{di}}{\sqrt{1 - \zeta_i^2}} \tag{6.17}$$

where ω_i, is the undamped natural frequency for the ith mode, ω_{di}, is the damped natural frequency for the ith mode ($\omega_{di} = 2\pi f_{di}$), ζ_i, is the damping ratio for the ith mode.
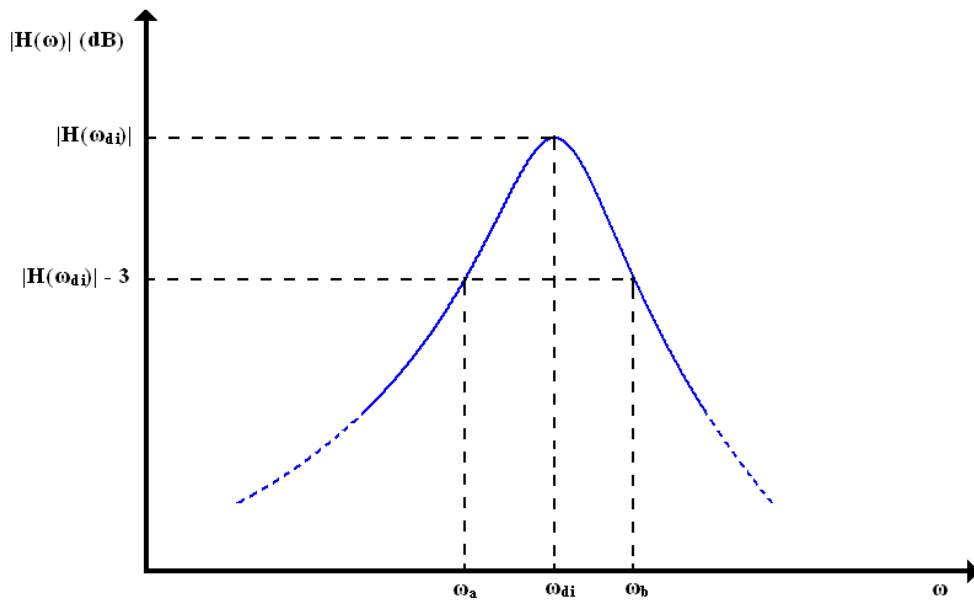
Figure 6.10. Modal damping ratio estimation.

For obtaining ζ_0 and ω_0 we use the same procedure mentioned above but in a slightly different way. For approximation purposes we take ω_0 directly as;

$$\omega_0 = 2\pi 0.01 \tag{6.18}$$

and we find our ζ_0 as;

$$\zeta_0 = \frac{\omega_b}{2\omega_0} \tag{6.19}$$

where ω_b is found with the same procedure mentioned above.

Now, we use linear least squares technique to get estimates for A_i's and B_i's.

When expanding Equation 6.14 we get;

$$G_{appx}(s) = \frac{A_0 + B_0 s}{s^2 + 2\zeta_0\omega_0 s + \omega_0^2} + \ldots + \frac{A_5 + B_5 s}{s^2 + 2\zeta_5\omega_5 s + \omega_5^2} \tag{6.20}$$

In order to obtain least squares estimates, we apply the following procedure:

Firstly, we take these individual transfer functions into a common denominator. So, the resulting approximate transfer function is rational with numerator degree 11 and denominator degree 12. It has the following form:

$$G_{appx}(s) = \frac{n_1 s^{11} + n_2 s^{10} + \ldots + n_{10} s + n_{11}}{s^{12} + d_1 s^{11} + \ldots + d_{11} s + d_{12}} \tag{6.21}$$

where n_i's are real coefficients for numerator polynomial, d_i's are coefficients for denominator polynomial. Note that, if we put $s = j\omega$ in Equation 6.21, then we obtain a complex value at ω such that:

$$G_{appx}(j\omega) = \frac{e + fj}{g + hj} \tag{6.22}$$

where e, f, g, h are real numbers and $j = \sqrt{-1}$.

In order to apply our proposed method we should get rid of complex denominator values obtained in Equation 6.22. For this purpose, we should multiply both the numerator and the denominator with complex conjugate of the denominator, namely $(g - hj)$. As a result, we obtained a complex number in numerator and a pure real number in denominator:

$$G_{appx}(jw) = \frac{(e + fj)}{(g + hj)} \frac{(g - hj)}{(g - hj)} \tag{6.23}$$

$$G_{appx}(jw) = \frac{k + mj}{n} \tag{6.24}$$

where k, m, n are real numbers and $j = \sqrt{-1}$.

After applying the procedure mentioned through Equation 6.21 - 6.24, we obtain such a relationship after straightforward but tedious calculations:

$$G_{appx}(j\omega) = (A_0 x_1 + ... + A_5 x_6 + B_1 x_7 + ... + B_5 x_{12})$$
$$+ (A_0 z_1 + ... + A_5 z_6 + B_1 z_7 + ... + B_5 z_{12})j \tag{6.25}$$

where x_i's and z_i's are the corresponding regressors.

We can write Equation 6.25 in a more compact way as:

$$real(G_{appx}(j\omega)) = A_0 x_1 + ... + A_5 x_6 + B_1 x_7 + ... + B_5 x_{12} \tag{6.26}$$

$$imag(G_{appx}(j\omega)) = A_0 z_1 + ... + A_5 z_6 + B_1 z_7 + ... + B_5 z_{12} \tag{6.27}$$

where $real(G_{appx}(j\omega))$ is the real part of $G_{appx}(j\omega)$, $imag(G_{appx}(j\omega))$ is the imaginary part of $G_{appx}(j\omega)$.

In Equation 6.26 and 6.27, for the data point $j\omega$, only unknowns are $A_0,.....,A_5$ and $B_0,.....,B_5$. Therefore, Equation 6.26 and 6.27 form a linear least squares problem

as mentioned below:

$$real(G_{exact}(j\omega)) \cong A_0 x_1 + ... + A_5 x_6 + B_0 x_7 + ... + B_5 x_{12} \qquad (6.28)$$

$$imag(G_{exact}(j\omega)) \cong A_0 z_1 + ... + A_5 z_6 + B_0 z_7 + ... + B_5 z_{12} \qquad (6.29)$$

where $real(G_{exact}(j\omega))$ is the real part of the exact system transfer function to be approximated at $j\omega$, $imag(G_{exact}(j\omega))$ is the imaginary part of the exact system transfer function to be approximated at $j\omega$.

For N number of data points, we can represent this linear regression problem, described by Equation 6.28 and 6.29, in matrix form as;

$$\hat{\boldsymbol{\beta}} = (\mathbf{X_{fdie}^T X_{fdie}})^{-1} \mathbf{X_{fdie}^T y_{fdie}} \qquad (6.30)$$

where,

$$\mathbf{X_{fdie}} = \begin{bmatrix} \begin{pmatrix} . & . & . & . & . & . & . & . \\ . & . & . & . & . & . & . & . \\ x_1 & x_2 & . & . & . & x_{11} & x_{12} \\ . & . & . & . & . & . & . \\ . & . & . & . & . & . & . \end{pmatrix}_{N \times 12} \\ \begin{pmatrix} . & . & . & . & . & . & . \\ . & . & . & . & . & . & . \\ z_1 & z_2 & . & . & . & z_{11} & z_{12} \\ . & . & . & . & . & . & . \\ . & . & . & . & . & . & . \end{pmatrix}_{N \times 12} \end{bmatrix}_{2N \times 12}$$

$$\hat{\boldsymbol{\beta}}^{\boldsymbol{T}} = \begin{bmatrix} A_0 & . & . & . & A_5 & B_0 & . & . & . & B_5 \end{bmatrix}$$

$$\mathbf{y_{fdie}} = \left[\begin{array}{c} \begin{pmatrix} \cdot \\ \cdot \\ \cdot \\ real(G_{exact}(j\omega)) \\ \cdot \\ \cdot \\ \cdot \end{pmatrix}_{N \times 1} \\ \begin{pmatrix} \cdot \\ \cdot \\ imag(G_{exact}(j\omega)) \\ \cdot \\ \cdot \end{pmatrix}_{N \times 1} \end{array} \right]_{2N \times 1}$$

Subscript "fdie" denotes "frequency dependent impedance end".

6.2.1.2. Results. We obtain approximations by using $N = 25000$ data points which are equally spaced with 0.01 Hz in the frequency range $0 - 250$ Hz. By using such a large number of data points, we provide a good fit to the exact frequency response values. Note that, our regressor matrix $\mathbf{X_{fdie}}$ is 50000×12, and our exact data vector $\mathbf{y_{fdie}}$ is 50000×1.

Now, we present results of the approximation scheme mentioned just above, for three different points which are located towards the end of the duct. In Figure 6.11-6.16, red lines represent infinite dimensional system transfer functions, whereas, blue lines represent finite dimensional approximations of the corresponding system transfer functions.

Figure 6.11 and 6.12 show the results for $d(s)$ to $P(x_m, s)$ and $q(s)$ to $P(x_m, s)$ transfer functions where $x_m = 2.8$ m. Figure 6.13 and 6.14 show the results for $d(s)$ to $P(x, s)$ and $q(s)$ to $P(x, s)$ transfer functions at $x = 3.1$ m. Figure 6.15 and 6.16 show the results for $d(s)$ to $P(x, s)$ and $q(s)$ to $P(x, s)$ transfer functions at the duct end $(x = 3.4$ m).

Figure 6.11. Bode magnitude and phase plot for $d(s)$ to $P(x_m, s)$ transfer function at $x_m = 2.8$ m (red - exact system transfer functions, blue - approximated transfer functions).
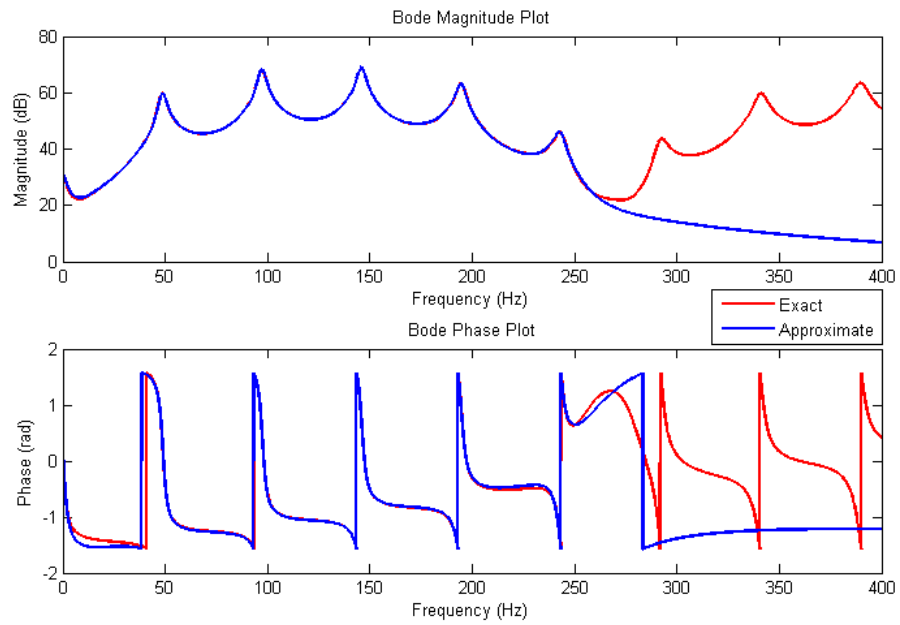
Figure 6.12. Bode magnitude and phase plot for $q(s)$ to $P(x_m, s)$ transfer function at $x_m = 2.8$ m (red - exact system transfer functions, blue - approximated transfer functions).
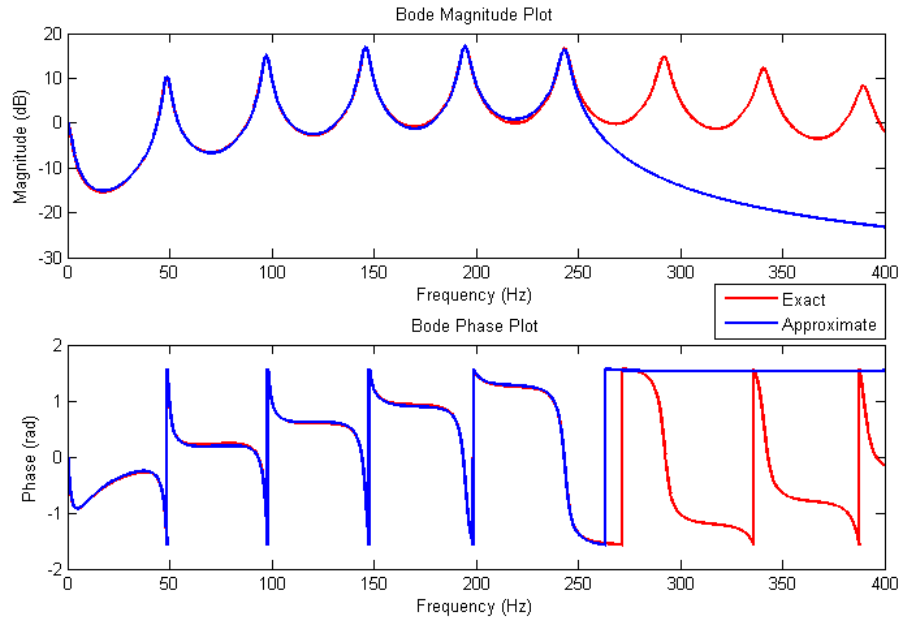
Figure 6.13. Bode magnitude and phase plot for $d(s)$ to $P(x,s)$ transfer function at $x = 3.1$ m (red - exact system transfer functions, blue - approximated transfer functions).
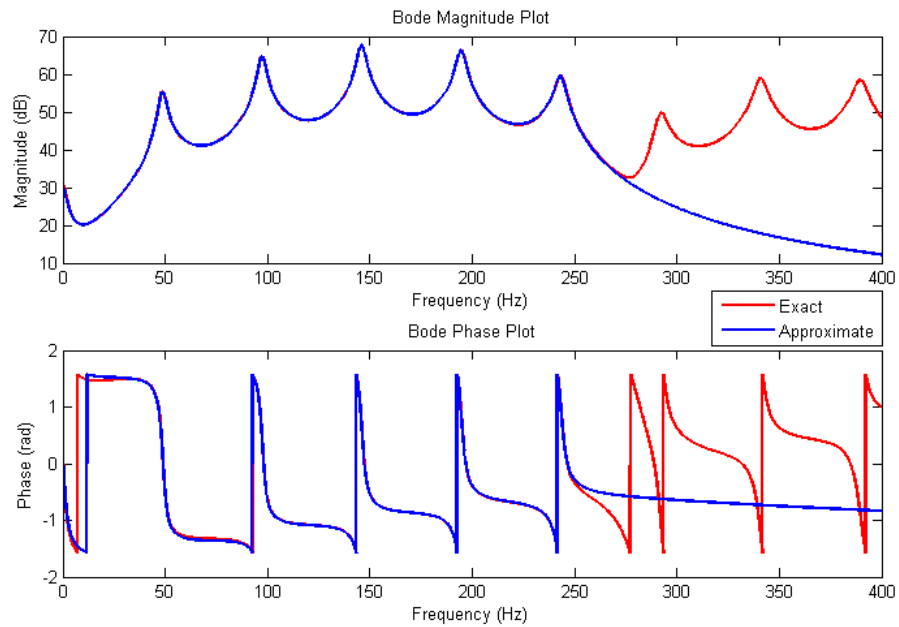
Figure 6.14. Bode magnitude and phase plot for $q(s)$ to $P(x,s)$ transfer function at $x = 3.1$ m (red - exact system transfer functions, blue - approximated transfer functions).
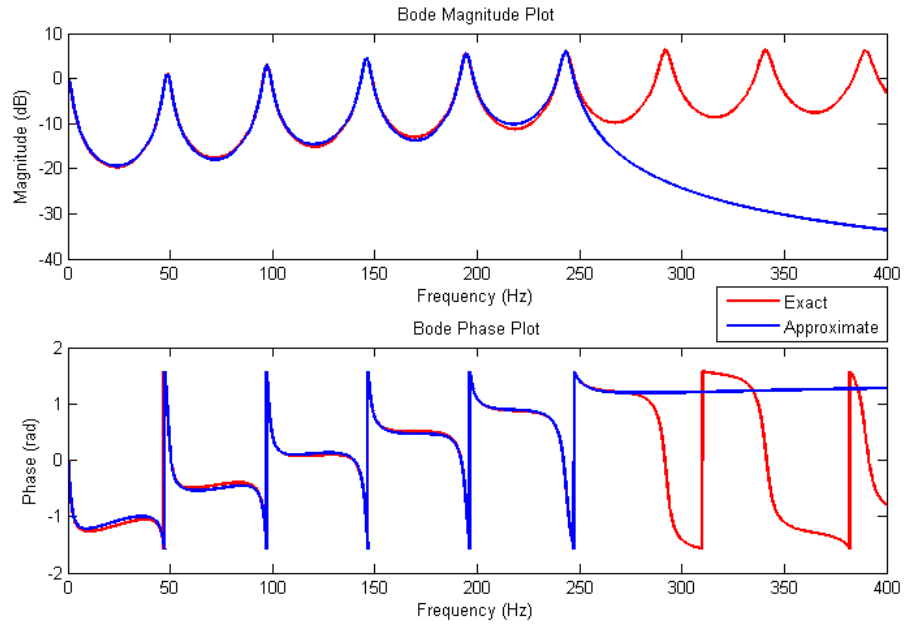
Figure 6.15. Bode magnitude and phase plot for $d(s)$ to $P(x, s)$ transfer function at the duct end $x = 3.4$ m (red - exact system transfer functions, blue - approximated transfer functions).
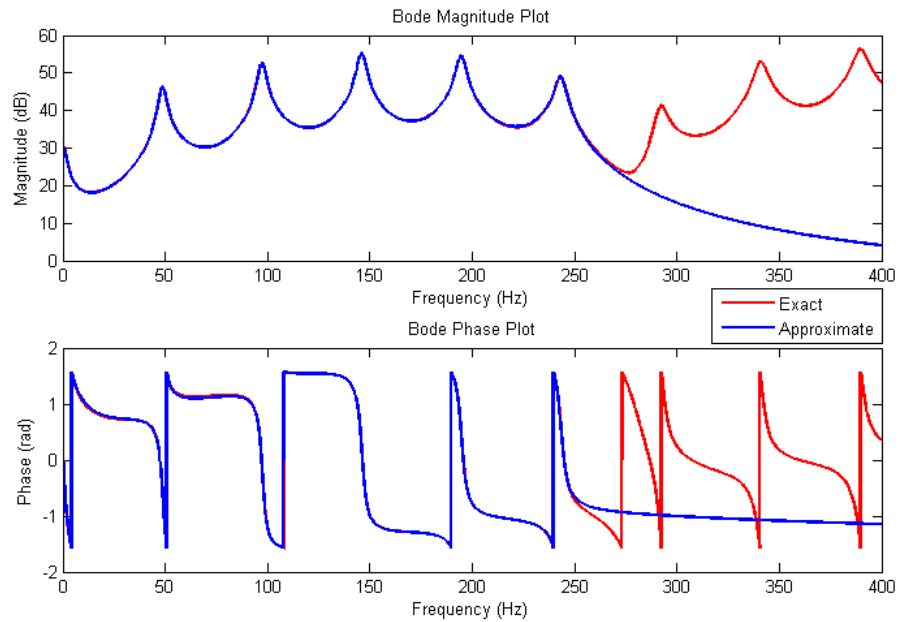
Figure 6.16. Bode magnitude and phase plot for $q(s)$ to $P(x, s)$ transfer function at the duct end $x = 3.4$ m (red - exact system transfer functions, blue - approximated transfer functions).

6.2.1.3. Discussions. As it can be observed in Figure 6.11-6.16, our approximating scheme is satisfactory for the frequency range of interest $(0 - 250 \text{ Hz})$. Compared to the open end case, it has some slight discrepencies in the representation of the actual system. But, it should be noted that, open end case is an ideal situation and does not represent a real physical system. In the open end case, system transfer functions can be described by a simple relationship mentioned in Equation 6.1. On the other hand, for our realistic duct case, we have a more complicated transfer function form mentioned in Equation 6.14. Thus, it is reasonable to get better results in the ideal case.

We used our approximating scheme by considering the damped natural frequencies of the system as mentioned in Section 6.2.1.1. Because of that, we achieved quite nice fits for both magnitude and phase plots at pole locations. On the other hand, we observe some deficiencies at locations other than pole locations. Generally, Figure 6.11-6.16 show that, at edge frequencies, our approximation begins to deviate. But for the frequency range of interest $(0 - 250 \text{ Hz})$, it can be readily used for representing the original system, since deviations are not considered as problematic. Beyond 250 Hz, our approximations are no longer valid, since we did not take into account that region in our model.

Our approximated real, rational, finite dimensional system transfer functions have denominator order of 12 and numerator order of 11, thus it is strictly proper and low order. As indicated before, this causes our controller to be low order as well.

As a conclusion, our approximations work well at our frequency range of interest and will be used in finite dimensional controller synthesis.

6.2.2. Performance of Controllers

Here we present our controllers performances, which are synthesized according to Chapter 5. We begin with, general procedure applied in order to synthesize low order controllers and continue with, frequency and time domain performances.

For the spatial region, $x = 2.8$ m to $x = 3.4$ m in the duct, Bode magnitude value's maximum value for $d(s)$ to $P(x, s)$ transfer function occurs at $x = 2.8$ m with 18.73 dB. So, it would be reasonable to suppress the noise levels at that point in the duct. Thus, as was done in the open end case, our performance point for frequency dependent impedance end is selected as $x_p = 2.8$ m as well.

Our controlled output (z) and measured output (y) are the same since, we take measurements from $x_m = 2.8$ m and want to reduce the noise at $x_p = 2.8$ m in the duct. Thus, we have $\mathbf{A_{dz}} = \mathbf{A_{dy}}$ and $\mathbf{A_{qz}} = \mathbf{A_{qy}}$. This condition automatically reduces plant order by half. To further reduce the order, we use the similarity of damping ratios and damped natural frequencies of approximated system transfer functions. In Table 6.1 and 6.2, we can see that, damping ratios $(\zeta_i\text{'s})$ and damped natural frequencies $(f_{di}\text{'s})$, which are used in transfer function approximations, do not change their value dramatically at different locations along the duct. Thus, we can obtain a low order plant description, if we approximate damping ratios and damped natural frequencies of approximated system transfer functions that are needed for controller design. For this purpose, we take arithmetic average of $(\zeta_i\text{'s})$ and $(f_{di}\text{'s})$ of corresponding modes, then use it to describe the plant. Therefore, we get a very close approximation while obtaining a low order plant.

Table 6.1. Damping ratios $(\zeta_i\text{'s})$ of approximated system transfer functions.

	ζ_0	ζ_1	ζ_2	ζ_3	ζ_4	ζ_5
$\mathbf{P(x,s)/d(s)}$ at $\mathbf{x = 2.8}$ m	82.5	0.0325	0.0172	0.0125	0.0106	0.0098
$\mathbf{P(x,s)/q(s)}$ at $\mathbf{x = 2.8}$ m	85.5	0.0326	0.0172	0.0125	0.0106	0.0102
$\mathbf{P(x,s)/d(s)}$ at $\mathbf{x = 3.1}$ m	80.0	0.0326	0.0172	0.0125	0.0105	0.0095
$\mathbf{P(x,s)/q(s)}$ at $\mathbf{x = 3.1}$ m	83.0	0.0327	0.0173	0.0126	0.0105	0.0096
$\mathbf{P(x,s)/d(s)}$ at $\mathbf{x = 3.4}$ m	79.5	0.0325	0.0172	0.0126	0.0105	0.0095
$\mathbf{P(x,s)/q(s)}$ at $\mathbf{x = 3.4}$ m	82.0	0.0326	0.0172	0.0125	0.0105	0.0096

Table 6.2. Damped natural frequencies(f_{di}'s) of approximated system transfer functions (in Hz).

	$\mathbf{f_{d0}}$	$\mathbf{f_{d1}}$	$\mathbf{f_{d2}}$	$\mathbf{f_{d3}}$	$\mathbf{f_{d4}}$	$\mathbf{f_{d5}}$
$\mathbf{P(x,s)/d(s)}$ **at x = 2.8 m**	0.01	48.67	97.28	145.91	194.54	243.08
$\mathbf{P(x,s)/q(s)}$ **at x = 2.8 m**	0.01	48.72	97.30	145.91	194.51	242.95
$\mathbf{P(x,s)/d(s)}$ **at x = 3.1 m**	0.01	48.68	97.29	145.93	194.60	243.29
$\mathbf{P(x,s)/q(s)}$ **at x = 3.1 m**	0.01	48.72	97.31	145.93	194.57	243.16
$\mathbf{P(x,s)/d(s)}$ **at x = 3.4 m**	0.01	48.64	97.29	145.94	194.61	243.31
$\mathbf{P(x,s)/q(s)}$ **at x = 3.4 m**	0.01	48.69	97.30	145.93	194.58	243.18

Then, we reduced the order of the plant to 12 states. Thus, we provided that our controllers have 12 states as well. Having low order controllers mean less computation time and fast response, which is crucial in real physical system implementations.

6.2.2.1. Frequency Domain Results. Here, we give frequency response results for uncontrolled and controlled systems. In Bode plots, approximated finite dimensional transfer functions are used.

Figure 6.17 shows the frequency response of uncontrolled and controlled systems at $x_m = 2.8$ m. Figure 6.18 shows the frequency response of uncontrolled and controlled systems at $x = 3.1$ m. Figure 6.19 shows the frequency response of uncontrolled and controlled systems at the duct end $x = 3.4$ m.
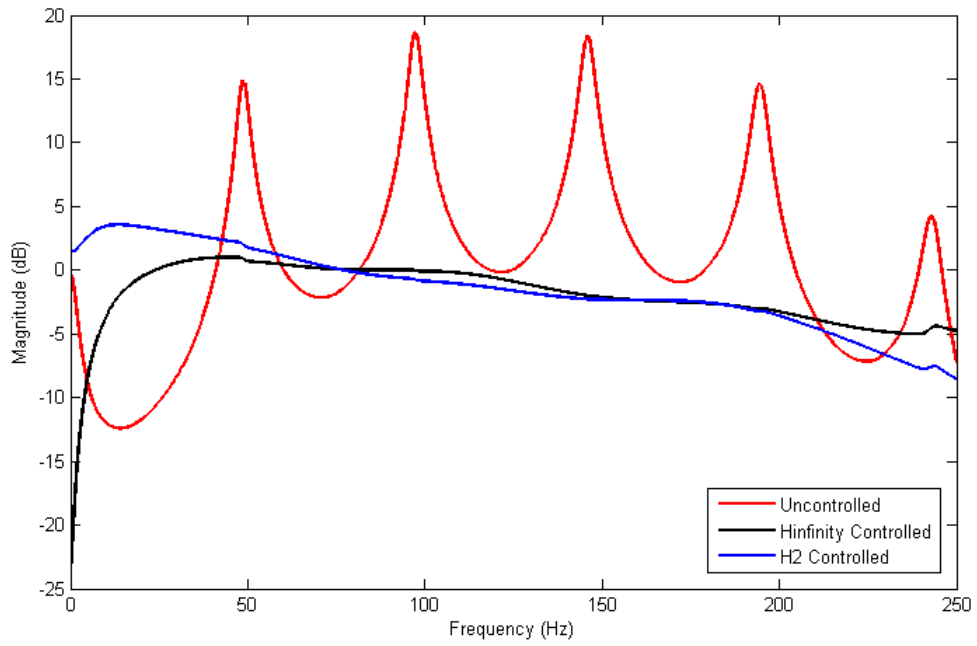
Figure 6.17. Frequency response of uncontrolled and controlled systems at $x_m = 2.8$ m (red - uncontrolled, blue - H_2 controlled, black - H_∞ controlled).
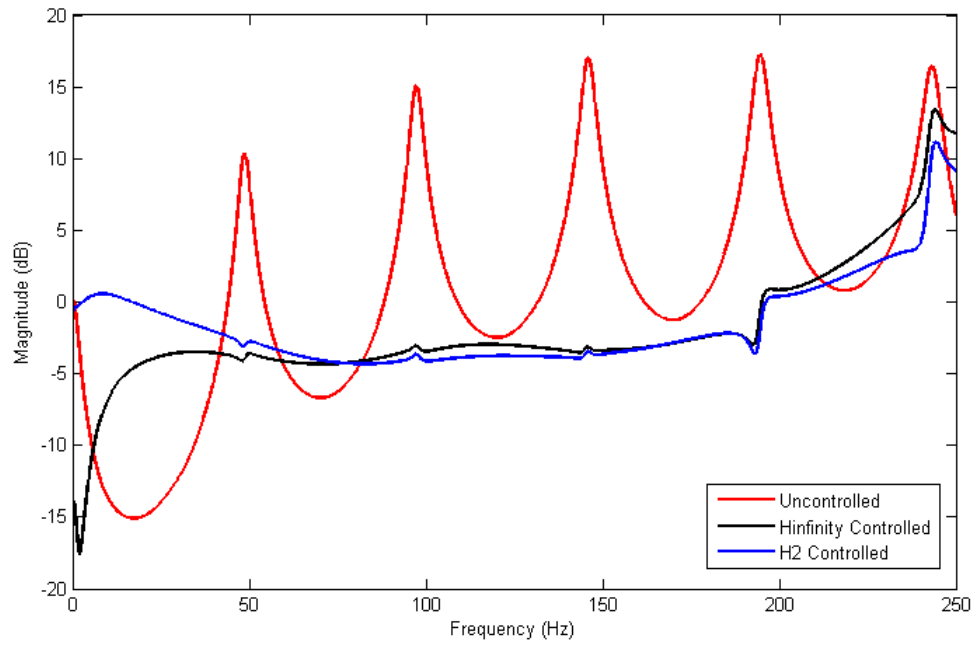
Figure 6.18. Frequency response of uncontrolled and controlled systems at $x = 3.1$ m (red - uncontrolled, blue - H_2 controlled, black - H_∞ controlled).
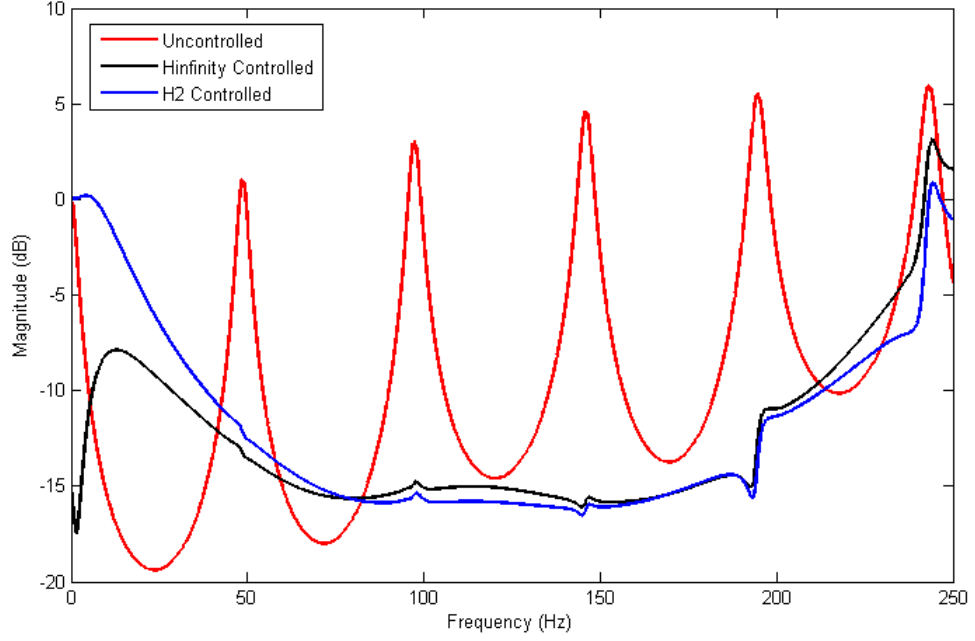
Figure 6.19. Frequency response of uncontrolled and controlled systems at the duct end $x = 3.4$ m (red - uncontrolled, blue - H_2 controlled, black - H_∞ controlled).

<u>6.2.2.2. Time Domain Results.</u> In this part, we give time domain simulation results obtained from Simulink by using approximated system transfer functions.

The disturbance signal used in time domain simulations is a summation of ten sine waves. All of these sine waves have amplitude 1 Pa. Ten different frequencies for these sine waves are: 25, 48.67, 75, 97.28, 125, 145.91, 175, 194.54, 225 and 243.08 Hz. Note that; 48.67, 97.28, 145.91, 194.54, 243.08 Hz frequencies are duct's first five damped natural frequencies. This broadband disturbance signal is shown in Figure 6.20.

Time domain uncontrolled and controlled system response at measuring point $(x_m = 2.8$ m) to this disturbance signal is shown in Figure 6.21. Time domain uncontrolled and controlled system response at $x = 3.1$ m to disturbance signal shown in Figure 6.20 is given in Figure 6.22. Time domain uncontrolled and controlled system response at the duct end $(x = 3.4$ m) to disturbance signal shown in Figure 6.20 is given below in Figure 6.23.
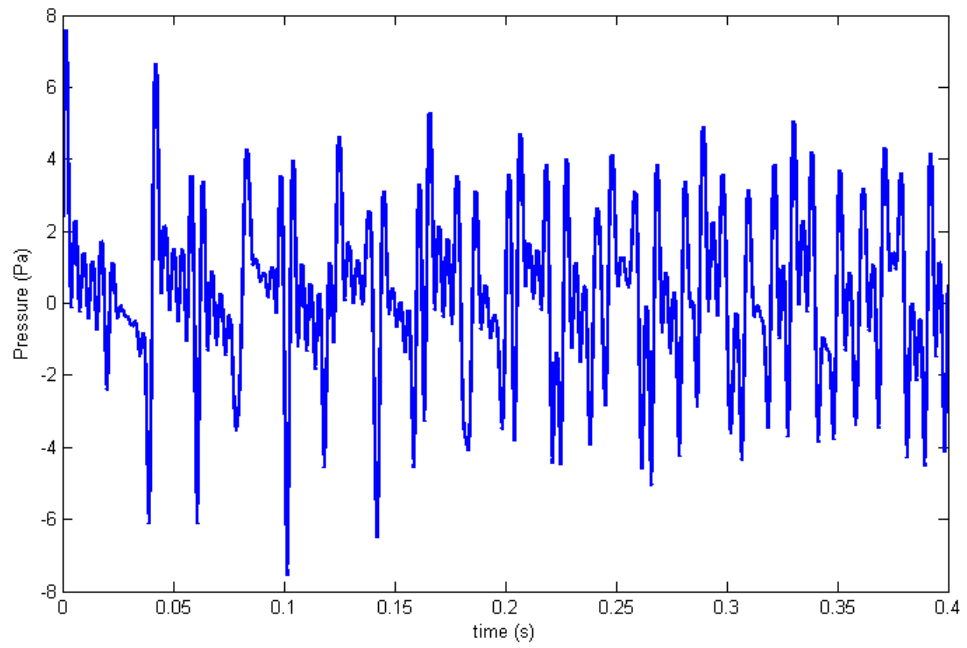
Figure 6.20. Disturbance signal used in time domain simulations for frequency dependent impedance boundary condition.
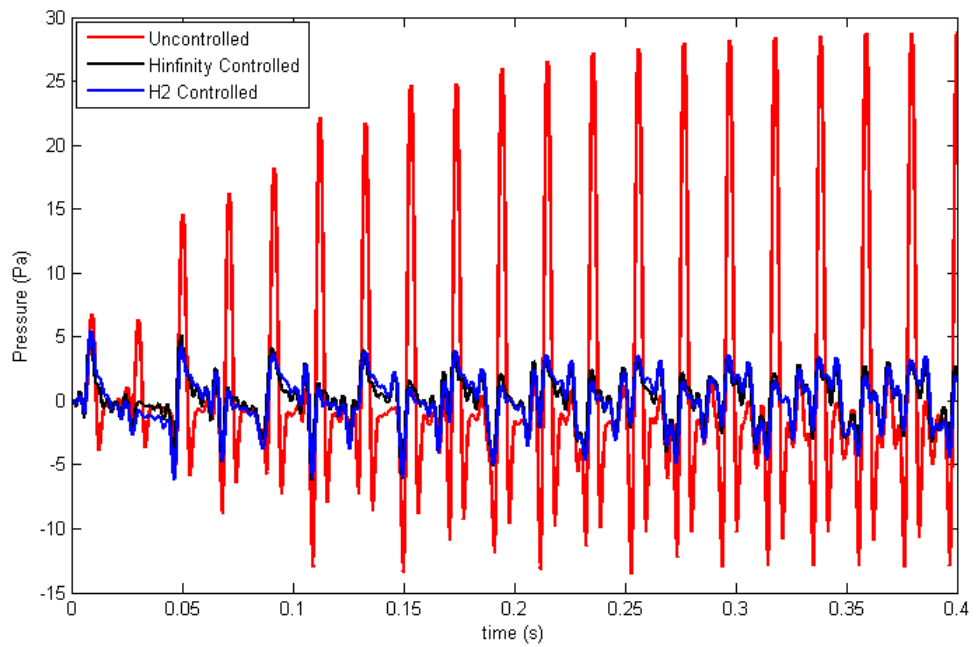
Figure 6.21. Time domain uncontrolled and controlled system responses at $x_m = 2.8$ m (red - uncontrolled, blue - H_2 controlled, black - H_∞ controlled).
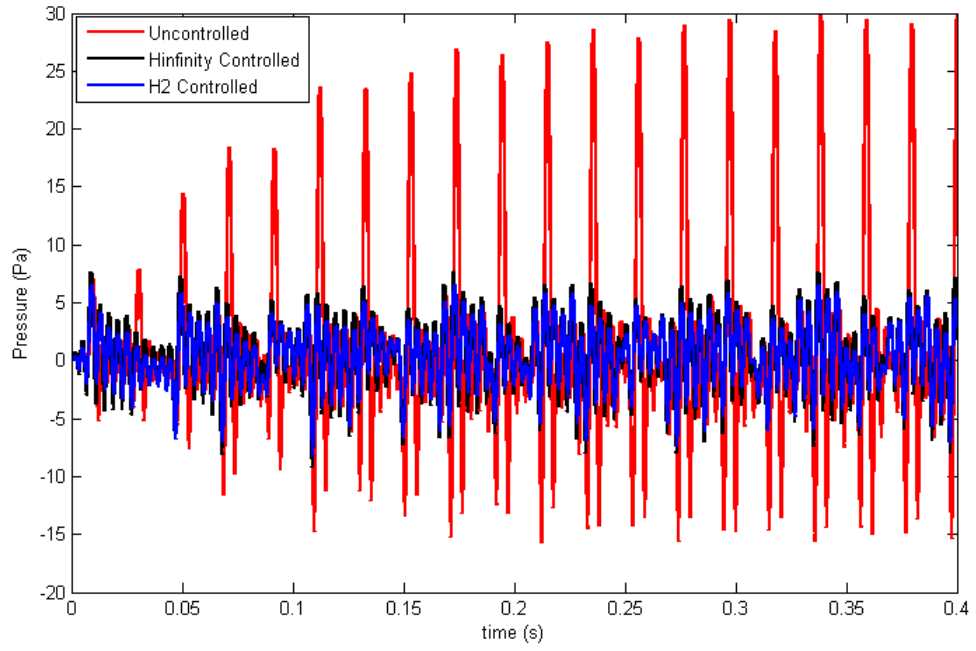
Figure 6.22. Time domain uncontrolled and controlled system responses at $x = 3.1$ m (red - uncontrolled, blue - H_2 controlled, black - H_∞ controlled).
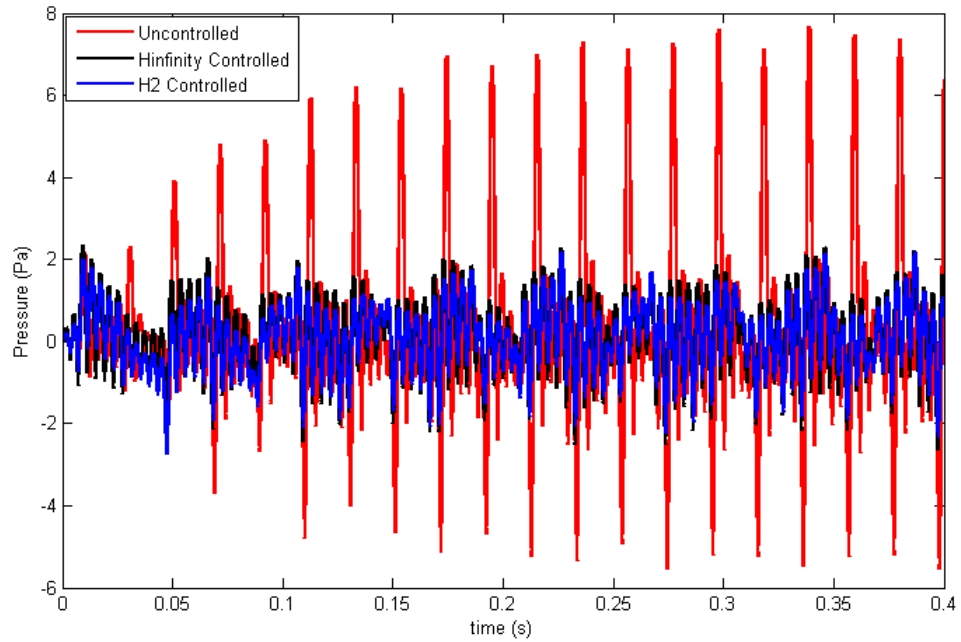
Figure 6.23. Time domain uncontrolled and controlled system responses at the duct end $x = 3.4$ m (red - uncontrolled, blue - H_2 controlled, black - H_∞ controlled).

6.2.2.3. Discussions.   As it can be seen from Figure 6.17, our optimal controllers show good noise reduction behavior at microphone point (x_m). So, our suggested reduced order approximated plant is adequate for controller synthesis. As can be seen from the same figure, near the first and the last mode natural frequencies, the closed loop frequency response deviates a little. It is probably because of approximated damping ratios and damped natural frequencies. But, since the variation of these parameters are very small, it does not cause a serious problem.

From Figure 6.17, we observe that H_∞ performance is better at low frequencies, whereas H_2 performance is superior at high frequencies. But overall, we can conclude that, H_∞ design demonstrates better performance characteristics throughout the frequency range of interest. At some frequencies, closed loop system shows worse results than the uncontrolled system. But at overall, this does not cause a big problem because of the low dB values observed. With controllers, we provide a smooth frequency response plot and avoided resonance peaks. Thus, at the performance point we achieved good noise reduction.

In Figure 6.18, we observe similar characteristics which are considered above. Again H_2 performance is better at high frequencies. But, even though we achieved to reduce the noise levels at most of the bandwidth, our controllers' performances are low at the fifth mode. In addition to that, at resonance frequencies we have a more wavy plot. Those defects in performance are encountered because we design our controllers to reduce noise levels at one particular point. But, since variation in damping ratios and damped natural frequencies are low, our low order controller works reasonably well at most of the target bandwidth.

Figure 6.19 shows the controller's performance at the duct end. Again, H_2 is better at high frequencies. But overall, H_∞ is superior then H_2. All of the peaks are suppressed. At the fifth mode again performance decreases but it does not cause a problem because of the low dB values observed. Similarly, around resonance frequency regions wavy closed loop plots are observed.

To sum up, by our low order controller designs we obtained smooth closed loop frequency responses and, we achieved to suppress noise levels along the end section of the duct. H_2 and H_∞ performances are similar, but overall H_∞ shows better results.

Time domain simulations shown in Figure 6.21 - 6.23 also validate the results obtained in the frequency domain. A broadband signal shown in Figure 6.20 is significantly suppressed.

Using simple low pass weights in controller designs did not change closed loop performance dramatically. Waterbed effect is observed due to weights used, i.e., at some frequencies, closed loop performance is getting better, whereas at some other frequencies, it is getting worse. The controllers' orders also increase depending on the orders of weights that are used. Despite the increase in orders of controllers, the closed loop performances did not improve much. Thus, we avoided to include weights in our controller designs.

7. CONCLUSIONS

In this thesis, active noise control in a duct, in which mean flow of fluid medium exists, is studied. We derive a one-dimensional acoustic duct model with flow; by using equation of state, equation of motion and equation of continuity. Our acoustic sources are disturbance signal at one end of the duct and canceling source's (actuator's) control signal somewhere inside the duct. Our canceling source is considered as a point source. At the other end of the duct, both open and frequency dependent acoustic impedance boundary conditions are considered.

We solve the acoustic duct model in Laplace domain to get infinite dimensional system transfer functions. For this purpose, initial conditions are taken as "zero" which is a routine procedure for obtaining transfer functions in control theory. System transfer functions are obtained for; no flow case with open BC, no flow case with frequency dependent impedance BC, mean flow case with open BC and mean flow case with frequency dependent impedance BC. It is observed that, mean flow cause a shift in resonance frequencies. We also see that, resonance frequencies in open boundary condition case are undamped natural frequencies, whereas resonance frequencies in frequency dependent impedance boundary condition case are damped natural frequencies which is more realistic.

For controller synthesis purposes, we suggest a duct configuration in which any antiresonances due to canceling source (actuator) and measuring device (microphone) are avoided. Depending on our target frequency range in which we want to suppress unwanted noise, we can move source and microphone to get rid of any antiresonances. By this way, we avoided to measure "zero" pressure values, and provided that canceling source will always work for the selected frequency region.

In our ANC system, we use a feedback configuration in which, microphone is located at downstream, and source is located at upstream of the duct. A microphone and a source are used, thus a SISO system is obtained. In controller synthesis LTI

finite dimensional control theory is utilized and H_2 and H_∞ optimal controllers are designed with LMI formulations.

In our case studies, we proposed two approximation schemes (for open BC and frequency dependent impedance BC) to obtain finite dimensional transfer function approximations of infinite dimensional system transfer functions. We avoided all antiresonances (zeros) in our frequency range, therefore, in our approximations we only consider the resonances (poles). In the selected frequency range, our approximations represent the original system well. According to the duct parameters specified, we obtain low order approximations, and these approximations are used in finite dimensional optimal controller synthesis.

A control objective, which neglects small variations in damping ratios and damped natural frequencies of approximated transfer functions, is specified. As a result, a minimal and balanced plant realization is obtained, i.e., our plant order is further reduced. Thus, our controllers' orders are reduced as well. Designed low order H_2 and H_∞ controllers show potential to suppress the unwanted noise. For open BC case, nearly flat and very smooth frequency response plots of closed loop system are observed. For frequency dependent impedance BC case, synthesized controllers still work. But, closed loop frequency responses are not as smooth as the open end case, since frequency dependent impedance BC case represents a more realistic case. Nevertheless, we achieved noise reduction at the end section of the duct. Time domain simulations also validate the results obtained from the frequency domain analyses.

8. FUTURE WORK

Here are some of the possible future studies about this subject:

- Robustness is not considered in this study. It could be included in a future work, in which uncertainties in transfer function approximations are taken into account. These uncertainties are small variations in damping ratios and damped natural frequencies in frequency dependent impedance BC case.
- Experiments can be conducted to validate the theoretical and numerical studies done in this thesis.
- In a more advanced study, theoretical findings and signal processing tools can be combined to synthesize an advanced robust controller. Then, in an experimental setup, this advanced controller can be tested. By this kind of controller synthesis, one could benefit from both physical laws and digital data obtained from actual system.

APPENDIX A: MATLAB CODES FOR MEAN FLOW CASE

In this section we give our MATLAB codes used in our study. We give our primary attention to mean flow case impedance end boundary condition system, for the sake of saving space in our thesis. The codes for other relatively simple cases (open end boundary condition and no flow cases) can also be obtained in the same manner.

A.1. Codes for Open Boundary Condition

A.1.1. Least Squares Approximation for $d(s)$ to $P(x, s)$ Transfer Function

```
%This program calculates the frequency response of the transfer function
%from disturbance d to P for open end boundary condition
%for MEAN FLOW case
clear all
clc
c=340;
L=3.4;
U=34;
a=c^2/(c^2-U^2);
x=3.0;
f=0.01;
for i=1:40000
    s=j*2*pi*f;
    AA=exp(x*s*U/(c^2-U^2));
    BB=exp(-x*s/c*a);
    DD=exp(-(2*L-x)*s/c*a);
    EE=exp(-2*L*s/c*a);
    Pexact(i)=AA*(BB-DD)/(1-EE);
    Gexact(i)=20*log10(abs(Pexact(i)));
    Phiexact(i)=atan(imag(Pexact(i))/real(Pexact(i)));
    f=f+0.01;
end
for i=1:25000
    YB(i)=imag(Pexact(i));
    YA(i)=real(Pexact(i));
end
for i=1:5
    w(i)=2*pi*49.5*i;
```

```
end
f=0.01;
for m=1:25000
    for n=1:5
        s=j*2*pi*f;
        Xreal(m,n)=1/(s^2+w(n)^2);
    end
    f=f+0.01;
end
Aestimated=inv(Xreal'*Xreal)*Xreal'*YA'
f=0.01;
for m=1:25000
    for n=1:5
        s=j*2*pi*f;
        Xdummy(m,n)=s/(s^2+w(n)^2);
        Ximag(m,n)=imag(Xdummy(m,n));
    end
    f=f+0.01;
end
Bestimated=inv(Ximag'*Ximag)*Ximag'*YB'
f=0.01;
for i=1:40000
    s=j*2*pi*f;
    P(i)=(Aestimated(1)+Bestimated(1)*s)/(s^2+w(1)^2)+
    (Aestimated(2)+Bestimated(2)*s)/(s^2+w(2)^2)+
    (Aestimated(3)+Bestimated(3)*s)/(s^2+w(3)^2)+
    (Aestimated(4)+Bestimated(4)*s)/(s^2+w(4)^2)+
    (Aestimated(5)+Bestimated(5)*s)/(s^2+w(5)^2);
    G(i)=20*log10(abs(P(i)));
    Phi(i)=atan(imag(P(i))/real(P(i)));
    f=f+0.01;
end
```

A.1.2. Least Squares Approximation for $q(s)$ to $P(x, s)$ Transfer Function

The codes for least squares approximation for $q(s)$ to $P(x, s)$ transfer function is also similar to the one just mentioned above. The only difference is; exact frequency domain values are obtained from $q(s)$ to $P(x, s)$ infinite dimensional system transfer function.

A.2. Codes for Frequency Dependent Impedance Boundary Condition

A.2.1. Least Squares Approximation for $d(s)$ to $P(x, s)$ Transfer Function

The codes for least squares approximation for $d(s)$ to $P(x, s)$ transfer function is similar to the one just mentioned below. The only difference is; exact frequency domain values are obtained from $d(s)$ to $P(x, s)$ infinite dimensional system transfer function. In previous section, we gave explicit code for $d(s)$ to $P(x, s)$ transfer function, thus in this section we decided to give $q(s)$ to $P(x, s)$ transfer function to provide complete view of subject while avoiding unnecessary information.

A.2.2. Least Squares Approximation for $q(s)$ to $P(x, s)$ Transfer Function

```
%This program calculates the least squares estimates for mean flow case for
%impedance end BC for q to P transfer function
clear all
clc
c=340;
u=34;
L=3.4;
rho=1.2;
a=c^2/(c^2-u^2);
%------------------------------------------
x=3.4;
xs=0.6;
%------------------------------------------
r=0.1;
R2=rho*c/(pi*r^2);
R1=0.504*R2;
CC=5.44*r^3/(rho*c^2);
M=0.1952*rho/r;
%------------------------------------------
%CALCULATIONS FOR ZETAO
f=0.01;
for i=1:2000
    s=j*2*pi*f;
    %--------------------------------------------------
    Z(i)=pi*r^2*((R1+R2)*M*s+R1*R2*M*CC*s^2)/((R1+R2)+(M+R1*R2*CC)*s+R1*M*CC*s^2);
    %--------------------------------------------------
    delay1=exp(-s*x*a/c);
    delay2=exp(s*x*a/c);
    delay3=exp(s*x*u*a/c^2);
```

```
    delay4=exp(-s*xs*a/c);
    delay5=exp(s*xs*a/c);
    delay6=exp(-s*xs*u*a/c^2);
    delay7=exp(2*L*s*a/c);
    %----------------------------------------------------
    AA=delay1*delay3*delay4*delay6*delay7;
    BB=delay2*delay3*delay4*delay6*delay7;
    DD=delay1*delay3*delay5*delay6;
    EE=delay2*delay3*delay5*delay6;
    FF=delay2*delay3*delay4*delay6;
    GG=delay1*delay3*delay5*delay6*delay7;
    %----------------------------------------------------
    COMP1=(c*rho+Z(i))*(c+u)^2;
    COMP2=(c*rho-Z(i))*(c-u)^2;
    COMP3=(c+u)*(c*rho+Z(i));
    COMP4=(-c+u)*(c*rho-Z(i));
    COMP5=FF*(c^2-u^2)-DD*(c-u)^2;
    COMP6=GG*(c^2-u^2)-BB*(c+u)^2;
    COMP7=BB-AA;
    COMP8=DD-EE;
    COMP9=(c*rho-Z(i));
    COMP10=(c*rho+Z(i));
    %----------------------------------------------------
    Pqexactxltxs0(i)=1/2*a*(COMP1*COMP7+COMP2*COMP8)/(delay7*COMP3+COMP4);
    Pqexactxgexs0(i)=Pqexactxltxs0(i)+1/2*a*(COMP9*COMP5+COMP10*COMP6)/(delay7*COMP3+COMP4);
    if x < xs
        Pqexact0(i)=Pqexactxltxs0(i);
    else
        Pqexact0(i)= Pqexactxgexs0(i);
    end
    Gqexact0(i)=20*log10(abs(Pqexact0(i)));
    Phiqexact0(i)=atan(imag(Pqexact0(i))/real(Pqexact0(i)));
    %----------------------------------------------------
    f=f+0.01;
end
fd0=0.01;
for i=1:2000
    OSY0=abs(max(Gqexact0)-Gqexact0(i));
    if OSY0>3
        if OSY0<3.1
            ffff(i)=0.01+0.01*(i-1);
        else
            ffff(i)=-1000;
        end
    else
        ffff(i)=-1000;
    end
end
```

```
fb0=max(ffff);
zeta0=(fb0-0)/2/fd0;
%fd0=0.01;
%zeta0=80;
clear ffff
clear Z
%CALCULATIONS FOR ZETA1
f=40;
for i=1:2000
    s=j*2*pi*f;
    %----------------------------------------------------
    Z(i)=pi*r^2*((R1+R2)*M*s+R1*R2*M*CC*s^2)/((R1+R2)+(M+R1*R2*CC)*s+R1*M*CC*s^2);
    %----------------------------------------------------
    delay1=exp(-s*x*a/c);
    delay2=exp(s*x*a/c);
    delay3=exp(s*x*u*a/c^2);
    delay4=exp(-s*xs*a/c);
    delay5=exp(s*xs*a/c);
    delay6=exp(-s*xs*u*a/c^2);
    delay7=exp(2*L*s*a/c);
    %----------------------------------------------------
    AA=delay1*delay3*delay4*delay6*delay7;
    BB=delay2*delay3*delay4*delay6*delay7;
    DD=delay1*delay3*delay5*delay6;
    EE=delay2*delay3*delay5*delay6;
    FF=delay2*delay3*delay4*delay6;
    GG=delay1*delay3*delay5*delay6*delay7;
    %----------------------------------------------------
    COMP1=(c*rho+Z(i))*(c+u)^2;
    COMP2=(c*rho-Z(i))*(c-u)^2;
    COMP3=(c+u)*(c*rho+Z(i));
    COMP4=(-c+u)*(c*rho-Z(i));
    COMP5=FF*(c^2-u^2)-DD*(c-u)^2;
    COMP6=GG*(c^2-u^2)-BB*(c+u)^2;
    COMP7=BB-AA;
    COMP8=DD-EE;
    COMP9=(c*rho-Z(i));
    COMP10=(c*rho+Z(i));
    %----------------------------------------------------
    Pqexactxltxs1(i)=1/2*a*(COMP1*COMP7+COMP2*COMP8)/(delay7*COMP3+COMP4);
    Pqexactxgexs1(i)=Pqexactxltxs1(i)+1/2*a*(COMP9*COMP5+COMP10*COMP6)/(delay7*COMP3+COMP4);
    if x < xs
        Pqexact1(i)=Pqexactxltxs1(i);
    else
        Pqexact1(i)= Pqexactxgexs1(i);
    end
    Gqexact1(i)=20*log10(abs(Pqexact1(i)));
    Phiqexact1(i)=atan(imag(Pqexact1(i))/real(Pqexact1(i)));
```

```
    %------------------------------------------------------
    f=f+0.01;
end
[MAXMAG1,IMAX1] = max(Gqexact1);
fd1=40+0.01*(IMAX1-1);
for i=1:2000
    OSY1=MAXMAG1-Gqexact1(i);
    if OSY1<3
        if OSY1<3.1
            ffff(i)=40+0.01*(i-1);
        else
            ffff(i)=1000;
        end
    else
        ffff(i)=1000;
    end
end
fa1=min(ffff);
clear ffff
for i=1:2000
    OSY1=MAXMAG1-Gqexact1(i);
    if OSY1<3
        if OSY1<3.1
            ffff(i)=40+0.01*(i-1);
        else
            ffff(i)=0;
        end
    else
        ffff(i)=0;
    end
end
fb1=max(ffff);
zeta1=(fb1-fa1)/2/fd1;
clear ffff
clear Z
%--------------------------------------------------------------
%CALCULATIONS FOR ZETA2
f=90;
for i=1:2000
    s=j*2*pi*f;
    %--------------------------------------------------
    Z(i)=pi*r^2*((R1+R2)*M*s+R1*R2*M*CC*s^2)/((R1+R2)+(M+R1*R2*CC)*s+R1*M*CC*s^2);
    %--------------------------------------------------
    delay1=exp(-s*x*a/c);
    delay2=exp(s*x*a/c);
    delay3=exp(s*x*u*a/c^2);
    delay4=exp(-s*xs*a/c);
    delay5=exp(s*xs*a/c);
```

```
        delay6=exp(-s*xs*u*a/c^2);
        delay7=exp(2*L*s*a/c);
        %--------------------------------------------------
        AA=delay1*delay3*delay4*delay6*delay7;
        BB=delay2*delay3*delay4*delay6*delay7;
        DD=delay1*delay3*delay5*delay6;
        EE=delay2*delay3*delay5*delay6;
        FF=delay2*delay3*delay4*delay6;
        GG=delay1*delay3*delay5*delay6*delay7;
        %--------------------------------------------------
        COMP1=(c*rho+Z(i))*(c+u)^2;
        COMP2=(c*rho-Z(i))*(c-u)^2;
        COMP3=(c+u)*(c*rho+Z(i));
        COMP4=(-c+u)*(c*rho-Z(i));
        COMP5=FF*(c^2-u^2)-DD*(c-u)^2;
        COMP6=GG*(c^2-u^2)-BB*(c+u)^2;
        COMP7=BB-AA;
        COMP8=DD-EE;
        COMP9=(c*rho-Z(i));
        COMP10=(c*rho+Z(i));
        %--------------------------------------------------
        Pqexactxltxs2(i)=1/2*a*(COMP1*COMP7+COMP2*COMP8)/(delay7*COMP3+COMP4);
        Pqexactxgexs2(i)=Pqexactxltxs2(i)+1/2*a*(COMP9*COMP5+COMP10*COMP6)/(delay7*COMP3+COMP4);
        if x < xs
            Pqexact2(i)=Pqexactxltxs2(i);
        else
            Pqexact2(i)= Pqexactxgexs2(i);
        end
        Gqexact2(i)=20*log10(abs(Pqexact2(i)));
        Phiqexact2(i)=atan(imag(Pqexact2(i))/real(Pqexact2(i)));
        %--------------------------------------------------
        f=f+0.01;
end
[MAXMAG2,IMAX2] = max(Gqexact2);
fd2=90+0.01*(IMAX2-1);
for i=1:2000
    OSY2=MAXMAG2-Gqexact2(i);
    if OSY2<3
        if OSY2<3.1
            ffff(i)=90+0.01*(i-1);
        else
            ffff(i)=1000;
        end
    else
        ffff(i)=1000;
    end
end
fa2=min(ffff);
```

```
clear ffff
for i=1:2000
    OSY2=MAXMAG2-Gqexact2(i);
    if OSY2<3
        if OSY2<3.1
            ffff(i)=90+0.01*(i-1);
        else
            ffff(i)=0;
        end
    else
        ffff(i)=0;
    end
end
fb2=max(ffff);
zeta2=(fb2-fa2)/2/fd2;
clear ffff
clear Z
%CALCULATIONS FOR ZETA3
f=140;
for i=1:2000
    s=j*2*pi*f;
    %---------------------------------------------------
    Z(i)=pi*r^2*((R1+R2)*M*s+R1*R2*M*CC*s^2)/((R1+R2)+(M+R1*R2*CC)*s+R1*M*CC*s^2);
    %---------------------------------------------------
    delay1=exp(-s*x*a/c);
    delay2=exp(s*x*a/c);
    delay3=exp(s*x*u*a/c^2);
    delay4=exp(-s*xs*a/c);
    delay5=exp(s*xs*a/c);
    delay6=exp(-s*xs*u*a/c^2);
    delay7=exp(2*L*s*a/c);
    %---------------------------------------------------
    AA=delay1*delay3*delay4*delay6*delay7;
    BB=delay2*delay3*delay4*delay6*delay7;
    DD=delay1*delay3*delay5*delay6;
    EE=delay2*delay3*delay5*delay6;
    FF=delay2*delay3*delay4*delay6;
    GG=delay1*delay3*delay5*delay6*delay7;
    %---------------------------------------------------
    COMP1=(c*rho+Z(i))*(c+u)^2;
    COMP2=(c*rho-Z(i))*(c-u)^2;
    COMP3=(c+u)*(c*rho+Z(i));
    COMP4=(-c+u)*(c*rho-Z(i));
    COMP5=FF*(c^2-u^2)-DD*(c-u)^2;
    COMP6=GG*(c^2-u^2)-BB*(c+u)^2;
    COMP7=BB-AA;
    COMP8=DD-EE;
    COMP9=(c*rho-Z(i));
```

```
    COMP10=(c*rho+Z(i));
    %----------------------------------------------------
    Pqexactxltxs3(i)=1/2*a*(COMP1*COMP7+COMP2*COMP8)/(delay7*COMP3+COMP4);
    Pqexactxgexs3(i)=Pqexactxltxs3(i)+1/2*a*(COMP9*COMP5+COMP10*COMP6)/(delay7*COMP3+COMP4);
    if x < xs
        Pqexact3(i)=Pqexactxltxs3(i);
    else
        Pqexact3(i)= Pqexactxgexs3(i);
    end
    Gqexact3(i)=20*log10(abs(Pqexact3(i)));
    Phiqexact3(i)=atan(imag(Pqexact3(i))/real(Pqexact3(i)));
    %----------------------------------------------------
    f=f+0.01;
end
[MAXMAG3,IMAX3] = max(Gqexact3);
fd3=140+0.01*(IMAX3-1);
for i=1:2000
    OSY3=MAXMAG3-Gqexact3(i);
    if OSY3<3
        if OSY3<3.1
            ffff(i)=140+0.01*(i-1);
        else
            ffff(i)=1000;
        end
    else
        ffff(i)=1000;
    end
end
fa3=min(ffff);
clear ffff
for i=1:2000
    OSY3=MAXMAG3-Gqexact3(i);
    if OSY3<3
        if OSY3<3.1
            ffff(i)=140+0.01*(i-1);
        else
            ffff(i)=0;
        end
    else
        ffff(i)=0;
    end
end
fb3=max(ffff);
zeta3=(fb3-fa3)/2/fd3;
clear ffff
clear Z
%CALCULATIONS FOR ZETA4
f=190;
```

```
for i=1:2000
    s=j*2*pi*f;
    %--------------------------------------------------
    Z(i)=pi*r^2*((R1+R2)*M*s+R1*R2*M*CC*s^2)/((R1+R2)+(M+R1*R2*CC)*s+R1*M*CC*s^2);
    %--------------------------------------------------
    delay1=exp(-s*x*a/c);
    delay2=exp(s*x*a/c);
    delay3=exp(s*x*u*a/c^2);
    delay4=exp(-s*xs*a/c);
    delay5=exp(s*xs*a/c);
    delay6=exp(-s*xs*u*a/c^2);
    delay7=exp(2*L*s*a/c);
    %--------------------------------------------------
    AA=delay1*delay3*delay4*delay6*delay7;
    BB=delay2*delay3*delay4*delay6*delay7;
    DD=delay1*delay3*delay5*delay6;
    EE=delay2*delay3*delay5*delay6;
    FF=delay2*delay3*delay4*delay6;
    GG=delay1*delay3*delay5*delay6*delay7;
    %--------------------------------------------------
    COMP1=(c*rho+Z(i))*(c+u)^2;
    COMP2=(c*rho-Z(i))*(c-u)^2;
    COMP3=(c+u)*(c*rho+Z(i));
    COMP4=(-c+u)*(c*rho-Z(i));
    COMP5=FF*(c^2-u^2)-DD*(c-u)^2;
    COMP6=GG*(c^2-u^2)-BB*(c+u)^2;
    COMP7=BB-AA;
    COMP8=DD-EE;
    COMP9=(c*rho-Z(i));
    COMP10=(c*rho+Z(i));
    %--------------------------------------------------
    Pqexactxltxs4(i)=1/2*a*(COMP1*COMP7+COMP2*COMP8)/(delay7*COMP3+COMP4);
    Pqexactxgexs4(i)=Pqexactxltxs4(i)+1/2*a*(COMP9*COMP5+COMP10*COMP6)/(delay7*COMP3+COMP4);
    if x < xs
        Pqexact4(i)=Pqexactxltxs4(i);
    else
        Pqexact4(i)= Pqexactxgexs4(i);
    end
    Gqexact4(i)=20*log10(abs(Pqexact4(i)));
    Phiqexact4(i)=atan(imag(Pqexact4(i))/real(Pqexact4(i)));
    %--------------------------------------------------
    f=f+0.01;
end
[MAXMAG4,IMAX4] = max(Gqexact4);
fd4=190+0.01*(IMAX4-1);
for i=1:2000
    OSY4=MAXMAG4-Gqexact4(i);
    if OSY4<3
```

```
        if OSY4<3.1
            ffff(i)=190+0.01*(i-1);
        else
            ffff(i)=1000;
        end
    else
        ffff(i)=1000;
    end
end
fa4=min(ffff);
clear ffff
for i=1:2000
    OSY4=MAXMAG4-Gqexact4(i);
    if OSY4<3
        if OSY4<3.1
            ffff(i)=190+0.01*(i-1);
        else
            ffff(i)=0;
        end
    else
        ffff(i)=0;
    end
end
fb4=max(ffff);
zeta4=(fb4-fa4)/2/fd4;
clear ffff
clear Z
%CALCULATIONS FOR ZETA5
f=235;
for i=1:2000
    s=j*2*pi*f;
    %--------------------------------------------------
    Z(i)=pi*r^2*((R1+R2)*M*s+R1*R2*M*CC*s^2)/((R1+R2)+(M+R1*R2*CC)*s+R1*M*CC*s^2);
    %--------------------------------------------------
    delay1=exp(-s*x*a/c);
    delay2=exp(s*x*a/c);
    delay3=exp(s*x*u*a/c^2);
    delay4=exp(-s*xs*a/c);
    delay5=exp(s*xs*a/c);
    delay6=exp(-s*xs*u*a/c^2);
    delay7=exp(2*L*s*a/c);
    %--------------------------------------------------
    AA=delay1*delay3*delay4*delay6*delay7;
    BB=delay2*delay3*delay4*delay6*delay7;
    DD=delay1*delay3*delay5*delay6;
    EE=delay2*delay3*delay5*delay6;
    FF=delay2*delay3*delay4*delay6;
    GG=delay1*delay3*delay5*delay6*delay7;
```

```
    %------------------------------------------------
    COMP1=(c*rho+Z(i))*(c+u)^2;
    COMP2=(c*rho-Z(i))*(c-u)^2;
    COMP3=(c+u)*(c*rho+Z(i));
    COMP4=(-c+u)*(c*rho-Z(i));
    COMP5=FF*(c^2-u^2)-DD*(c-u)^2;
    COMP6=GG*(c^2-u^2)-BB*(c+u)^2;
    COMP7=BB-AA;
    COMP8=DD-EE;
    COMP9=(c*rho-Z(i));
    COMP10=(c*rho+Z(i));
    %--------------------------------------------------
    Pqexactxltxs5(i)=1/2*a*(COMP1*COMP7+COMP2*COMP8)/(delay7*COMP3+COMP4);
    Pqexactxgexs5(i)=Pqexactxltxs5(i)+1/2*a*(COMP9*COMP5+COMP10*COMP6)/(delay7*COMP3+COMP4);
    if x < xs
        Pqexact5(i)=Pqexactxltxs5(i);
    else
        Pqexact5(i)= Pqexactxgexs5(i);
    end
    Gqexact5(i)=20*log10(abs(Pqexact5(i)));
    Phiqexact5(i)=atan(imag(Pqexact5(i))/real(Pqexact5(i)));
    %----------------------------------------------------
    f=f+0.01;
end
[MAXMAG5,IMAX5] = max(Gqexact5);
fd5=235+0.01*(IMAX5-1);
for i=1:2000
    OSY5=MAXMAG5-Gqexact5(i);
    if OSY5<3
        if OSY5<3.1
            ffff(i)=235+0.01*(i-1);
        else
            ffff(i)=1000;
        end
    else
        ffff(i)=1000;
    end
end
fa5=min(ffff);
clear ffff
for i=1:2000
    OSY5=MAXMAG5-Gqexact5(i);
    if OSY5<3
        if OSY5<3.1
            ffff(i)=235+0.01*(i-1);
        else
            ffff(i)=0;
        end
```

```
    else
        ffff(i)=0;
    end
end
fb5=max(ffff);
zeta5=(fb5-fa5)/2/fd5;
clear ffff
clear Z
%-----------------------------------------------------------
%THIS SECTION CALCULATES THE EXACT FREQUENCY RESPONSE VALUES FOR 25000 DATA
%POINTS
f=0.01;
for i=1:40000
    s=j*2*pi*f;
    %--------------------------------------------------
    Z(i)=pi*r^2*((R1+R2)*M*s+R1*R2*M*CC*s^2)/((R1+R2)+(M+R1*R2*CC)*s+R1*M*CC*s^2);
    %--------------------------------------------------
    delay1=exp(-s*x*a/c);
    delay2=exp(s*x*a/c);
    delay3=exp(s*x*u*a/c^2);
    delay4=exp(-s*xs*a/c);
    delay5=exp(s*xs*a/c);
    delay6=exp(-s*xs*u*a/c^2);
    delay7=exp(2*L*s*a/c);
    %--------------------------------------------------
    AA=delay1*delay3*delay4*delay6*delay7;
    BB=delay2*delay3*delay4*delay6*delay7;
    DD=delay1*delay3*delay5*delay6;
    EE=delay2*delay3*delay5*delay6;
    FF=delay2*delay3*delay4*delay6;
    GG=delay1*delay3*delay5*delay6*delay7;
    %--------------------------------------------------
    COMP1=(c*rho+Z(i))*(c+u)^2;
    COMP2=(c*rho-Z(i))*(c-u)^2;
    COMP3=(c+u)*(c*rho+Z(i));
    COMP4=(-c+u)*(c*rho-Z(i));
    COMP5=FF*(c^2-u^2)-DD*(c-u)^2;
    COMP6=GG*(c^2-u^2)-BB*(c+u)^2;
    COMP7=BB-AA;
    COMP8=DD-EE;
    COMP9=(c*rho-Z(i));
    COMP10=(c*rho+Z(i));
    %--------------------------------------------------
    Pqexactxltxs(i)=1/2*a*(COMP1*COMP7+COMP2*COMP8)/(delay7*COMP3+COMP4);
    Pqexactxgexs(i)=Pqexactxltxs(i)+1/2*a*(COMP9*COMP5+COMP10*COMP6)/(delay7*COMP3+COMP4);
    if x < xs
        Pqexact(i)=Pqexactxltxs(i);
    else
```

```
        Pqexact(i)= Pqexactxgexs(i);
    end
    Gqexact(i)=20*log10(abs(Pqexact(i)));
    Phiqexact(i)=atan(imag(Pqexact(i))/real(Pqexact(i)));
    %-----------------------------------------------------
    f=f+0.01;
end
%----------------------------------------------------------------
%THIS SECTION CALCULATES Y vector for Least Squares Estimation
for i=1:25000
    Y1(i)=real(Pqexact(i));
    Y2(i)=imag(Pqexact(i));
end
%----------------------------------------------------------------
Y=[Y1';Y2'];
%----------------------------------------------------------------
%THIS SECTION DECLARES wn's
w0=2*pi*fd0;
w1=2*pi*fd1/(sqrt(1-zeta1^2));
w2=2*pi*fd2/(sqrt(1-zeta2^2));
w3=2*pi*fd3/(sqrt(1-zeta3^2));
w4=2*pi*fd4/(sqrt(1-zeta4^2));
w5=2*pi*fd5/(sqrt(1-zeta5^2));
%----------------------------------------------------------------
%THIS SECTION CALCULATES THE REGROSSOR MATRIX X
f=0.01;
for i=1:25000
w=2*pi*f;
Z0=2*zeta0*w0;
Z1=2*zeta1*w1;
Z2=2*zeta2*w2;
Z3=2*zeta3*w3;
Z4=2*zeta4*w4;
Z5=2*zeta5*w5;
P1=Z1+Z2;
P2=w1^2+w2^2+Z1*Z2;
P3=w1^2*Z2+w2^2*Z1;
P4=w1^2*w2^2;
P5=P1+Z3;
P6=P1*Z3+P2+w3^2;
P7=P1*w3^2+P2*Z3+P3;
P8=P2*w3^2+P3*Z3+P4;
P9=P3*w3^2+P4*Z3;
P10=P4*w3^2;
P11=Z4+P5;
P12=w4^2+P5*Z4+P6;
P13=P5*w4^2+P6*Z4+P7;
P14=P6*w4^2+P7*Z4+P8;
```

```
P15=P7*w4^2+P8*Z4+P9;
P16=P8*w4^2+P9*Z4+P10;
P17=P9*w4^2+P10*Z4;
P18=P10*w4^2;
P19=Z5+P11;
P20=w5^2+P11*Z5+P12;
P21=P11*w5^2+P12*Z5+P13;
P22=P12*w5^2+P13*Z5+P14;
P23=P13*w5^2+P14*Z5+P15;
P24=P14*w5^2+P15*Z5+P16;
P25=P15*w5^2+P16*Z5+P17;
P26=P16*w5^2+P17*Z5+P18;
P27=P17*w5^2+P18*Z5;
P28=P18*w5^2;
P29=P27*w;
P30=P26*(-w^2);
P31=P25*(-w^3);
P32=P24*w^4;
P33=P23*w^5;
P34=P22*(-w^6);
P35=P21*(-w^7);
P36=P20*w^8;
P37=P19*w^9;
P38=-w^10;
P39=Z2+Z3;
P40=w2^2+w3^2+Z2*Z3;
P41=w2^2*Z3+w3^2*Z2;
P42=w2^2*w3^2;
P43=Z4+Z5;
P44=w4^2+w5^2+Z4*Z5;
P45=Z4*w5^2+w4^2*Z5;
P46=w4^2*w5^2;
P47=Z1+Z3;
P48=w1^2+w3^2+Z1*Z3;
P49=Z1*w3^2+w1^2*Z3;
P50=w1^2*w3^2;
P51=P39+P43;
P52=P40+P44+P39*P43;
P53=P45+P39*P44+P40*P43+P41;
P54=P46+P39*P45+P40*P44+P41*P43+P42;
P55=P39*P46+P40*P45+P41*P44+P42*P43;
P56=P40*P46+P41*P45+P42*P44;
P57=P41*P46+P42*P45;
P58=P42*P46;
P59=P43+P47;
P60=P44+P47*P43+P48;
P61=P45+P47*P44+P48*P43+P49;
P62=P46+P47*P45+P48*P44+P49*P43+P50;
```

```
P63=P47*P46+P48*P45+P49*P44+P50*P43;
P64=P48*P46+P49*P45+P50*P44;
P65=P49*P46+P50*P45;
P66=P50*P46;
P67=P43+P1;
P68=P44+P1*P43+P2;
P69=P45+P1*P44+P2*P43+P3;
P70=P46+P1*P45+P2*P44+P3*P43+P4;
P71=P1*P46+P2*P45+P3*P44+P4*P43;
P72=P2*P46+P3*P45+P4*P44;
P73=P3*P46+P4*P45;
P74=P4*P46;
P75=Z5+P5;
P76=w5^2+P5*Z5+P6;
P77=P5*w5^2+P6*Z5+P7;
P78=P6*w5^2+P7*Z5+P8;
P79=P7*w5^2+P8*Z5+P9;
P80=P8*w5^2+P9*Z5+P10;
P81=P9*w5^2+P10*Z5;
P82=P10*w5^2;
P83=w^8;
P84=P51*(-w^7);
P85=P52*(-w^6);
P86=P53*w^5;
P87=P54*w^4;
P88=P55*(-w^3);
P89=P56*(-w^2);
P90=P57*w;
P91=P59*(-w^7);
P92=P60*(-w^6);
P93=P61*w^5;
P94=P62*w^4;
P95=P63*(-w^3);
P96=P64*(-w^2);
P97=P65*w;
P98=P67*(-w^7);
P99=P68*(-w^6);
P100=P69*w^5;
P101=P70*w^4;
P102=P71*(-w^3);
P103=P72*(-w^2);
P104=P73*w;
P105=P75*(-w^7);
P106=P76*(-w^6);
P107=P77*w^5;
P108=P78*w^4;
P109=P79*(-w^3);
P110=P80*(-w^2);
```

```
P111=P81*w;
P112=P11*(-w^7);
P113=P12*(-w^6);
P114=P13*w^5;
P115=P14*w^4;
P116=P15*(-w^3);
P117=P16*(-w^2);
P118=P17*w;
P119=P38+P36+P34+P32+P30+P28;
P120=P37+P35+P33+P31+P29;
P121=P58+P83+P85+P87+P89;
P122=P84+P86+P88+P90;
P123=P66+P83+P92+P94+P96;
P124=P91+P93+P95+P97;
P125=P74+P83+P99+P101+P103;
P126=P98+P100+P102+P104;
P127=P82+P83+P106+P108+P110;
P128=P105+P107+P109+P111;
P129=P18+P83+P113+P115+P117;
P130=P112+P114+P116+P118;
P131=P121*P119+P122*P120;
P132=P122*P119-P121*P120;
P133=P123*P119+P124*P120;
P134=P124*P119-P123*P120;
P135=P125*P119+P126*P120;
P136=P126*P119-P125*P120;
P137=P127*P119+P128*P120;
P138=P128*P119-P127*P120;
P139=P129*P119+P130*P120;
P140=P130*P119-P129*P120;
K1=Z0+P19;
K2=w0^2+P19*Z0+P20;
K3=P19*w0^2+P20*Z0+P21;
K4=P20*w0^2+P21*Z0+P22;
K5=P21*w0^2+P22*Z0+P23;
K6=P22*w0^2+P23*Z0+P24;
K7=P23*w0^2+P24*Z0+P25;
K8=P24*w0^2+P25*Z0+P26;
K9=P25*w0^2+P26*Z0+P27;
K10=P26*w0^2+P27*Z0+P28;
K11=P27*w0^2+P28*Z0;
K12=P28*w0^2;
K13=Z0+P51;
K14=w0^2+P51*Z0+P52;
K15=P51*w0^2+P52*Z0+P53;
K16=P52*w0^2+P53*Z0+P54;
K17=P53*w0^2+P54*Z0+P55;
K18=P54*w0^2+P55*Z0+P56;
```

```
K19=P55*w0^2+P56*Z0+P57;
K20=P56*w0^2+P57*Z0+P58;
K21=P57*w0^2+P58*Z0;
K22=P58*w0^2;
K23=Z0+P59;
K24=w0^2+P59*Z0+P60;
K25=P59*w0^2+P60*Z0+P61;
K26=P60*w0^2+P61*Z0+P62;
K27=P61*w0^2+P62*Z0+P63;
K28=P62*w0^2+P63*Z0+P64;
K29=P63*w0^2+P64*Z0+P65;
K30=P64*w0^2+P65*Z0+P66;
K31=P65*w0^2+P66*Z0;
K32=P66*w0^2;
K33=Z0+P67;
K34=w0^2+P67*Z0+P68;
K35=P67*w0^2+P68*Z0+P69;
K36=P68*w0^2+P69*Z0+P70;
K37=P69*w0^2+P70*Z0+P71;
K38=P70*w0^2+P71*Z0+P72;
K39=P71*w0^2+P72*Z0+P73;
K40=P72*w0^2+P73*Z0+P74;
K41=P73*w0^2+P74*Z0;
K42=P74*w0^2;
K43=Z0+P75;
K44=w0^2+P75*Z0+P76;
K45=P75*w0^2+P76*Z0+P77;
K46=P76*w0^2+P77*Z0+P78;
K47=P77*w0^2+P78*Z0+P79;
K48=P78*w0^2+P79*Z0+P80;
K49=P79*w0^2+P80*Z0+P81;
K50=P80*w0^2+P81*Z0+P82;
K51=P81*w0^2+P82*Z0;
K52=P82*w0^2;
K53=Z0+P11;
K54=w0^2+P11*Z0+P12;
K55=P11*w0^2+P12*Z0+P13;
K56=P12*w0^2+P13*Z0+P14;
K57=P13*w0^2+P14*Z0+P15;
K58=P14*w0^2+P15*Z0+P16;
K59=P15*w0^2+P16*Z0+P17;
K60=P16*w0^2+P17*Z0+P18;
K61=P17*w0^2+P18*Z0;
K62=P18*w0^2;
K63=-w^10;
K64=K13*w^9;
K65=K14*w^8;
K66=K15*(-w^7);
```

```
K67=K16*(-w^6);

K68=K17*w^5;

K69=K18*w^4;

K70=K19*(-w^3);

K71=K20*(-w^2);

K72=K21*w;

K73=K63+K65+K67+K69+K71+K22;

K74=K64+K66+K68+K70+K72;

K75=K23*w^9;

K76=K24*w^8;

K77=K25*(-w^7);

K78=K26*(-w^6);

K79=K27*w^5;

K80=K28*w^4;

K81=K29*(-w^3);

K82=K30*(-w^2);

K83=K31*w;

K84=K63+K76+K78+K80+K82+K32;

K85=K75+K77+K79+K81+K83;

K86=K33*w^9;

K87=K34*w^8;

K88=K35*(-w^7);

K89=K36*(-w^6);

K90=K37*w^5;

K91=K38*w^4;

K92=K39*(-w^3);

K93=K40*(-w^2);

K94=K41*w;

K95=K63+K87+K89+K91+K93+K42;

K96=K86+K88+K90+K92+K94;

K97=K43*w^9;

K98=K44*w^8;

K99=K45*(-w^7);

K100=K46*(-w^6);

K101=K47*w^5;

K102=K48*w^4;

K103=K49*(-w^3);

K104=K50*(-w^2);

K105=K51*w;

K106=K63+K98+K100+K102+K104+K52;

K107=K97+K99+K101+K103+K105;

K108=K53*w^9;

K109=K54*w^8;

K110=K55*(-w^7);

K111=K56*(-w^6);

K112=K57*w^5;

K113=K58*w^4;

K114=K59*(-w^3);
```

```
K115=K60*(-w^2);
K116=K61*w;
K117=K63+K109+K111+K113+K115+K62;
K118=K108+K110+K112+K114+K116;
K119=w^12;
K120=K1*(-w^11);
K121=K2*(-w^10);
K122=K3*w^9;
K123=K4*w^8;
K124=K5*(-w^7);
K125=K6*(-w^6);
K126=K7*w^5;
K127=K8*w^4;
K128=K9*(-w^3);
K129=K10*(-w^2);
K130=K11*w;
K131=K119+K121+K123+K125+K127+K129+K12;
K132=K120+K122+K124+K126+K128+K130;
K133=P119*K131+P120*K132;
K134=P120*K131-P119*K132;
K135=K73*K131+K74*K132;
K136=K74*K131-K73*K132;
K137=K84*K131+K85*K132;
K138=K85*K131-K84*K132;
K139=K95*K131+K96*K132;
K140=K96*K131-K95*K132;
K141=K106*K131+K107*K132;
K142=K107*K131-K106*K132;
K143=K117*K131+K118*K132;
K144=K118*K131-K117*K132;
%regressors for real(G(jw))
x1(i)=K135/(K131^2+K132^2);
x2(i)=K137/(K131^2+K132^2);
x3(i)=K139/(K131^2+K132^2);
x4(i)=K141/(K131^2+K132^2);
x5(i)=K143/(K131^2+K132^2);
x6(i)=K133/(K131^2+K132^2);
x7(i)=w*(-K136)/(K131^2+K132^2);
x8(i)=w*(-K138)/(K131^2+K132^2);
x9(i)=w*(-K140)/(K131^2+K132^2);
x10(i)=w*(-K142)/(K131^2+K132^2);
x11(i)=w*(-K144)/(K131^2+K132^2);
x12(i)=w*(-K134)/(K131^2+K132^2);
%regressor for imag(G(jw))
y1(i)=K136/(K131^2+K132^2);
y2(i)=K138/(K131^2+K132^2);
y3(i)=K140/(K131^2+K132^2);
y4(i)=K142/(K131^2+K132^2);
```

```
y5(i)=K144/(K131^2+K132^2);
y6(i)=K134/(K131^2+K132^2);
y7(i)=w*(K135)/(K131^2+K132^2);
y8(i)=w*(K137)/(K131^2+K132^2);
y9(i)=w*(K139)/(K131^2+K132^2);
y10(i)=w*(K141)/(K131^2+K132^2);
y11(i)=w*(K143)/(K131^2+K132^2);
y12(i)=w*(K133)/(K131^2+K132^2);
f=f+0.01;
end
X=[x1' x2' x3' x4' x5' x6' x7' x8' x9' x10' x11' x12'
y1' y2' y3' y4' y5' y6' y7' y8' y9' y10' y11' y12'];
%------------------------------------------------------------------------
%THIS SECTION CALCULATES LEAST SQUARES ESTIMATE OF Ai's and Bi's
Estimated=inv(X'*X)*X'*Y;
A_estimated=Estimated(1:6);
B_estimated=Estimated(7:12);
%------------------------------------------------------------------------
%THIS SECTION CALCULATES THE APPROXIMATED TF FREQUENCY RESPONSE
f=0.01;
for i=1:40000
    s=j*2*pi*f;
    Pqapproximated(i)=(A_estimated(6)+B_estimated(6)*s)/(s^2+2*zeta0*w0*s+w0^2)+
    (A_estimated(1)+B_estimated(1)*s)/(s^2+2*zeta1*w1*s+w1^2)+
    (A_estimated(2)+B_estimated(2)*s)/(s^2+2*zeta2*w2*s+w2^2)+
    (A_estimated(3)+B_estimated(3)*s)/(s^2+2*zeta3*w3*s+w3^2)+
    (A_estimated(4)+B_estimated(4)*s)/(s^2+2*zeta4*w4*s+w4^2)+
    (A_estimated(5)+B_estimated(5)*s)/(s^2+2*zeta5*w5*s+w5^2);
    Gqapproximated(i)=20*log10(abs(Pqapproximated(i)));
    Phiqapproximated(i)=atan(imag(Pqapproximated(i))/real(Pqapproximated(i)));
    f=f+0.01;
end
```

A.2.3. Plant Construction for Controller Synthesis

```
%After obtaining transfer function approximations at xm=2.8m
clear all
clc
load ENSONSYSTEMINFOatxm28m
fd0=(fd0dxm+fd0qxm)/2;
fd1=(fd1dxm+fd1qxm)/2;
fd2=(fd2dxm+fd2qxm)/2;
fd3=(fd3dxm+fd3qxm)/2;
fd4=(fd4dxm+fd4qxm)/2;
fd5=(fd5dxm+fd5qxm)/2;
zeta0=(zeta0dxm+zeta0qxm)/2;
```

```
zeta1=(zeta1dxm+zeta1qxm)/2;
zeta2=(zeta2dxm+zeta2qxm)/2;
zeta3=(zeta3dxm+zeta3qxm)/2;
zeta4=(zeta4dxm+zeta4qxm)/2;
zeta5=(zeta5dxm+zeta5qxm)/2;
w0=2*pi*fd0;
w1=2*pi*fd1/(sqrt(1-zeta1^2));
w2=2*pi*fd2/(sqrt(1-zeta2^2));
w3=2*pi*fd3/(sqrt(1-zeta3^2));
w4=2*pi*fd4/(sqrt(1-zeta4^2));
w5=2*pi*fd5/(sqrt(1-zeta5^2));
%_____
SYSdPxm0=tf([B_estimated_dxm(6) A_estimated_dxm(6)],[1 2*zeta0*w0 w0^2]);
SYSdPxm1=tf([B_estimated_dxm(1) A_estimated_dxm(1)],[1 2*zeta1*w1 w1^2]);
SYSdPxm2=tf([B_estimated_dxm(2) A_estimated_dxm(2)],[1 2*zeta2*w2 w2^2]);
SYSdPxm3=tf([B_estimated_dxm(3) A_estimated_dxm(3)],[1 2*zeta3*w3 w3^2]);
SYSdPxm4=tf([B_estimated_dxm(4) A_estimated_dxm(4)],[1 2*zeta4*w4 w4^2]);
SYSdPxm5=tf([B_estimated_dxm(5) A_estimated_dxm(5)],[1 2*zeta5*w5 w5^2]);
SYSdPxm=SYSdPxm0+SYSdPxm1+SYSdPxm2+SYSdPxm3+SYSdPxm4+SYSdPxm5;
SYSTEMdPxm=ss(SYSdPxm);
%_____
SYSqPxm0=tf([B_estimated_qxm(6) A_estimated_qxm(6)],[1 2*zeta0*w0 w0^2]);
SYSqPxm1=tf([B_estimated_qxm(1) A_estimated_qxm(1)],[1 2*zeta1*w1 w1^2]);
SYSqPxm2=tf([B_estimated_qxm(2) A_estimated_qxm(2)],[1 2*zeta2*w2 w2^2]);
SYSqPxm3=tf([B_estimated_qxm(3) A_estimated_qxm(3)],[1 2*zeta3*w3 w3^2]);
SYSqPxm4=tf([B_estimated_qxm(4) A_estimated_qxm(4)],[1 2*zeta4*w4 w4^2]);
SYSqPxm5=tf([B_estimated_qxm(5) A_estimated_qxm(5)],[1 2*zeta5*w5 w5^2]);
SYSqPxm=SYSqPxm0+SYSqPxm1+SYSqPxm2+SYSqPxm3+SYSqPxm4+SYSqPxm5;
SYSTEMqPxm=ss(SYSqPxm);
%_____
A_PLANT=[SYSTEMdPxm.a zeros(12,12) zeros(12,12) zeros(12,12)
    zeros(12,12) SYSTEMqPxm.a zeros(12,12) zeros(12,12)
    zeros(12,12) zeros(12,12) SYSTEMdPxm.a zeros(12,12)
    zeros(12,12) zeros(12,12) zeros(12,12) SYSTEMqPxm.a];
B_PLANT=[SYSTEMdPxm.b zeros(12,1)
    zeros(12,1) SYSTEMqPxm.b
    SYSTEMdPxm.b zeros(12,1)
    zeros(12,1) SYSTEMqPxm.b];
C_PLANT=[SYSTEMdPxm.c SYSTEMqPxm.c zeros(1,12) zeros(1,12)
    zeros(1,12) zeros(1,12) SYSTEMdPxm.c SYSTEMqPxm.c];
D_PLANT=[SYSTEMdPxm.d SYSTEMqPxm.d
    SYSTEMdPxm.d SYSTEMqPxm.d];
PLANT=ss(A_PLANT,B_PLANT,C_PLANT,D_PLANT);
PLANT =minreal(PLANT);
PLANT =balreal(PLANT);
%_____
A=PLANT.a;
B=PLANT.b;
```

```
C=PLANT.c;
Bu=B(:,2);
Bw=B(:,1);
Cy=C(2,:);
Cz=C(1,:);
```

A.2.4. H_2 Synthesis via LMIs

```
minusI=-1;
I=eye(12);
setlmis([])
X=lmivar(1,[12 1]);
Y=lmivar(1,[12 1]);
H=lmivar(1,[12 1]);
LLL=lmivar(2,[12 1]);
K=lmivar(2,[1 12]);
N=lmivar(2,[1 1]);
LAMBDA=lmivar(2,[1 1]);
LMI1=newlmi
lmiterm([LMI1 1 1 Y],A,1,'s');
lmiterm([LMI1 1 1 K],Bu,1,'s');
lmiterm([LMI1 1 2 0],A);
lmiterm([LMI1 1 2 N],Bu,Cy);
lmiterm([LMI1 1 2 H],1,1);
lmiterm([LMI1 1 3 0],Bw);
lmiterm([LMI1 2 2 X],1,A,'s');
lmiterm([LMI1 2 2 LLL],1,Cy,'s');
lmiterm([LMI1 2 3 X],1,Bw);
lmiterm([LMI1 3 3 0],minusI);
LMI2=newlmi
lmiterm([-LMI2 1 1 LAMBDA],1,1);
lmiterm([-LMI2 1 2 Y],Cz,1);
lmiterm([-LMI2 1 3 0],Cz);
lmiterm([-LMI2 2 2 Y],1,1);
lmiterm([-LMI2 2 3 0],I);
lmiterm([-LMI2 3 3 X],1,1);
LMISYSTEM=getlmis
nnn=decnbr(LMISYSTEM);
ccc=zeros(nnn,1);
for iii=1:nnn,
    [LAMBDAiii]=defcx(LMISYSTEM,iii,LAMBDA);
    ccc(iii)=trace(LAMBDAiii);
end
[COPT,XOPT]=mincx(LMISYSTEM,ccc,[0 0 0 0 0],[],2500)
X=dec2mat(LMISYSTEM,XOPT,X);
Y=dec2mat(LMISYSTEM,XOPT,Y);
```

```
H=dec2mat(LMISYSTEM,XOPT,H);
LLL=dec2mat(LMISYSTEM,XOPT,LLL);
K=dec2mat(LMISYSTEM,XOPT,K);
N=dec2mat(LMISYSTEM,XOPT,N);
LAMBDA=dec2mat(LMISYSTEM,XOPT,LAMBDA);
%_____
UUU=eye(12);
Vtrans=eye(12)-X*Y;
CONTROLLERMATRICE=inv([UUU X*Bu;zeros(1,12) 1])*[H'-X*A*Y LLL;K N]
                  *inv([Vtrans zeros(12,1);Cy*Y 1]);
Ac=CONTROLLERMATRICE(1:12,1:12);
Bc=CONTROLLERMATRICE(1:12,13);
Cc=CONTROLLERMATRICE(13,1:12);
Dc=CONTROLLERMATRICE(13,13);
A_closed_loop=[A+Bu*Dc*Cy Bu*Cc;Bc*Cy Ac];
B_closed_loop=[Bw;zeros(12,1)];
C_closed_loop=[Cz zeros(1,12)];
D_closed_loop=0;
CLOSED_LOOP_SYSTEM=ss(A_closed_loop,B_closed_loop,C_closed_loop,D_closed_loop)
CONTROLLERSS=ss(Ac,Bc,Cc,Dc);
[NUMCONTROLLER,DENCONTROLLER]=ss2tf(Ac,Bc,Cc,Dc);
CONTROLLERTF=tf(NUMCONTROLLER,DENCONTROLLER);
```

A.2.5. H_∞ Synthesis via LMIs

```
I=eye(12);
Cztrans=Cz';
setlmis([])
X=lmivar(1,[12 1]);
Y=lmivar(1,[12 1]);
H=lmivar(1,[12 1]);
LLL=lmivar(2,[12 1]);
K=lmivar(2,[1 12]);
N=lmivar(2,[1 1]);
gama=lmivar(1,[1 1]);
LMI1=newlmi
lmiterm([LMI1 1 1 Y],A,1,'s');
lmiterm([LMI1 1 1 K],Bu,1,'s');
lmiterm([LMI1 1 2 0],A);
lmiterm([LMI1 1 2 N],Bu,Cy);
lmiterm([LMI1 1 2 H],1,1);
lmiterm([LMI1 1 3 0],Bw);
lmiterm([LMI1 1 4 Y],1,Cztrans);
lmiterm([LMI1 2 2 X],1,A,'s');
lmiterm([LMI1 2 2 LLL],1,Cy,'s');
lmiterm([LMI1 2 3 X],1,Bw);
```

```
lmiterm([LMI1 2 4 0],Cztrans);
lmiterm([LMI1 3 3 gama],-1,1);
lmiterm([LMI1 3 4 0],0);
lmiterm([LMI1 4 4 gama],-1,1);
LMI2=newlmi
lmiterm([-LMI2 1 1 Y],1,1);
lmiterm([-LMI2 1 2 0],I);
lmiterm([-LMI2 2 2 X],1,1);
LMISYSTEM=getlmis
nnn=decnbr(LMISYSTEM);
ccc=zeros(nnn,1);
for iii=1:nnn,
    [gamaiii]=defcx(LMISYSTEM,iii,gama);
    ccc(iii)=trace(gamaiii);
end
[COPT,XOPT]=mincx(LMISYSTEM,ccc,[0 0 0 0 0],[],3.25)
X=dec2mat(LMISYSTEM,XOPT,X);
Y=dec2mat(LMISYSTEM,XOPT,Y);
H=dec2mat(LMISYSTEM,XOPT,H);
LLL=dec2mat(LMISYSTEM,XOPT,LLL);
K=dec2mat(LMISYSTEM,XOPT,K);
N=dec2mat(LMISYSTEM,XOPT,N);
gama=dec2mat(LMISYSTEM,XOPT,gama);
%------------------------------------------------------------------------
UUU=eye(12);
Vtrans=inv(UUU)*(eye(12)-X*Y);
CONTROLLERMATRICE=inv([UUU X*Bu;zeros(1,12) 1])*[H-X*A*Y LLL;K N]
                 *inv([Vtrans zeros(12,1);Cy*Y 1]);
Ac=CONTROLLERMATRICE(1:12,1:12);
Bc=CONTROLLERMATRICE(1:12,13);
Cc=CONTROLLERMATRICE(13,1:12);
Dc=CONTROLLERMATRICE(13,13);
A_closed_loop=[A+Bu*Dc*Cy Bu*Cc;Bc*Cy Ac];
B_closed_loop=[Bw;zeros(12,1)];
C_closed_loop=[Cz zeros(1,12)];
D_closed_loop=0;
CLOSED_LOOP_SYSTEM=ss(A_closed_loop,B_closed_loop,C_closed_loop,D_closed_loop)
CONTROLLERSS=ss(Ac,Bc,Cc,Dc);
[NUMCONTROLLER,DENCONTROLLER]=ss2tf(Ac,Bc,Cc,Dc);
CONTROLLERTF=tf(NUMCONTROLLER,DENCONTROLLER);
```

REFERENCES

1. Snyder, S. D., *Active Noise Control Primer*, Springer-Verlag Inc., New York, 2000.

2. Hansen, C. H., "Does Active Noise Control Have a Future?", *The Eighth Western Pacific Acoustics Conference*, 2003.

3. Kuo, S. M. and D. R. Morgan, "Active Noise Control: A Tutorial Review", *Proceedings of the IEEE*, Vol. 87, No. 6, pp. 943–973, 1999.

4. Gordon, R. T. and W. D. Vining, "Active Noise Control: A Review of the Field", *The American Industrial Hygiene Association Journal*, Vol. 53, No. 11, pp. 721–725, 1992.

5. Wise, S. and G. Leventhall, "Active Noise Control as a Solution to Low Frequency Noise Problems", *Journal of Low Frequency Noise, Vibration and Active Control*, Vol. 29, No. 2, pp. 129–137, 2010.

6. Elliott, S. J. and P. A. Nelson, "Active Noise Control", *IEEE Signal Processing Magazine*, Vol. 10, No. 4, pp. 12–35, 1993.

7. Hansen, C. H., "Current and Future Industrial Applications of Active Noise Control", *Noise Control Engineering Journal*, Vol. 53, No. 5, pp. 181–196, 2005.

8. Gelin, L. J., "Active Noise Control: A Tutorial for HVAC Designers", *ASHRAE Journal*, Vol. 39, No. 8, pp. 43–49, 1997.

9. Lueg, P., "Process of Silencing Sound Oscillations", US Patent 2,043,416, 1936.

10. Warnaka, G. E., "Active Attenuation of Noise - The State of the Art", *Noise Control Engineering Journal*, Vol. 18, No. 3, pp. 100–110, 1982.

11. Olson, H. F. and E. G. May, "Electronic Sound Absorber", *The Journal of the*

Acoustical Society of America, Vol. 25, No. 6, pp. 1130–1136, 1953.

12. Conover, W. B., "Noise Reducing System for Transformers", US Patent 2,776,020, 1957.

13. Terzigni, M., "HVAC-System Acoustics - Methods of Reducing Unwanted Sound Associated with Mechanical Systems in Commercial Buildings", *HPAC Engineering*, Vol. 80, No. 8, pp. 18–23, 2008.

14. Niv, R., "Silence Simplified", *Appliance Design*, Vol. 56, No. 8, pp. 30–33, 2008.

15. Milani, A. A., G. Kannan, and I. M. S. Panahi, "On Maximum Achievable Noise Reduction in ANC Systems", *2010 IEEE International Conference on Acoustics Speech and Signal Processing (ICASSP)*, pp. 349–352, 2010.

16. Papini, G. S. and R. L. U. F. Pinto, "Active Noise Control for Small-Diameter Exhaustion System", *ABCM Symposium Series in Mechatronics*, Vol. 3, pp. 148–156, 2008.

17. Eriksson, L. J. and M. C. Allie, "Use of Random Noise for On-Line Transducer Modeling in an Adaptive Active Attenuation System", *The Journal of the Acoustical Society of America*, Vol. 85, No. 2, pp. 797–802, 1989.

18. Akhtar, M. T., M. Abe, and M. Kawamata, "Acoustic Feedback Path Modeling in Active Noise Control Systems", *Proceedings of SICE Annual Conference*, pp. 157–161, Okayama, Japan, 2005.

19. Babu, P. and A. Krishnan, "Modified FxAFA Algorithm Using Dynamic Step Size for Active Noise Control Systems", *International Journal of Recent Trends in Engineering*, Vol. 2, No. 7, pp. 37–39, 2009.

20. Akhtar, M. T., M. Abe, and M. Kawamata, "A Method for Online Secondary Path Modeling in Active Noise Control Systems", *ISCAS IEEE International Symposium on Circuits and Systems*, pp. 264–267, 2005.

21. Zhou, D. and V. DeBrunner, "A New Active Noise Control Algorithm that Requires No Secondary Path Identification Based on the SPR Property", *IEEE Transactions on Signal Processing*, Vol. 55, No. 5, pp. 1719–1729, 2007.

22. Eghtesadi, K. and H. G. Leventhall, "Active Attenuation of Noise: The Chelsea Dipole", *Journal of Sound and Vibration*, Vol. 75, No. 1, pp. 127–134, 1981.

23. Eghtesadi, K. and H. G. Leventhall, "Active Attenuation of Noise - The Monopole System", *The Journal of the Acoustical Society of America*, Vol. 71, No. 3, pp. 608–611, 1982.

24. Eghtesadi, K. and H. G. Leventhall, "A Study of n-Source Active Attenuator Arrays for Noise in Ducts", *Journal of Sound and Vibration*, Vol. 91, No. 1, pp. 11–19, 1983.

25. Trinder, M. C. J. and P. A. Nelson, "Active Noise Control in Finite Length Ducts", *Journal of Sound and Vibration*, Vol. 89, No. 1, pp. 95–105, 1983.

26. Hull, A. J., C. J. Radcliffe, M. Miklavčič, and C. R. MacCluer, "State Space Representation of the Nonself-Adjoint Acoustic Duct System", *Journal of Vibration and Acoustics*, Vol. 112, pp. 483–488, 1990.

27. Hull, A. J. and C. J. Radcliffe, "Experimental Verification of the Nonself-Adjoint State Space Duct Model", *Journal of Vibration and Acoustics*, Vol. 114, pp. 404–408, 1992.

28. Hull, A. J., C. J. Radcliffe, and C. R. MacCluer, "State Estimation of the Nonself-Adjoint Acoustic Duct System", *Journal of Dynamic Systems, Measurement and Control*, Vol. 113, pp. 122–126, 1991.

29. Hull, A. J., C. J. Radcliffe, and S. C. Southward, "Global Active Noise Control of a One-Dimensional Acoustic Duct Using a Feedback Controller", *Journal of Dynamic Systems, Measurement and Control*, Vol. 115, pp. 488–494, 1993.

30. Hu, J. S., "Active Sound Attenuation in Finite-Length Ducts Using Close-Form Transfer Function Models", *Journal of Dynamic Systems, Measurement and Control*, Vol. 117, pp. 143–154, 1995.

31. Bai, M. R. and C. Shieh, "Active Noise Cancellation by Using the Linear Quadratic Gaussian Independent Modal Space Control", *The Journal of the Acoustical Society of America*, Vol. 97, No. 5, pp. 2664–2674, 1995.

32. Hong, J., J. C. Akers, R. Venugopal, M. N. Lee, A. G. Sparks, P. D. Washabaugh, and D. S. Bernstein, "Modeling, Identification and Feedback Control of Noise in an Acoustic Duct", *IEEE Transactions on Control Systems Technology*, Vol. 4, No. 3, pp. 283–291, 1996.

33. Wu, Z., V. K. Varadan, and V. V. Varadan, "Time-Domain Analysis and Synthesis of Active Noise Control Systems in Ducts", *Journal of the Acoustical Society of America*, Vol. 101, No. 3, pp. 1502–1511, 1997.

34. Lee, Y. S., *The Active Noise Control of a One-Dimensional Duct*, M.S. Thesis, Michigan State University, 1997.

35. Grad, J. R., H_∞ *Control of Acoustic Noise*, Ph.D. Thesis, University of Waterloo, 1997.

36. Morris, K. A., "Noise Reduction in Ducts Achievable by Point Control", *Journal of Dynamic Systems, Measurement and Control*, Vol. 120, pp. 216–223, 1998.

37. Pota, H. R. and A. G. Kelkar, "Modeling and Control of Acoustic Ducts", *Journal of Vibration and Acoustics*, Vol. 123, pp. 2–10, 2001.

38. Toochinda, V., *Fundamental Limitations of ANC in One-Dimensional Ducts Using 2 Sensors and 1 Actuator*, Ph.D. Thesis, University of Massachusetts Amherst, 2002.

39. Zimmer, B. J., S. P. Lipshitz, K. A. Morris, J. Vanderkooy, and E. E. Obasi, "An

Improved Acoustic Model for Active Noise Control in a Duct", *Journal of Dynamic Systems, Measurement and Control*, Vol. 125, pp. 382–395, 2003.

40. Morris, K. A., "H_∞-Control of Acoustic Noise in a Duct with a Feedforward Configuration", *15th International Symposium on Mathematical Theory of Networks and Systems*, South Bend, Indiana, USA, 2002.

41. Yang, Z., "Design of Active Noise Control Using Feedback Control Techniques for an Acoustic Duct System", *Proceedings of the 2004 IEEE Conference on Robotics, Automation and Mechatronics*, Vol. 1, pp. 467–472, Singapore, 2004.

42. Yang, Z., "Active Noise Control for a One-Dimensional Acoustic Duct Using Feedback Control Techniques: Modelling and Simulation", *Proceedings of IASTED Conference on Applied Simulation and Modeling*, Marbella, Spain, 2003.

43. Yang, Z. and D. L. Hicks, "A Study of Active Noise Control for an Acoustic Duct System Using Feedback Control Techniques", *Proc. of IEEE 2003 Int. Sym. on Intelligent Signal Processing and Communication Systems*, pp. 720–728, Awaji Island, Japan, 2003.

44. Swinbanks, M. A., "The Active Control of Sound Propagation in Long Ducts", *Journal of Sound and Vibration*, Vol. 27, No. 3, pp. 411–436, 1973.

45. Poole, J. H. B. and H. G. Leventhall, "An Experimental Study of Swinbanks' Method of Active Attenuation of Sound in Ducts", *Journal of Sound and Vibration*, Vol. 49, No. 2, pp. 257–266, 1976.

46. Poole, J. H. B. and H. G. Leventhall, "Active Attenuation of Noise in Ducts", *Journal of Sound and Vibration*, Vol. 57, No. 2, pp. 308–309, 1978.

47. Berengier, M. and A. Roure, "Broad-Band Active Sound Absorption in a Duct Carrying Uniformly Flowing Fluid", *Journal of Sound and Vibration*, Vol. 68, No. 3, pp. 437–449, 1980.

48. Hong, W. K. W., K. Eghtesadi, and H. G. Leventhall, "The Tight-Coupled Monopole (TCM) and Tight-Coupled Tandem (TCT) Attenuators: Theoretical Aspects and Experimental Attenuation in an Air Duct", *The Journal of the Acoustical Society of America*, Vol. 81, No. 2, pp. 376–388, 1987.

49. Bai, M. R. and H. Lin, "Plant Uncertainty Analysis in a Duct Active Noise Control Problem by Using the H_∞ Theory", *The Journal of the Acoustical Society of America*, Vol. 104, No. 1, pp. 237–247, 1998.

50. Sawada, Y. and A. Ohsumi, "Active Attenuation of the Sound Outflowing from a One-Dimensional Duct", *Proceedings of the 2001 IEEE International Conference on Control Applications*, pp. 1008–1013, Mexico City, Mexico, 2001.

51. Yucelen, T., A. S. Sadahalli, and F. Pourboghrat, "Active Noise Control in a Duct Using Output Feedback Robust Control Techniques", *2010 American Control Conference (ACC)*, pp. 3506–3511, Baltimore, USA, 2010.

52. Morse, P. M. and K. U. Ingard, *Theoretical Acoustics*, Princeton University Press, Princeton, 1986.

53. Kinsler, L. E., A. R. Frey, A. B. Coppens, and J. V. Sanders, *Fundamentals of Acoustics*, John Wiley & Sons Inc., 3rd edition, 1982.

54. Cole, J. E., "Acoustic Pulse Propagation in a Duct with Flow", *Journal of Sound and Vibration*, Vol. 47, No. 1, pp. 95–105, 1976.

55. Swinbanks, M. A., "The Sound Field Generated by a Source Distribution in a Long Duct Carrying Sheared Flow", *Journal of Sound and Vibration*, Vol. 40, No. 1, pp. 51–76, 1975.

56. Munjal, M. L., *Acoustics of Ducts and Mufflers with Application to Exhaust and Ventilation System Design*, John Wiley & Sons Inc., 1987.

57. Venugopal, R., *Modeling and Adaptive Control of Acoustic Noise*, Ph.D. Thesis,

University of Michigan, 1997.

58. Hong, J., *Experimental Implementation of Fixed-Gain and Adaptive Disturbance Rejection Controllers*, Ph.D. Thesis, University of Michigan, 1998.

59. Doak, P. E., "Excitation, Transmission and Radiation of Sound from Source Distributions in Hard-Walled Ducts of Finite Length (I): The Effects of Duct Cross-Section Geometry and Source Distribution Space-Time Pattern", *Journal of Sound and Vibration*, Vol. 31, No. 1, pp. 1–72, 1973.

60. Haberman, R., *Applied Partial Differential Equations with Fourier Series and Boundary Value Problems*, Pearson Prentice Hall, New Jersey, 4th edition, 2004.

61. Beranek, L. L., *Acoustics*, McGraw-Hill Book Company Inc., New York, 1954.

62. Scherer, C. and S. Weiland, *Linear Matrix Inequalities in Control*, Lecture Notes, Dutch Institute for Systems and Control, Delft, The Netherlands, 2000.

63. Inman, D. J., *Engineering Vibration*, Prentice Hall Inc., New Jersey, 1996.